Science of Ultrasound and Echocardiography

1

Pierre C. Wong

Abstract

For anyone seeking to achieve proficiency in transesophageal echocardiography, it is important to have a solid understanding of the underlying science of ultrasound, along with knowledge of the instrumentation and equipment utilized for cardiac imaging. This chapter provides a review of all of these topics, particularly as they apply to echocardiography. Basic principles of sound will first be discussed, followed by the process of ultrasonic two-dimensional image formation. Principles of Doppler echocardiography (and its applications) will then be presented. Finally, echocardiography instrumentation, echocardiographic artifacts, and digital archiving/networking of echocardiographic studies will be discussed. Familiarity with the information in this chapter will provide readers a greater understanding of the many technical aspects of echocardiography, enabling them to optimize their cardiac ultrasound platforms so that the best possible information can be obtained.

Keywords

Ultrasound physics • B-mode imaging • Phased array transducers • Doppler echocardiography • Spectral Doppler • Color flow Doppler • DICOM

Introduction

This is a textbook on transesophageal echocardiography (TEE), specifically TEE for the evaluation of congenital heart disease (CHD). But what is TEE? It is a specialized form of echocardiography, which is itself a specialized form of ultrasonography focusing upon the heart and related vascular structures. Thus, anyone seeking to achieve proficiency in echocardiography and TEE needs to have a solid understanding of the underlying science of ultrasound, particularly its strengths and weaknesses as applied to the evaluation of the cardiovascular system.

P.C. Wong, MD
Division of Cardiology, Children's Hospital Los Angeles, Department of Pediatrics, Keck School of Medicine, University of Southern California, 4650 Sunset Blvd, Mailstop #34, Los Angeles, CA 90027, USA
e-mail: pwong@chla.usc.edu

This chapter reviews the physics and instrumentation of ultrasound and echocardiography. It is not intended to be an exhaustive review of the subject—that would require a separate textbook, and a number of excellent and comprehensive references have already been written on this topic [1–4]. Rather, its purpose is to provide an overview of the science of ultrasound, focusing on aspects that apply especially to modern day echocardiography and TEE technology, and touching upon details pertinent to the echocardiographic evaluation of CHD.

This chapter is divided into six major sections: (1) Physics of Sound and Ultrasound; (2) Important Principles of Echocardiographic Image Formation; (3) Doppler Echocardiography; (4) Overview of the Echocardiography Machine; (5) Artifacts; (6) Digital Imaging and DICOM. While knowledge of the material in earlier sections aids in the comprehension of later sections, readers should feel free to peruse the chapter in whatever order they find most applicable.

P.C. Wong, W.C. Miller-Hance (eds.), *Transesophageal Echocardiography for Congenital Heart Disease*,
DOI 10.1007/978-1-84800-064-3_1, © Springer-Verlag London 2014

Background

The concept of utilizing sound for the purposes of location and imaging has its origins in nature. It is well known that bats use ultrasound (high frequency sound above the range of human hearing) in order to fly and locate their prey, even in complete darkness. This capability, which evolved over millions of years, is known as "echolocation". Dolphins, porpoises, and toothed whales are also known to utilize ultrasound underwater for echolocation. In World War I, SONAR (**SO**und **NA**vigation and **R**anging) was developed, in which piezoelectric materials were formulated as senders and receivers of high frequency sound waves, and these were employed to detect enemy submarines underwater. This technology was further developed and put to good use in World War II, and is still widely utilized today in both the commercial and military nautical industry. Medical diagnostic ultrasound was first developed in the 1940s–1950s. Over the past 50–60 years, rapid advancements in computing and probe miniaturization technology have made possible the development of high resolution, real-time two-dimensional (2D) ultrasonography, leading to the ability to define precisely the anatomy and physiology of the heart by echocardiography [5].

Regardless of whether it is used in bats, SONAR, or medical imaging, the basic principle (known as the *pulse-echo* principle) remains the same. Sound waves of known frequency are generated and sent (*pulsed*) in a specific direction, with the intention that a target object (or objects) will reflect some or all of the sound waves back to the source (Fig. 1.1). The sender then "listens" for the returning signals (*echoes*) from the target object; these returning echoes carry important information that can be used to abstract details about the object, including distance, image, size, movement, etc.

The following sections discuss the physical process in which ultrasound, specifically through the use of the pulse-echo principle, is utilized to obtain detailed information for medical diagnostic imaging—particularly in regard to noninvasive cardiac evaluation by echocardiography, including TEE.

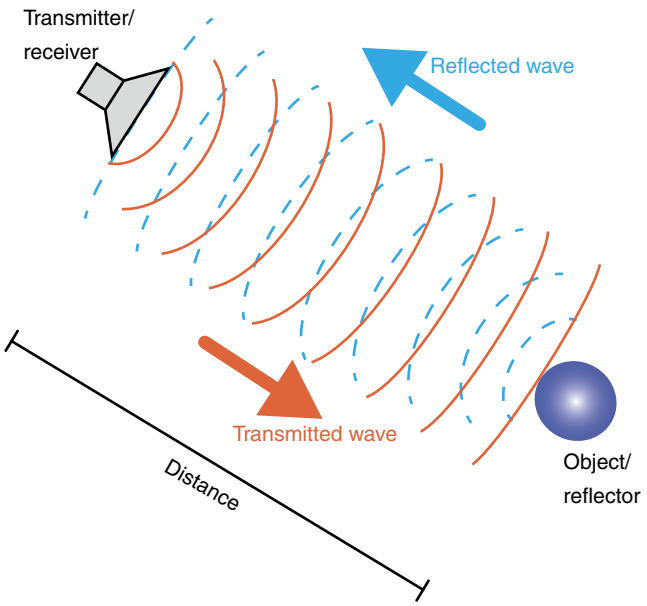

Fig. 1.1 Pulse-echo principle. A *pulse* of sound of known frequency is generated and emitted in a known direction. The *echoes* returning from an object can be used to derive information regarding the object, including distance, size, etc.

Physics of Sound and Ultrasound

Sound: Definition and Properties

Sound is a form of mechanical energy that requires a physical medium for transmission; this medium must contain molecules (such as air, water, etc.) that are used to propagate the sound. Unlike electromagnetic waves, which do not require a medium for propagation, sound cannot be transmitted in a vacuum. A sound wave is created when a discrete source—a vibrating or oscillating object—pushes and pulls adjacent molecules, causing them in turn to vibrate; this vibration spreads to adjacent molecules, and thus a disturbance is propagated away from the source in the form of a longitudinal wave characterized by a series of back and forth vibrations of molecules (Fig. 1.2). The direction of this back and forth vibration is parallel to the direction of wave propagation. The wave that is created represents a series of *compressions*, when the molecules are pushed together, and *rarefactions*, when the molecules are pulled apart (Fig. 1.2). If one could measure the instantaneous pressure at different points, the regions of compression, in which there is a greater density of molecules, would have a higher pressure than normal, and the regions of rarefaction (with a lesser density) would have a lower pressure than normal. Plotting a graph of pressure vs. distance from the source (along the line of propagation) would produce a curve in the shape of a sine wave (Fig. 1.2). The importance of this sine wave is that, like any wave, it has certain properties that can be used to describe it. The peak of one wave to the next peak (or valley to valley) represents one full wave or one complete cycle or period; the number of times per second that the cycle is repeated is termed the **frequency**, and the unit to measure this is cycles per second, or **Hertz** (**Hz**). This frequency is determined by the number of oscillations per second made by the sound source. The physical distance between two peaks (or valleys) is termed the **wavelength** and often designated by the symbol λ. This is the distance the sound wave travels in one complete cycle. The importance here is that frequency and

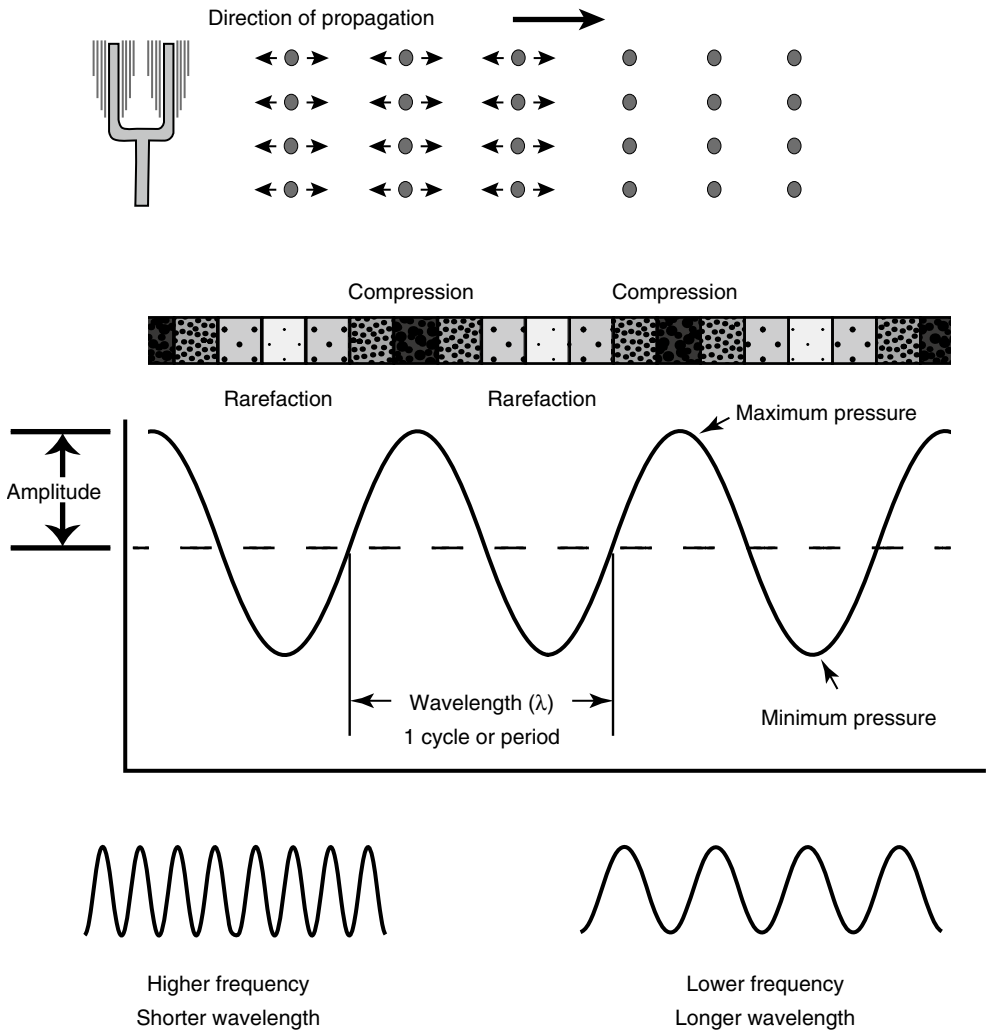

Fig. 1.2 Generation of a sound wave. A vibrating source (in this case, a tuning fork) causes adjacent air molecules to vibrate in a back-and-forth direction. This oscillating motion propagates away from the source in a series of compressions and rarefactions; when the air pressure at any one point is plotted as a function of time, a sine wave is obtained with a wavelength (**λ**) and pressure amplitude (P). Shorter wavelengths are associated with higher wave frequencies; longer wavelengths with lower frequencies. This example shows sound propagation in air, but the same principles apply in water or in the soft tissue of the human body

wavelength are inversely related, and their magnitude depends upon the speed of sound in the medium (Table 1.1A). The equation relating these three variables is given as follows:

$$\lambda = \frac{c}{f} \tag{1.1}$$

λ = wavelength
c = speed of sound in the medium
f = frequency in cycles/second

The speed of sound varies depending upon the medium: the denser the medium, the faster the speed of propagation. In biological systems, the speed of sound exhibits wide variation: it is lowest in the lungs, which are air-filled structures (about 600 m/s), and highest in bone (about 4,080 m/s) (Table 1.1A). In the soft tissues, the average speed of sound is about **1,540 m/s**, and this is the number generally used when calibrating the range-measuring circuits of most diagnostic ultrasound instrumentation [1]. As will be shown throughout this chapter, the speed of sound in the human body plays an important role in a number of considerations related to echocardiography.

The importance of Eq. 1.1 is that, by knowing the speed of sound in the medium, the wavelength can be calculated for a given sound frequency, and vice-versa. The range of sound frequencies audible by the human ear is between 20 and 20,000 Hz. However, if sound waves of these frequencies were transmitted in the body, the corresponding wavelengths would be far too large for use in the medical field. For diagnostic medical imaging, adequate resolution is possible only when the wavelength of the sound wave is comparable to the size of the smallest objects being imaged [6, 7]. For echocardiography, this translates to millimeters or less, which means that sound frequencies in the *millions* of Hertz (megahertz, or MHz) must be used. Note that these frequencies are extremely high, several orders of magnitude beyond the range of human hearing—hence the term *ultrasound*. Echocardiography generally utilizes frequencies between 1 and 15 MHz, which by Eq. 1.1 yields a wavelength between

Table 1.1 Physical properties of sound for various tissues in the human body

A. Speed of sound	
Material	*Speed of sound (m/s)*
Lung	600
Fat	1,460
Liver	1,555
Blood	1,560
Kidney	1,565
Muscle	1,600
Lens of eye	1,620
Skull bone	4,080
B. Acoustic impedance	
Tissue	*Acoustic impedance (Rayls × 10^{-4})*
Air	0.0004
Lung	0.18
Water	1.5
Brain	1.55
Blood	1.61
Liver	1.65
Kidney	1.62
Human soft tissue, mean	1.63
Muscle	1.71
Skull bone	7.8
C. Attenuation coefficient	
Tissue	*Attenuation coefficient (dB/cm)*
Water	0.0022
Blood	0.18
Brain	0.85
Liver	0.9
Fat	0.6
Kidney	1.0
Muscle	1.2
Skull bone	20
Lung	40

Source: Zagzebski [1]

For each table, measurements are listed from lowest to highest value

0.1 mm (15 MHz) and 1.54 mm (1 MHz). The higher the frequency, the smaller the wavelength, and the better the spatial resolution.

The other important property of a sound wave is its amplitude, which describes the strength of the wave, or maximum pressure elevation from baseline (Fig. 1.2). This corresponds to the "loudness" of the sound. This property, also known as **acoustic pressure**, is measured in **Pascals** (**P**). The amplitude of the sound represents the energy associated with the sound wave: the more the energy, the "louder" the sound and the greater the amplitude. Another parameter used to express the "loudness" of the sound is known as **intensity**. This term is used to describe the energy flowing a cross-sectional area per second and is proportional to the square of acoustic pressure, as noted by the equation:

$$I = \frac{P^2}{2\rho c} \tag{1.2}$$

I = intensity
P = acoustic pressure in Pascals
ρ = density of the medium
c = speed of sound in the medium

Intensity is the parameter used to characterize the spatial distribution of ultrasound energy. As noted, it describes the amount of ultrasonic power per unit area (given in watts/square meter, or more commonly milliwatts per square centimeter), and can vary depending upon location. The difference between acoustical power and intensity can be illustrated in the following example: two beams (one focused, one unfocused) are emitted with the same acoustic power. While the unfocused beam has a more uniform distribution of energy; the focused beam will produce more concentrated energy in the area focused. Hence, the intensity is greater in that area. Intensity is also one of the parameters used to evaluate the biological effects of ultrasound. At sufficiently high intensities and long enough exposure times, ultrasound can produce a measurable effect on tissues, notably in the form of heating and cavitation (tiny bubbles from dissolved gases in the medium) [1]. The subject of the biological effects of ultrasound on human tissue is beyond the scope of this chapter. Suffice it to say that while no known ill effects have been noted from the intensity levels and scan times commonly used in diagnostic medical ultrasound, it is still important to be mindful of the remote possibility—particularly if equipment manufacturers were to increase output intensities to improve imaging [3, 8].

For medical imaging, a standard method for quantifying intensities or power levels is to use the decibel (dB) system. Instead of providing an absolute number, this method produces a value that represents a relative change (or ratio) between two amplitudes or two intensities. Using two echo signal intensities I_1 and I_2 or two echo signal amplitudes A_1 and A_2 (I_1 and A_1 representing the reference signal), the signal level in dB is calculated as follows:

$$Signal\ level = 10\log\frac{I_2}{I_1} \text{ or } Signal\ level = 20\log\frac{A_2}{A_1} \tag{1.3}$$

It is meaningless to use a dB level as an absolute value. Rather, the dB notation provides a value obtained when comparing a particular intensity or amplitude to a reference value. In diagnostic medical ultrasound, the transmitted signal generally serves as the reference value. Note that the dB represents a logarithmic scale, therefore an intensity change of +3 dB represents a doubling of intensity, and −3 dB a halving of intensity. The dB system is used to express output power, dynamic range, or ultrasonic attenuation in tissue (see

below). It represents a simpler, more compact method to express large differences in power levels or intensity, and will be used throughout the remainder of this chapter.

Reflection: The Key to Ultrasonic Imaging

As an ultrasound wave propagates through the body, several different interactions are possible as it encounters the various tissues interfaces. These interactions, analogous to those occurring with light waves, include: (a) continued transmission, (b) reflection, (c) refraction, (d) absorption. Of these, **reflection** is the key interaction that makes possible the generation of ultrasonographic/echocardiographic information. As mentioned above, diagnostic medical ultrasound consists of emitting sound pulses in a known direction, and then collecting and processing the returning echo signals—that is, the signals that have been *reflected* from the various internal structures in the body (in the case of echocardiography, the heart, blood, and vascular structures). The differences in the strength of the returning signals enable the ultrasound machine to build an image of the various tissues, as well as the tissue-tissue and tissue-blood interfaces, and this forms the basis of echocardiographic imaging. What determines how echo signals are reflected, and the strength of these signals? A fundamental factor is **acoustic impedance**, an intrinsic property of tissue that characterizes its capacity for sound transmission. The acoustic impedance of a tissue is directly proportional to its underlying density—the denser the tissue, the higher the acoustic impedance. Each type of tissue has a different acoustic impedance: air has an extremely low impedance, bone has a very high impedance, and the various soft tissues have impedances that differ from each other but vary within a much narrower range (Table 1.1B). At a tissue interface, the degree of reflection vs. transmission of an incident sound wave depends upon the relative difference in acoustic impedance between the two tissues—that is, the degree of *impedance matching*. When there is a small impedance mismatch, most of the sound energy is transmitted, and only a small amount is reflected and returns to the source (transducer) to be used as imaging information (Fig. 1.3). As the transmitted energy continues further, some is reflected in a similar manner at more distant interfaces, yielding imaging information from deeper structures. This process continues along the length of the ultrasound beam. In this manner, ultrasonic information is progressively obtained, and imaging is possible to significant depths because the acoustic impedance differences are small for most soft tissue-soft tissue interfaces. However, if a significant impedance mismatch exists between two tissues, then virtually all sound is reflected, and very little transmitted. Almost no usable information is available beyond the interface (a phenomenon known as "acoustic shadowing"). This is the reason that lung

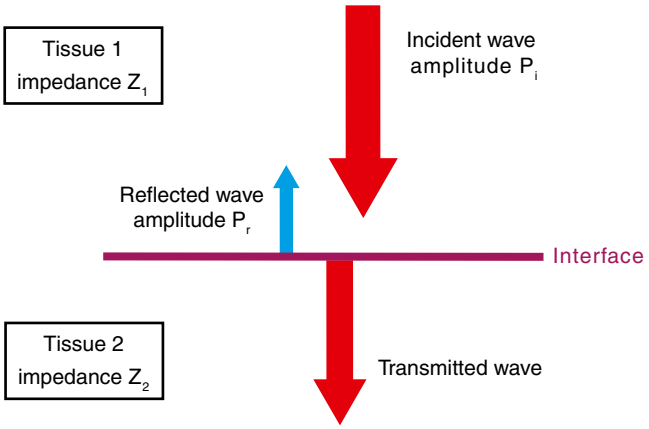

Fig. 1.3 Specular reflection. When an incident sound wave of amplitude P_i encounters a smooth interface perpendicular to the direction of propagation, some is reflected (amplitude P_r) and the remainder transmitted. The degree of transmission vs. reflection depends upon the relative differences in acoustic impedance between the two tissues (Z_1 and Z_2)—the greater the impedance mismatch, the greater the amount of sound reflected

interferes with ultrasonic imaging: it is not that ultrasound cannot propagate through lung, it is that the impedance mismatch is so great between lung and soft tissue that virtually all ultrasound energy is reflected. It is also the reason that ultrasonic gel is used with transthoracic imaging: to improve the acoustic coupling (impedance matching) between the transducer and the chest wall.

Acoustic impedance matching is important whenever a sound wave encounters an interface between two tissues, and it is particularly important for those interfaces that are much larger than the size of the ultrasound wavelength. When such interfaces are large and smooth, they are termed **specular reflectors** and they behave like a large acoustic mirror (*speculum* = mirror in Latin). If there is a sizable impedance mismatch, incident ultrasound beams will undergo a great deal of reflection. If the incident beam is directed perpendicular to the surface, the reflected sound waves return to the transducer as a well-defined, redirected beam (echo), leading to a very bright appearance on the display screen (Fig. 1.4). If the incident ultrasound beam strikes the specular reflector at an angle, the reflected portion will be directed at an angle θ_r which is equal to the incident angle θ_i but in the opposite direction. The remainder of the incident beam that is transmitted can be "bent" or **refracted**, with the amount of refraction depending upon the difference between the speed of sound between the two tissues, as given by Snell's Law (Fig. 1.5). The greater the difference in the speed of sound between the two tissues, the greater the degree of refraction. Again, this is analogous to the behavior of light waves. In general, refraction is not a major problem with diagnostic ultrasound because there is little variation in the speed of sound among the soft tissues in the human body.

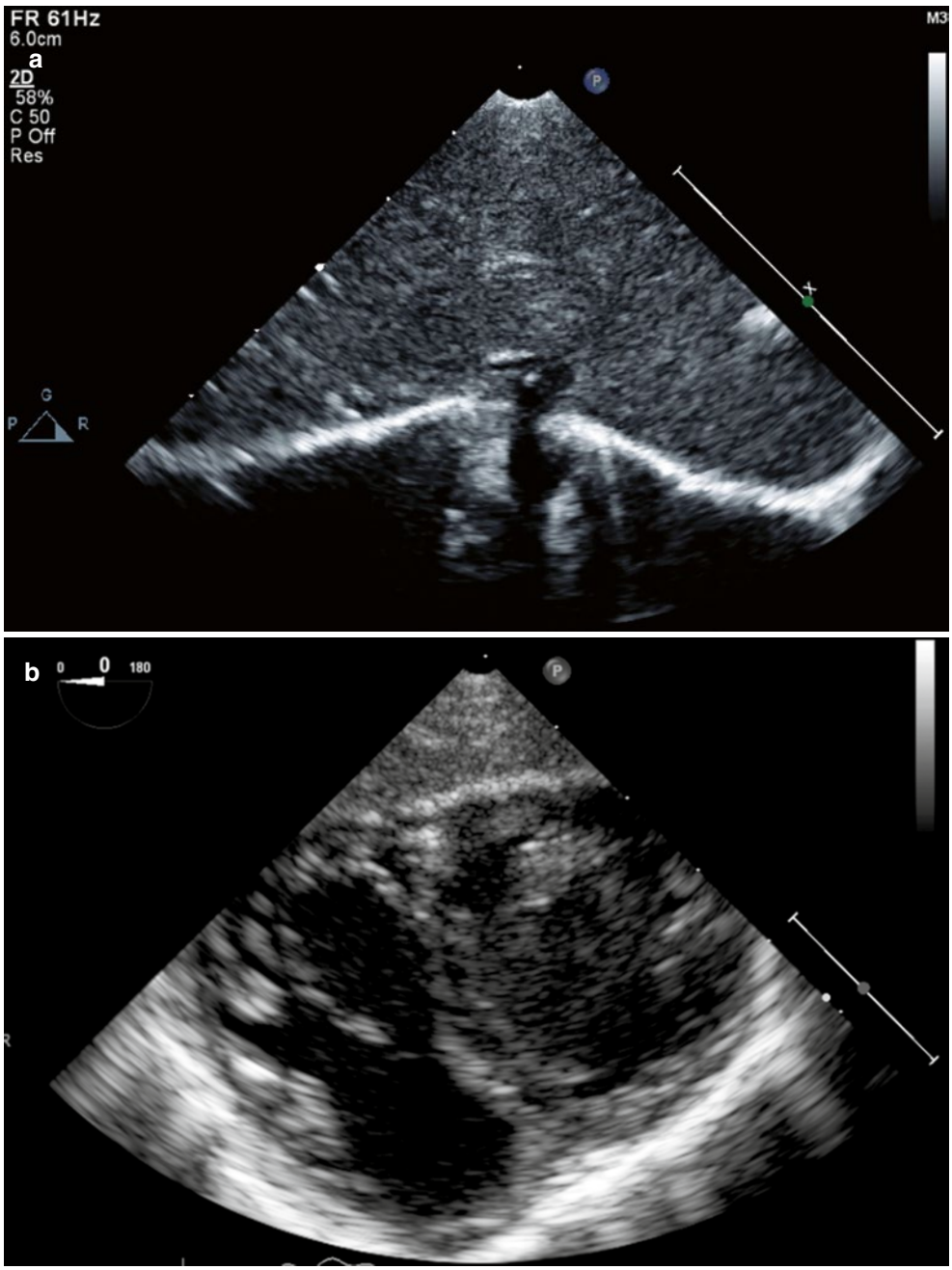

Fig. 1.4 Example of a large specular reflector (diaphragm) and acoustic scattering produced by imaging of the liver (**a**) and myocardium (**b**). Note that the echoes from the specular reflector have the largest amplitude (brightness) when the surface is perpendicular to the angle of insonation. In (**b**), the myocardium has the characteristic heterogeneous 2D appearance produced by natural acoustic reflections and interference patterns (scattering) from its various components, also known as "speckle"

However in certain situations, refraction can lead to image errors; this can be seen in the setting of interfaces between fat and soft tissue.

What if the large surface is not smooth, but rough? In this case the uneven surface causes incident energy to be reflected in a number of different directions. This is called **diffuse reflection** (Fig. 1.6). Such reflections can cause a loss of beam coherence and a weaker echo returning to the transducer. Some organ boundaries, as well as the walls of the heart chambers (irregular endocardial surfaces), fall within this category. At first glance, it would appear that that these signals, along with the nonperpendicular signals to a specular reflector (whether reflected at an angle or refracted) would not be as useful for imaging because they are not directed back to the transducer. However in practice, even these off-angle specular and diffuse reflectors are useful for ultrasonic imaging due to the range to different transducer positions that can be utilized. In addition, divergences of the ultrasound beam can result in sound waves that will be reflected back to the transducer [9]. In fact, echoes from diffuse reflectors, while weaker, can be useful because of the fact that they are not as sensitive to the orientation of the transducer.

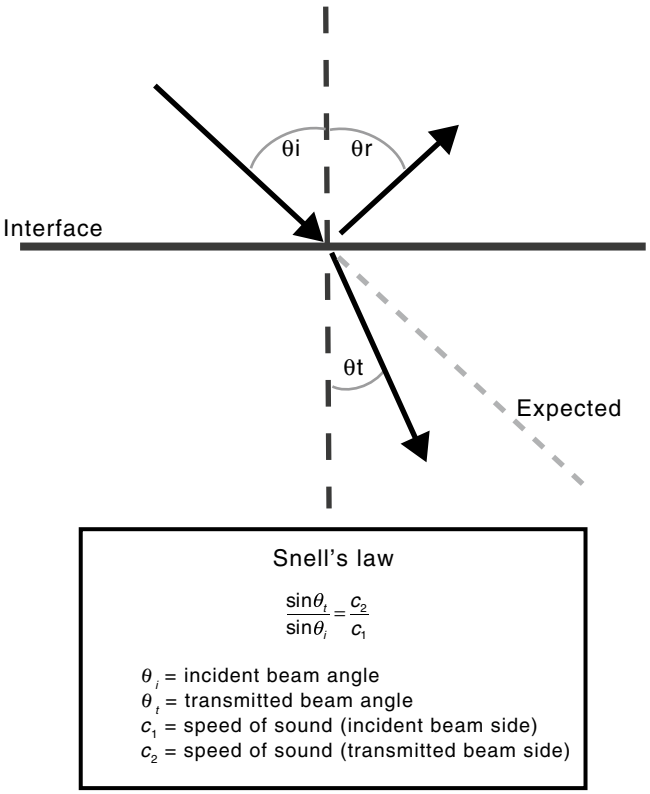

Fig. 1.5 Refraction and Snell's law. When the incident sound wave encounters a large specular reflector at a nonperpendicular angle θ_i (θ_i refers to the angle as measured from the perpendicular axis), the reflected beam travels off at an equivalent angle θ_r. The transmitted wave undergoes refraction or "bending". The amount of refraction can be predicted by Snell's law, which is itself based upon the difference in the speed of sound between the two tissues. The greater the difference, the greater the degree of refraction

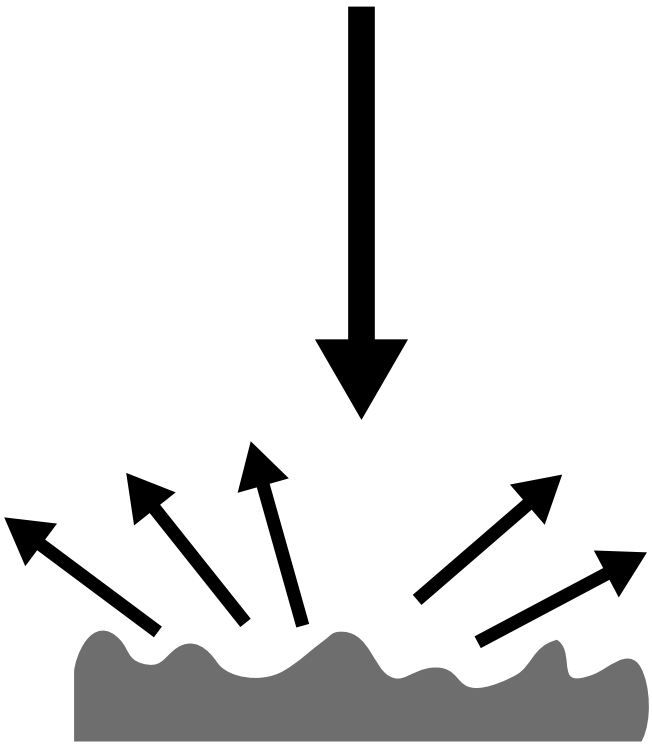

Fig. 1.6 Diffuse reflector. An incident beam striking a rough, uneven surface results in lower amplitude reflected waves that travel away from the reflector in multiple directions. This type of echo is not as dependent upon interface orientation as a specular reflector

The information from diffuse and specular reflectors is most useful at the boundaries of objects and organs, for example along the diaphragm or pericardium. However an even more important type of reflection accounts for much of the useful diagnostic information in ultrasonic imaging, including echocardiography. This type of reflection is called **acoustic scattering**, also known as *nonspecular reflection*. It refers to reflections from objects the size of the ultrasound wavelength or smaller. The parenchyma of most organs, including the heart, contains a number of objects (reflectors) of this size. The signals from these reflectors return to the transducer through multiple pathways. The sound from such reflectors is no longer a coherent beam; it is instead the sum of a number of component waves that produces a complex pattern of constructive and destructive interference. This interference pattern is known as "speckle" and provides the characteristic ultrasonic appearance of complex tissue such as myocardium (Fig. 1.4a) [7]. These signals tend to be weaker, and echo signal strength varies depending upon the degree of scattering. The degree of scattering is primarily based upon: (a) number of scatterers per unit volume; (b) acoustic impedance changes at the scatterer interfaces; (c) size of the scatterer—increased size produces increased scattering; (d) ultrasonic frequency—scattering increases with increasing frequency/decreasing wavelength [1]. The last point is important, because it contrasts to specular reflection, which is *frequency independent*. Therefore it is possible to enhance scattering selectively over specular reflection by using higher ultrasound frequencies. Also, because of the fact that scattering occurs in multiple directions, the incident beam angle/direction is not as important as with specular reflectors. This is why organ parenchyma (such as liver) can be readily viewed from a number of different transducer positions (Fig. 1.4b). Changes in scattering amplitude will result in brightness changes on the ultrasound image on the display, giving rise to the terms **hyperechoic** (increased scattering, brighter) and **hypoechoic** (decreased scattering, darker), and **anechoic** (no scattering, black appearance).

At the opposite extreme from the large specular reflectors are the very small reflectors whose dimensions are much less than the ultrasonic wavelength. Such reflectors also produce scattering, and are termed **Rayleigh scatterers**. This category most notably includes red blood cells, and the scattering that results from these gives rise to the echo signals from

blood for Doppler and color flow imaging. Scattering from Rayleigh scatterers increases exponentially (to the fourth power) as frequency is increased.

Attenuation and Ultrasonic Imaging

As ultrasound travels through tissue, the amplitude and intensity of the signal decreases as a function of distance. This is known as **attenuation**, and is due to several mechanisms. The first mechanism is one in which acoustic energy is converted into another form of energy, principally heat; this is known as *absorption*. The second mechanism involves redirection of beam energy, by a number of different processes including *scattering*, *reflection*, *refraction*, *diffraction*, and *divergence* (the latter two processes result in a spreading of the sound beam). Scattering and reflection (and also refraction) were discussed above; while both play an essential role in diagnostic medical imaging, each process also reduces the intensity of ultrasound energy transmitted distally, thereby attenuating the transmitted signal. The third mechanism involves interaction between sound waves, known as *interference*. Wave interference occurs when two waves meet. It can be constructive or destructive, depending upon whether the two waves are in phase or out of phase. When in phase (constructive), an additive effect is produced, increasing amplitude; when out of phase (destructive), the waves can effectively cancel each other out. The degree of attenuation can be given as an *attenuation coefficient* (α) in decibels per centimeter (dB/cm), representing the reduction in signal amplitude or intensity as a function of distance. The amount of attenuation, as measured in decibels, can be calculated by the equation: Attenuation (dB) = α × distance (cm). The attenuation coefficient varies with the type of medium through which the ultrasound is transmitted (Table 1.1C). As can be seen, there is little attenuation in blood, but significant attenuation in bone. Attenuation in muscle is twice that of other tissues such as liver. Another important determinant of attenuation is the frequency of the ultrasound beam. In most cases, attenuation increases approximately linearly with frequency: the higher the frequency, the greater the attenuation (Fig. 1.7).

However, as will be seen with much of ultrasound, there are tradeoffs. In this particular case, the tradeoff is depth. While higher frequencies provide enhanced spatial resolution, in soft tissue they are attenuated much more rapidly than lower frequencies, hence the depth of penetration is much less, and so the higher frequencies are not as useful for visualizing deeper structures. This is why higher frequency, higher resolution transthoracic imaging is much more feasible in pediatric compared to adult patients. It is also one of the reasons that TEE provides superior imaging compared to transthoracic imaging in larger patients: the proximity of the esophagus to the heart significantly reduces attenuation and enables the use of higher frequency ultrasonic imaging.

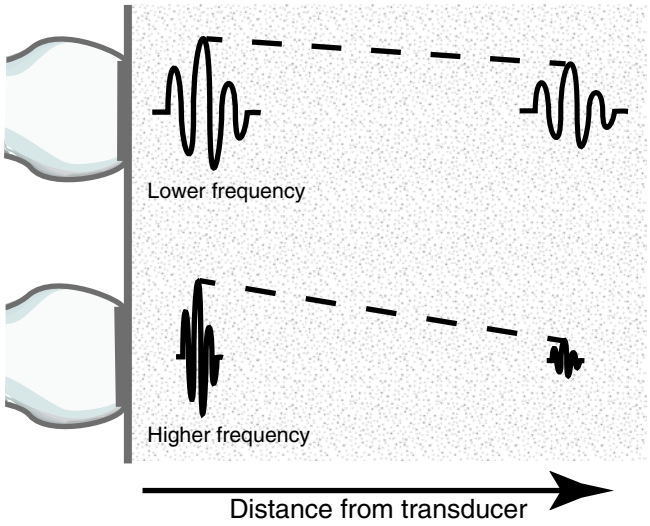

Fig. 1.7 Attenuation of ultrasound in parenchyma. As an ultrasound pulse travels through tissue, its amplitude and intensity decrease as a function of distance from the transducer. This is known as attenuation. Higher frequency sound waves are attenuated much more rapidly than lower frequencies

Important Principles of Echocardiographic Image Formation

At first glance, the basic premise behind 2D imaging in echocardiography seems relatively straightforward. Using the pulse-echo principle discussed above, an ultrasound pulse is emitted as a well-directed beam, and reflected echo signals are collected from the beam line. If this is continued while the ultrasound beam is swept in an arc (sector), a 2D image can be constructed, using echo arrival times and beam axis location to determine the precise location of reflectors within the sector (Fig. 1.8).

However, the actual process by which reflected ultrasound signals are converted into real-time, 2D echocardiographic images is deceptively complex, requiring sophisticated and technologically intricate hardware, along with highly advanced and powerful computing and digital signal processing capabilities. A number of different steps are involved: generation of high quality and well-directed ultrasound pulses, reception and digitization of the returning signals, multilayered digital signal processing, and conversion of these signals to a real-time 2D image of sufficient medical diagnostic quality (while at the same allowing operator manipulation and pre/post processing of the images). Moreover, for echocardiography and TEE the same process must be repeated rapidly and continuously in order to display the real time motion of the heart.

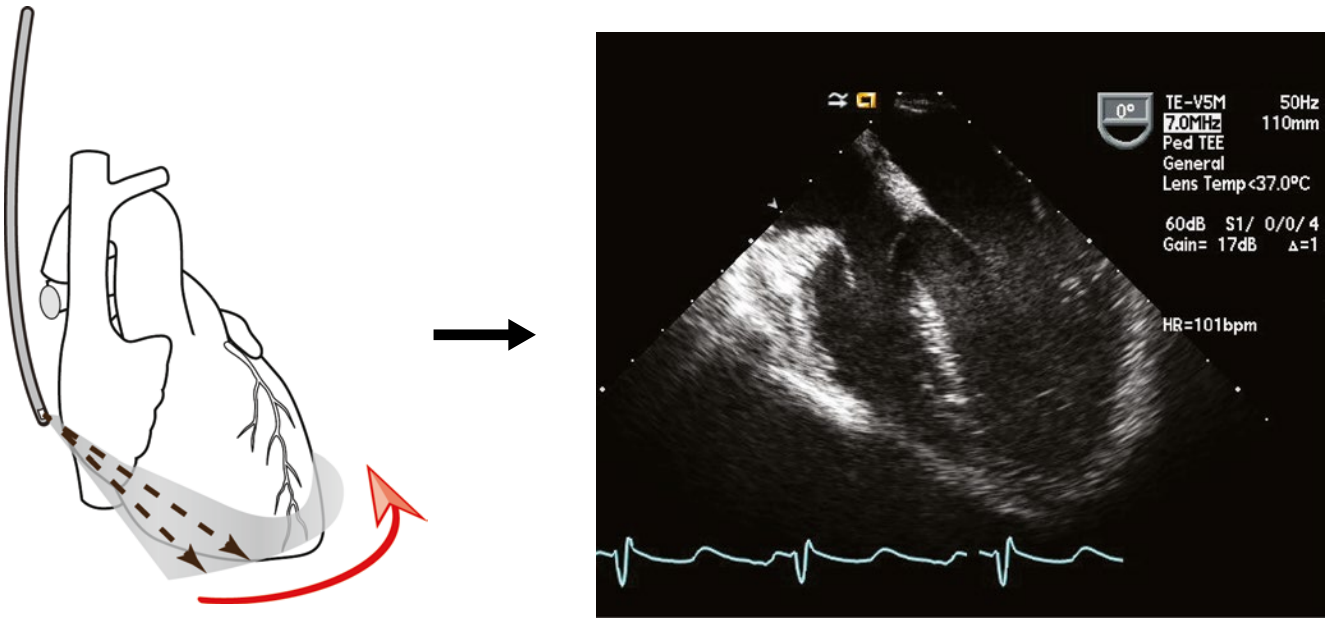

Fig. 1.8 Production of an ultrasound (echocardiographic) image. A pulse of ultrasound is transmitted in a well defined beam, and the transducer "listens" while echoes are received from the same beam path. These echoes appear as *dots* (brightness) corresponding to signal amplitude. During 2D imaging, the beam is swept across a sector (*red arrow*), and displaying all the beams along this sector results in a two-dimensional (B-mode) image. In this example, a transesophageal transducer is shown, but the same process occurs with transthoracic echocardiography

The sections that follow discuss the process by which ultrasound pulse generation leads to image formation, specifically as pertains to echocardiography. For simplicity's sake, the discussion will first cover basic ultrasound beam forming principles utilizing single element transducers. These principles will then be applied to array transducers, which form the basis for modern day echocardiography, including TEE.

Transducers

The first step in ultrasound imaging requires the creation and transmission of an appropriate sound wave; this is accomplished by the use of a **transducer**. Technically, the term transducer refers to any device that is used to convert one form of energy into another. The ultrasonic transducer converts electrical energy to mechanical (acoustic) energy in the form of sound waves that are then transmitted into the medium. When reflected sound waves return, the reverse process occurs: the transducer receives the acoustic energy and converts it into electrical signals for processing. Transducers in medical ultrasound achieve this conversion by the *piezoelectric* (PZE) effect. The PZE effect is a special property seen with certain types of crystals (quartz, ceramics, etc.). When an electrical signal is applied to such a crystal, it vibrates at a natural resonant frequency, sending a sound wave into the medium. Conversely, acoustic energy received by the crystal produces mechanical pressure or stress, which then causes the crystal to generate an electrical charge that can be amplified, yielding a useful electrical signal. Thus PZE transducers can serve as both detectors and transmitters of ultrasound. As noted previously, the signals must be appropriate for imaging of tissues in the human body—wavelengths must be no more than 1–2 mm, which means sound frequencies must be in the *millions* of Hertz. While several PZE crystals found in nature (e.g. quartz) have been used for ultrasonography, most present day ultrasound transducers utilize man-made PZE ceramic (such as lead zirconate titanate, also known as PZT) and composite ceramic elements. When excited, these PZE elements can produce the very high frequencies required for diagnostic medical imaging. A PZE transducer operates best at its natural resonance frequency, which corresponds to the crystal (element) thickness; however newer composite elements have wide frequency bandwidths and can operate at different frequencies, enabling generation of multiple frequencies from one transducer. In these instances, the native frequency, which usually represents the midpoint of the frequency distribution, is termed the "center" or "central carrier" frequency.

However, a transducer is not simply a housing surrounding a PZE element or collection of elements (see arrays below). While the PZE element serves as the most important component of an ultrasound transducer, a number of other essential components also reside in the transducer. These include backing (damping) material, electrodes, an insulating cover, housing, matching layer, and acoustic lens (in some transducers) (Fig. 1.9). The matching layer, which covers and attaches to the PZE element, is very important

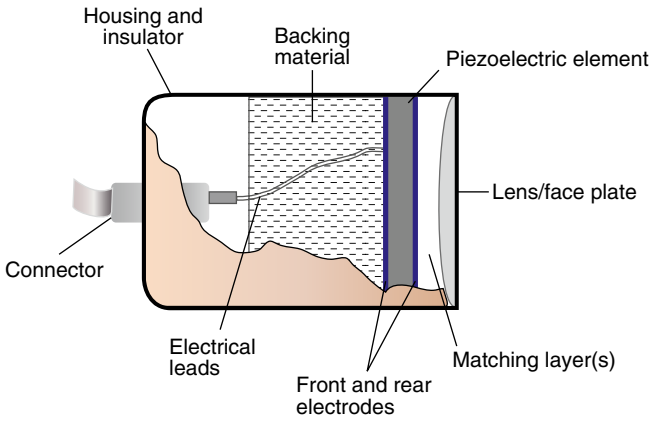

Fig. 1.9 Diagram of a single element transducer. The various components of the transducer are seen. In this example, there is a large, single piezoelectric crystal. For an array transducer, instead of a large single element, multiple elements would be laid in a single row, each with its own electrical connector. However the other parts of the transducer would be analogous to the single element transducer

because of the significant impedance mismatch that exists between the PZE element and surface (skin or esophagus). The matching layer contains an acoustic impedance intermediate between the two surfaces; this helps to match impedances from one surface to the other, allowing for efficient sound transmission between transducer element and soft tissue. In some transducers, multiple matching layers are used to facilitate transmission of a range of ultrasound frequencies. Also, newer composite PZE elements have acoustic impedances much closer to that of soft tissue.

The backing (damping) material also serves an important role. Pulse-echo ultrasound involves the transmission of a short pulse of sound, followed by a period in which the transducer "listens" for the returning echoes. As it turns out, for ultrasound imaging the transducer spends only a tiny fraction of time actually transmitting sound—this is known as the *duty factor*, and typically comprises less than 1 % of the total time. The rest of the time is spent listening for returning echoes. For this to occur, the transducer can emit only a very short pulse of acoustic energy, usually a small number of cycles in length. To produce these, short bursts of electrical energy cause the PZE element to vibrate or "ring", which generates the acoustic pulse. The length of the pulse train, also known as *pulse duration* or *spatial pulse length*, is truncated by *damping* the duration of the vibration as quickly as possible, and the backing material plays an important role here. An important point regarding pulse duration is that short pulses are desirable to optimize axial resolution, as will be discussed below. The typical pulse length is 1–3 cycles in length. Of note, a shorter pulse is a less "pure" tone, and contains a wider range of frequencies, also known as having a broader bandwidth (Fig. 1.10). This range of frequencies encompasses the labeled operating (center) frequency, which represents the midpoint of the frequency distribution. Wide bandwidth associated with short pulse duration is more desirable for imaging applications; narrower frequency bandwidth associated with longer pulse duration is more useful for pulsed Doppler applications.

Transducer Beam Formation and Geometry

When sound waves originate from a single, small point source whose size is similar to the wavelengths it produces (such as a bell), the waves radiate outward in all directions (Fig. 1.11a). However this results in an unfocused signal, unsuitable for medical imaging in which a directed, focused ultrasound beam becomes considerably more important. Diagnostic medical ultrasound transducers are designed to direct ultrasound pulses in a specific direction. A single element ultrasound source of large dimension (for example, a transducer face much larger than the wavelength of sound emanating from it) can produce equally spaced, linear wavefronts (Fig. 1.11b) also known as *planar wavefronts* [10]. Conceptually, these planar wavefronts can be described as a collection of multiple individual point sources, also known as *Huygen sources*, and the wavelets arising from these sources are known as *Huygen wavelets* [1]. Interference among wavelets results in the large planar waveform (Fig. 1.11c).

One of the important aspects of ultrasound beam formation concerns the geometry of the beam and its impact upon imaging. With a single element, unfocused ultrasound transducer, the individual wavelets from a transducer form a near parallel beam wave front, as noted in Fig. 1.11c. Two important zones develop in this beam. The first distance is the *near field*, or *Fresnel zone*. This area is characterized by many regions of constructive and destructive interference, leading to fluctuations in intensity. In this zone, the beam remains well collimated for a certain distance, and even narrows slightly (Fig. 1.12). Beyond the near field, the beam diverges, and some energy escapes along the periphery of the beam; this is known as the *far field* or *Fraunhofer zone* (Fig. 1.12). Fresnel (near-field) length is directly proportional to aperture of the transducer element and inversely proportional to transducer frequency, as given by the equation:

$$D_{Fresnel} = \frac{d^2}{4\lambda} \tag{1.4}$$

$D_{Fresnel}$ = Fresnel (near field) length
d = diameter, or aperture, of the transducer
λ = ultrasound wavelength

The importance of these two zones lies in the fact that lateral resolution is best before divergence of the beam, hence the best imaging and spatial detail are obtained within the Fresnel zone, or near-field. From Eq. 1.4, it becomes

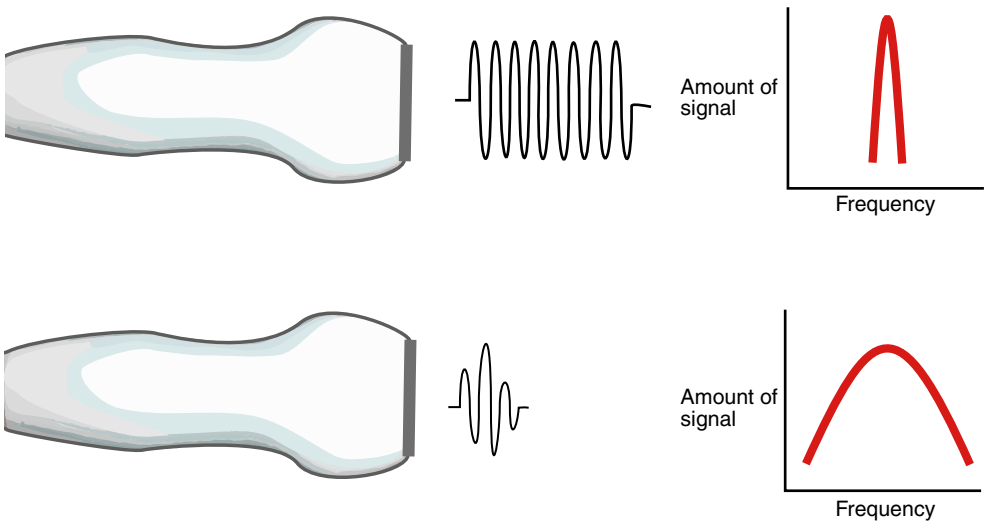

Fig. 1.10 Spatial pulse length. The top pulse has undergone less damping; therefore it has a longer duration, or spatial pulse length, and a purer "tone" with most of the sound at or near a certain frequency. Contrast this with the bottom pulse, which has undergone excellent damping that reduces the spatial pulse length. This type of pulse is characterized by a large frequency bandwidth

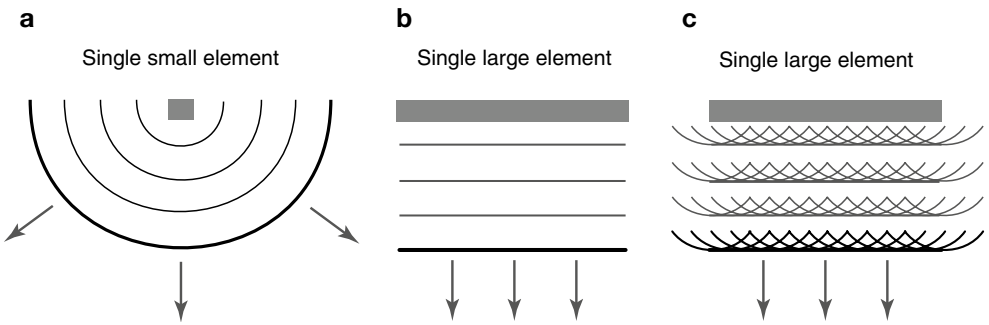

Fig. 1.11 Sound wave geometry. (**a**) A single small element has a size similar to the wavelength it produces. Sound from this element radiates in all directions. (**b**) The single element is much larger than the sound wavelengths it produces, resulting in equally spaced, planar wavefronts. These planar wavefronts can be thought of as a collection of individual point sources, each with its own wavelet. These are known as *Huygen wavelets* (**c**)

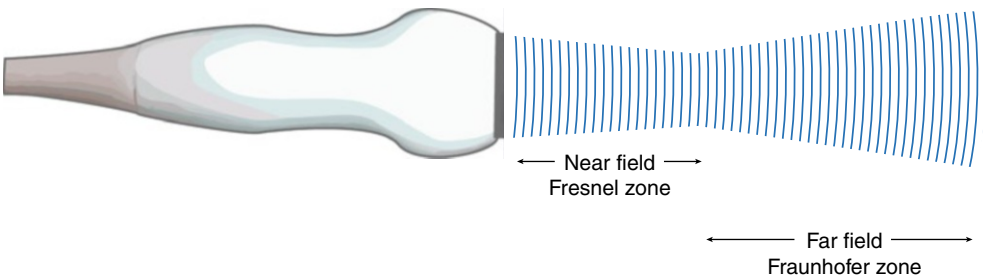

Fig. 1.12 Sound beam pattern from a single element, unfocused transducer. The near field is known as the *Fresnel zone*, the far field is known as the *Fraunhofer zone*. Note that the sound beam is well collimated in the near field and diverges in the far field

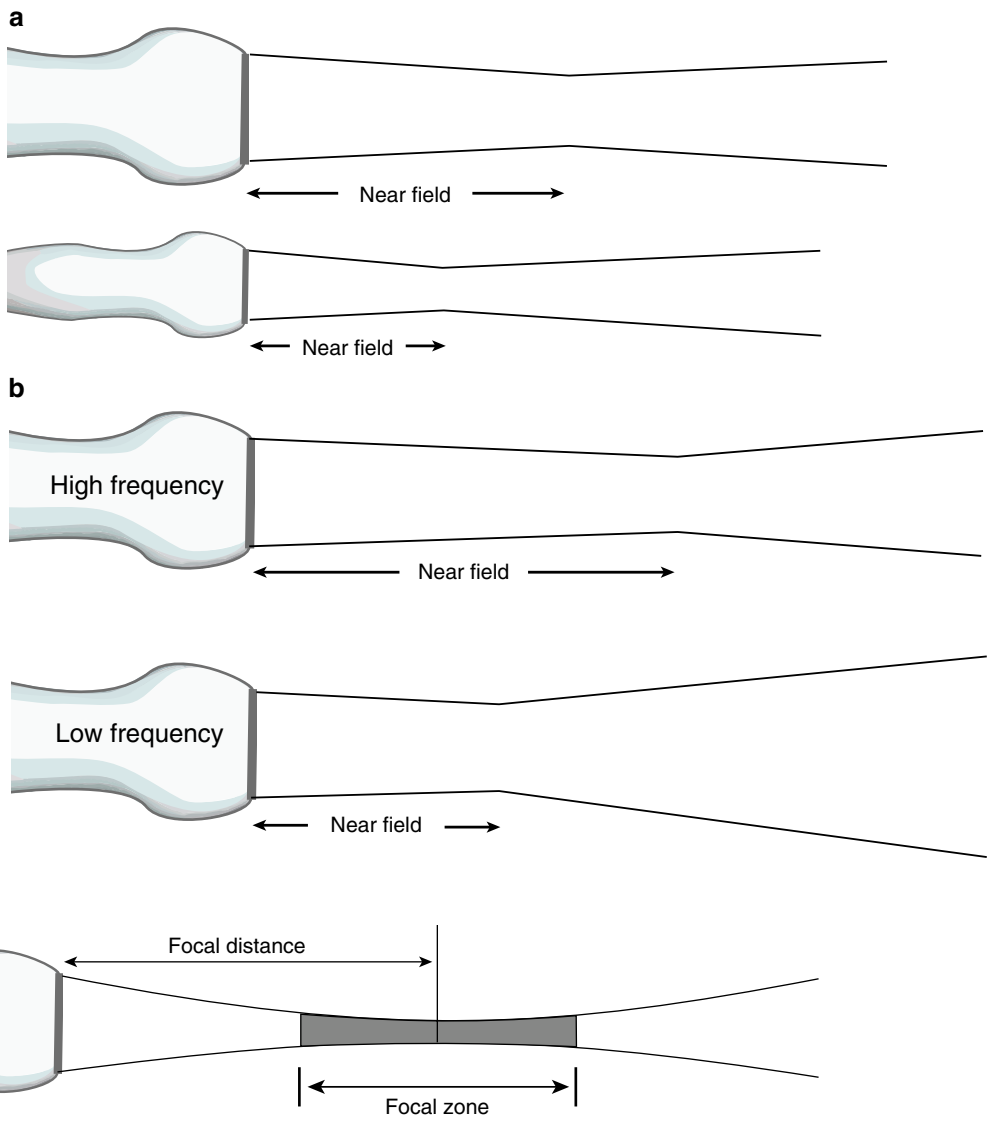

Fig. 1.13 Effect of transducer frequency and diameter on near field length. (**a**) Both transducers have the same frequency but the larger diameter transducer has a longer near field length, and less beam divergence. (**b**) Both transducers have the same diameter, but the transducer with the higher frequency has the longer near field length and less beam divergence

Fig. 1.14 Beam pattern for a focused transducer. The beam is narrowest at the focal distance, hence the best lateral resolution is within the focal zone. Focusing can either be done externally (e.g. acoustic lens) for a single element transducer or, in the case of an array transducer, focusing can be performed electronically and dynamically

apparent that a larger transducer diameter as well as higher frequencies (leading to shorter wavelengths) will increase the near field length and maximize image quality (Fig. 1.13). These have an immediate impact on lateral resolution.

The above considerations of frequency and transducer diameter were discussed in the context of a single element, unfocused transducer. It is clear that—even without beam focusing—it is desirable to perform imaging in the near field. However there is another very important aspect of beam geometry: that of *focusing* the beam, which has the effect of narrowing the beam profile. The narrowest portion of this beam is the *focal distance*, and the *focal zone* corresponds to the region over which the width of the beam is less than two times the beam width at the focal distance (Fig. 1.14). This is the area in which ultrasound intensity is highest, and also where the lateral resolution is best; whenever possible, imaging of key structures should be performed within this zone. As will be discussed below, a focused, narrow beam is desirable for 2D imaging. With single element transducers, this is performed by utilizing a curved PZE element or acoustic lens to focus and narrow the beam width; however in such cases the focal distance is generally fixed. Nonetheless in the past these focused, single element transducers formed the basis of the early mechanical sector echocardiography platforms. Obviously the ability to change a transmit focus dynamically would enhance the imaging capabilities of an ultrasound platform. The advent of array technology marked a significant advance in the field of echocardiography: variable beam

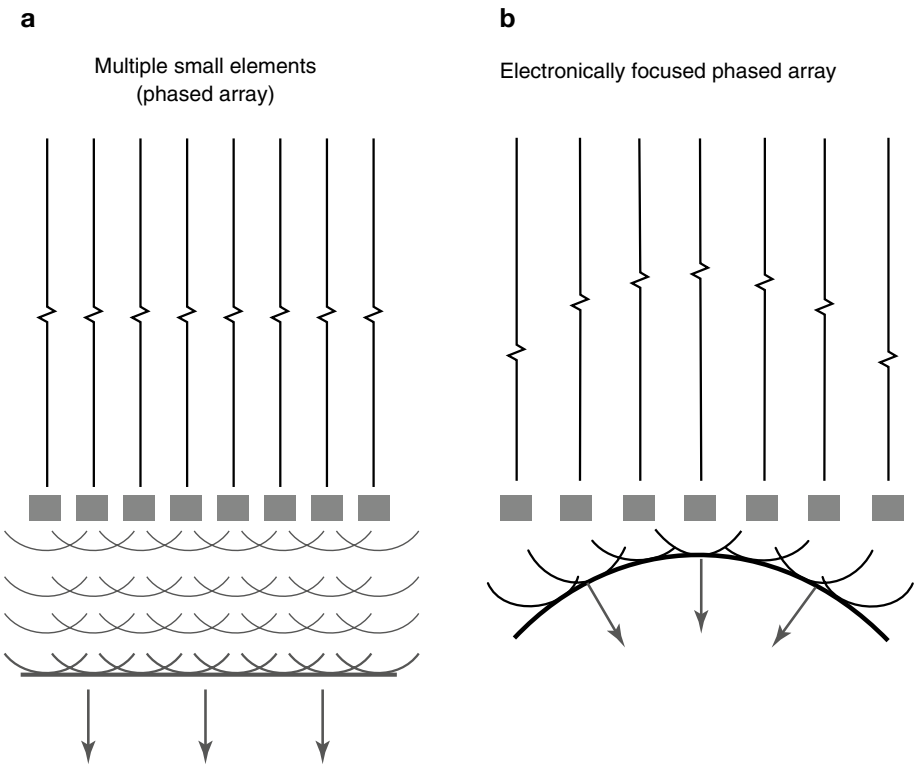

Fig. 1.15 Phased array transducer. When all elements are stimulated simultaneously, the waves from the individual elements act as Huygen point sources, merging to produce a large planar wavefront (**a**). With an array transducer, the beam can be focused by introducing time delays to the separate elements (**b**), producing beam geometry analogous to that obtained by an acoustic lens

focusing and beam shaping became a reality, adding a great deal of flexibility and versatility to echocardiographic imaging. Array technology is discussed in the next section.

Arrays

The foundation of current ultrasound transducer technology, particularly that used in echocardiography, is built upon the concept of transducer **arrays**. Rather than a single element, an array consists of a group of closely spaced PZE elements, each with its own electrical connection to the ultrasound machine. This enables the array elements to be excited individually or in groups. The resultant sound beam emitted by the transducer results from a summation of the sound beams produced by the individual elements. The wave from an individual element (which is quite small, often less than half a wavelength) is by itself broad and unfocused. However when a group of elements transmits simultaneously, there is reinforcement (constructive interference) of the waves along the beam direction, and cancellation (destructive interference) of the waves in other directions, yielding a more well-defined, planar ultrasound beam (Fig. 1.15a). The whole concept of arrays is based upon Huygens' principle, in which a large ultrasound beam wavefront can be divided into a large number of point sources (Huygen sources) from which small diverging waves (Huygen wavelets) merge to form a planar wavefront [1]. The resultant beam can also be focused electronically by introducing time delays to the separate elements, in a manner essentially the same as using a focusing lens or curved PZE element (Fig. 1.15b). Electronic beam steering can occur, in which beams can be swept across an imaged field without any mechanical motion in the transducer (unlike the older mechanical sector transducers). Moreover the focal distance is not fixed but dynamic, and can be adjusted by the operator. Furthermore, multiple transmit focal zones can be utilized to increase the focal zone of an instrument, thereby improving image quality throughout the sector (however this requires extra "pulses" and can result in a lower image frame rate). Thus the array transducer provides a tremendous amount of flexibility for imaging.

There are a number of different types of arrays available for ultrasonic imaging (linear, curvilinear, annular), but the **phased array** transducer is generally the one used for 2D transthoracic and transesophageal echocardiography. This type of array is smaller than linear and curvilinear arrays, thereby providing a transducer "footprint" that allows the transducers to be used with the smaller windows available for transthoracic (particularly pediatric) and transesophageal imaging. The number of PZE elements in a transthoracic phased array probe generally ranges between 64 and 256 (or more) elements. One of the important distinguishing characteristics of phased array transducers is that—unlike linear and curvilinear arrays—*all* elements of the phased array are excited during the production of one transmitted beam line (Fig. 1.16). The direction of the beam is steered electronically

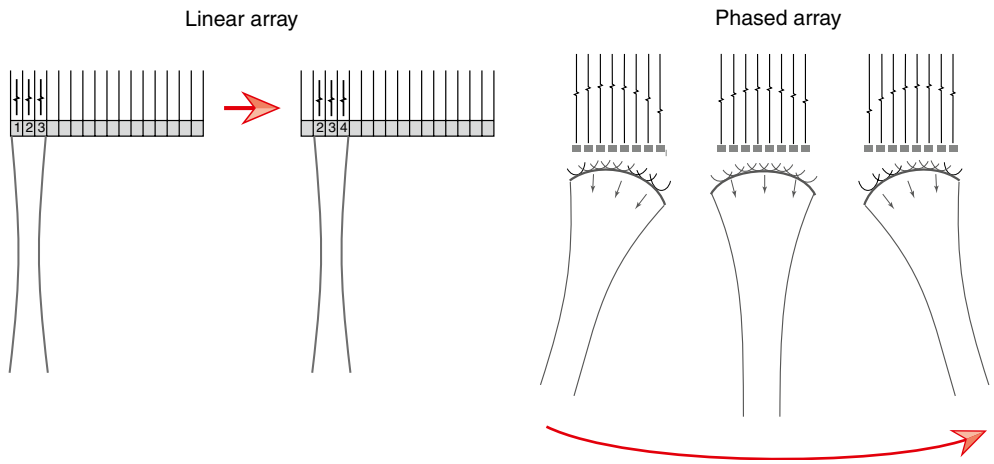

Fig. 1.16 Linear vs. phased array transducer. In the linear array, small groups of elements are stimulated to produce one beam line. Once the returning signals are received, a second adjacent group of elements is stimulated to produce the second beam line. This process continues sequentially down the length of the transducer. Not all elements are stimulated at one time. In contrast, the phased array transducer has a smaller footprint, and all elements are utilized to produce and steer every beam electronically. By varying the timing of pulses to the elements, sequential beam lines are generated and swept in an arc (*red arrow* under the right diagram)

by varying the timing sequence of excitation pulses; the term *phasing* describes the control of the timing of PZE element excitation in order to steer and focus the ultrasound beam. In this manner, timing sequence alterations allow successive beam lines to be generated (Fig. 1.16). Therefore in phased array transducers, the beam can be electronically swept in an arc, providing a wide field of view despite the relatively small footprint. In addition, the direction of echo reception ("listening") can be varied electronically. Returning echo signals from reflectors along each scan line are received by all the elements in the phased array; because of slightly different distances from a reflector to the individual elements, the returning signals will not be in phase and therefore electronic receive focusing must be performed to bring them back into phase to prevent destructive interference of returning signals. This is done by applying time delays to the individual element returning signals, analogous to the time delays used for transmission. In this way, the signals from the individual elements will be in phase when summed together to produce a single signal for each reflector. Receive focusing is adjusted dynamically and automatically by the ultrasound machine in order to compensate for different reflector depths.

An essential component of modern ultrasound systems that use array transducers is the *beam former*. This component of the system provides pulse-delay sequences to individual elements to achieve transmit focusing. In addition, it controls beam direction and dynamic focusing of received echoes, as well as other signal processing. It is located on the ultrasound system and electronically connected to the individual transducer PZE elements. Traditionally, beam formers have been analog, but most ultrasound manufacturers now utilize digital beam formers.

A newer type of array, the **matrix array**, has been developed for real-time three-dimensional (3D) transthoracic and transesophageal echocardiography. This consists of more than 2,500–3,000 elements laid out in a two-dimensional square array slightly larger than 50×50 elements [11] (Fig. 1.17). Analogous to 2D phased array, all elements in the matrix array are active during beam forming. Because of the large number of elements the process of beam forming is divided into two areas: (1) pre-beam forming by custom made integrated circuits within the transducer handle, and (2) traditional digital beam forming within the ultrasound system [12, 13]. The most important aspect of 3D beam forming is the ability to steer in both lateral and elevational directions, thereby providing a pyramidal 3D dataset. Three-dimensional technology and imaging (specifically in the context of 3D TEE) is discussed in Chap. 2 as well as Chaps. 19 and 20.

Transesophageal Echocardiographic Transducers

All current 2D TEE probes utilize phased array technology, usually in a row of 64 elements for current adult multiplane TEE probes (some pediatric probes have fewer elements—see Chap. 2). TEE probes are constructed similar to standard transthoracic transducers: they have a collection of piezoelectric elements, backing material, electrical connector, housing, and matching layer. In addition an acoustic lens is added below the matching layer to improve focusing. The important difference is that all the components, as well as the housing, are much smaller, and special cabling is required for anterior/posterior flexion (anteflexion/retroflexion) and (in some probes) right/left rotation (Fig. 1.18). In addition, with multiplane TEE probes the piezoelectric elements can be electronically or mechanically rotated by cables (Fig. 1.18), a rotor, or even a small motor housed in the probe tip, and attached to the elements, allowing the tomographic

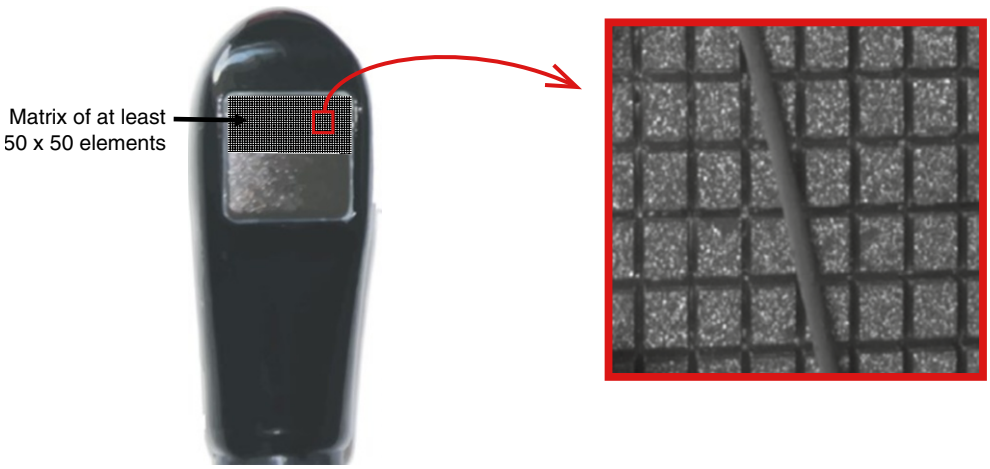

Fig. 1.17 Matrix array three-dimensional transesophageal echocardiography probe. The transducer is a square matrix of at least 50×50 elements (2,500–3,000 total elements). A pyramidal three dimensional dataset is produced from this. Each individual element is just larger than the diameter of a human hair (Photograph on the right, courtesy of Philips Medical Systems, Andover, MA)

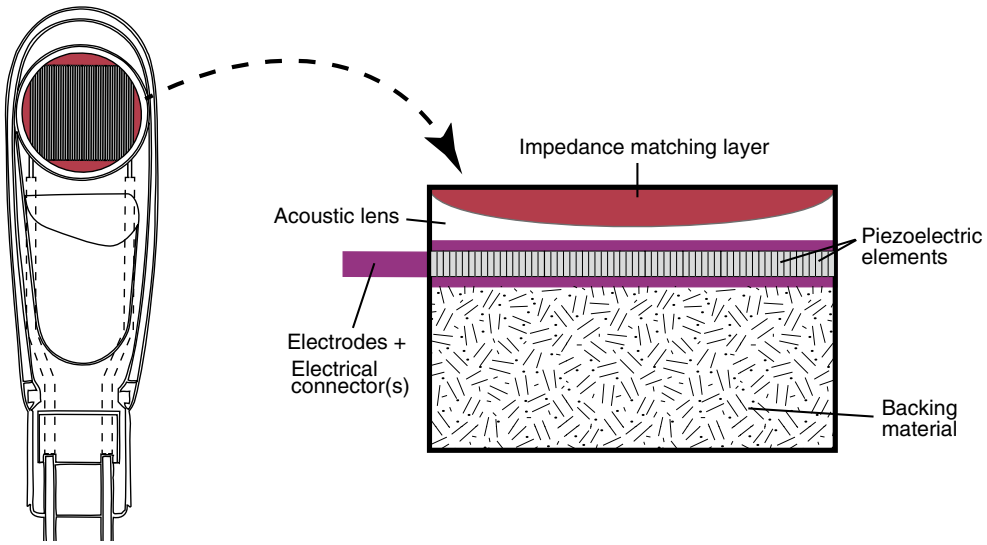

Fig. 1.18 Internal layout of model of a multiplane transesophageal echocardiographic (TEE) probe. The probe utilizes phased array technology; the transducer containing the array of elements is located at the probe tip and can be rotated between 0° and 180° by either an electronic or mechanical control in the probe handle. The principal transducer components (right diagram) are similar to those found in a transthoracic probe. Rotation of the transducer can be achieved using cables (as shown on left), a central rotor, or a small motor housed in the probe tip. The TEE probe itself is similar to a gastroscope, with controls in the probe handle (not shown, see Chap. 2) for tip movement anteriorly/posteriorly and right/left (Note: in some pediatric probes, the right/left control has been omitted)

plane to be varied between 0° and 180°. More detailed discussion of TEE technology is given in Chap. 2.

Pulse Repetition Frequency

Ultimately, one of the major factors determining the quality of information obtained by ultrasonic imaging, particularly that of echocardiography, is the speed of sound in tissue. This generally fixed value imposes certain restrictions on pulse-echo imaging as well as pulsed wave and color flow Doppler evaluation—specifically, it places limits on the at maximum rate at which ultrasound pulses can be emitted. A transducer cannot send and receive ultrasound pulses at the same time; once a pulse has been sent, the transducer must wait a certain period of time for returning echoes, with the round-trip time depending upon the depth of the reflector. The equation relating distance to time is:

$$T = \frac{2D}{c} \tag{1.5}$$

T = Time it takes a pulse of sound to travel to a reflector, and for an echo to return to the transducer (round-trip time)
D = Distance from the transducer
c = Speed of sound in the medium

Given a speed of sound in tissue of 1,540 m/s, the round-trip time is equivalent to **13 μs/cm of depth**, hence the time needed to collect all returning echoes from a scan line of depth D is equal to 13 μs×D. This time is also known as the *pulse repetition period*, and the reciprocal of this is known as

the **pulse repetition frequency**, or **PRF**. This is a very important concept in echocardiography, because *the maximum PRF represents the maximum number of times a pulse can be emitted per second*. PRF will vary with the speed of sound in different media. However, assuming a constant speed of sound (as is seen with soft tissues in the human body), *PRF is totally dependent upon depth*: *the greater the depth*, *the less the maximum PRF*. In the soft tissues of the human body, maximum PRF calculates to **77,000/s/cm of depth** (roughly equivalent to 1 divided by 13 μs). Typically, PRF is expressed in units of Hz or kiloHz (kHz). For example, for a depth of 10 cm, the maximum PRF for one scan line will be 77,000 ÷ 10 cm, or 7,700/s (also given as 7,700 Hz or 7.7 kHz). In other words, for this particular depth, the maximum number of times a sound pulse can be transmitted and received is 7,700 times/s. As will be seen, the PRF plays an important role in determining the limits of temporal resolution for both 2D imaging as well as the maximum velocities measurable by pulsed wave and color flow Doppler.

Generation of an Echocardiographic Image

The pulse-echo principle serves as the fundamental concept underlying ultrasonic and echocardiographic imaging. This principle is based upon a predictable and reliable constant: the speed of sound in the soft tissues of the human body, which, as noted above, is 1,540 m/s. When an acoustic pulse is emitted by a transducer, the time delay between transmission and signal detection can be used to calculate distance from the transducer, by rearranging Eq. 1.5 above:

$$D = \frac{cT}{2} \tag{1.6}$$

Thus for ultrasonography and echocardiography, it is axiomatic that *time equals distance*: the transmit/receive time (divided by 2) serves as the measurement for distance. Returning echoes along a scan line will have their various depths registered as a function of their time of return, as calculated by Eq. 1.6. In addition, these returning echoes will have different amplitudes that correspond to the different reflectors encountered. In the past, the amplitude of returning signals was displayed directly by an oscilloscope (known as "*A-mode*"). However, all modern-day echocardiography platforms convert the amplitude of returning echoes to a corresponding gray scale value for display on a computer monitor—this is known as brightness mode, or "*B-mode*". By plotting these varying brightness points as a function of distance from the transducer, one scan line can be displayed. If successive scan lines are rapidly swept across the object of interest, a 2D image can then be assembled, with echo signal location on the display corresponding to the reflector positions in relation to the transducer (Fig. 1.19). As discussed previously, this scan line sweep

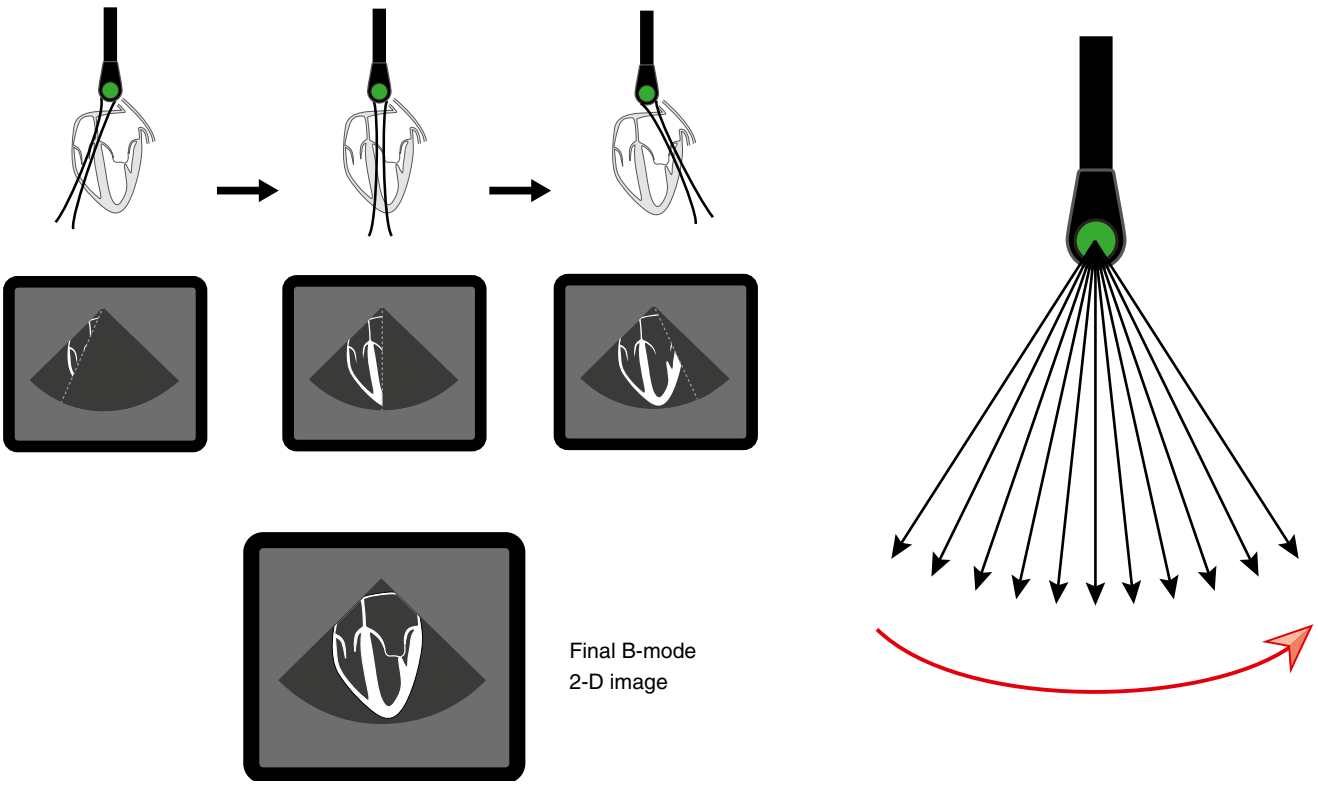

Fig. 1.19 Generation of a two dimensional (2D) echocardiographic image. The returning echo amplitudes from one scan line are converted to pixel gray scale brightness on a computer monitor. This is also known as "B-mode" (for brightness mode). If successive scan lines are obtained and rapidly swept across the sector, a 2D image can be generated (*red arrow* indicates the direction of the scan line sweep). This process must be repeated rapidly in order to depict accurate real-time cardiac motion

is performed electronically with a phased array transducer, using time delay sequences to vary the activation of the individual elements and sequentially "steer" the scan lines. Typically, 100–200 separate scan lines are used for a single 2D image [3]. For echocardiography, this process must be repeated rapidly in order to depict accurate, real-time cardiac motion.

The process whereby the reflected echoes are converted to real-time, 2D echocardiographic images requires highly specialized and advanced technology, as well as sophisticated digital signal processing capabilities. Returning echo signals from reflectors along each scan line are received by all the phased array elements in the transducer; as noted previously, electronic receive focusing is performed to bring returning signals into phase. Analog to digital conversion also occurs during this process. To compensate for different reflector depths, this receive focusing is adjusted dynamically and automatically by the digital beam former. These digital signals are then sent to a receiver in the ultrasound machine, where they undergo a number of preprocessing steps to "condition" the signal; these include signal preamplification and demodulation, as well as operator-adjustable time gain compensation (TGC), noise reduction (known as reject), and dynamic range/compression (that varies contrast). The TGC is a selective form of amplification used to compensate for the weaker, attenuated signals from increased depths. Some of this can be performed by the operator, but modern echocardiography machines now incorporate an adaptive TGC that automatically adjusts the TGC in real-time [3]. The operator-adjusted TGC controls will be discussed in a separate section below.

Once the signals have been amplified and processed, they are sent to a **scan converter**, which is a digital imaging matrix used to store and buffer returning signal information. In the process, the returning echo signal locations are converted from polar to Cartesian coordinates—in other words, angle and depth information are converted to a matrix format for display on a computer monitor. A common setup is a matrix of 512×512 pixels, with each pixel having 8 bits of storage allowing 256 levels of gray scale (though other types of setup are possible) (Fig. 1.20). Location information is

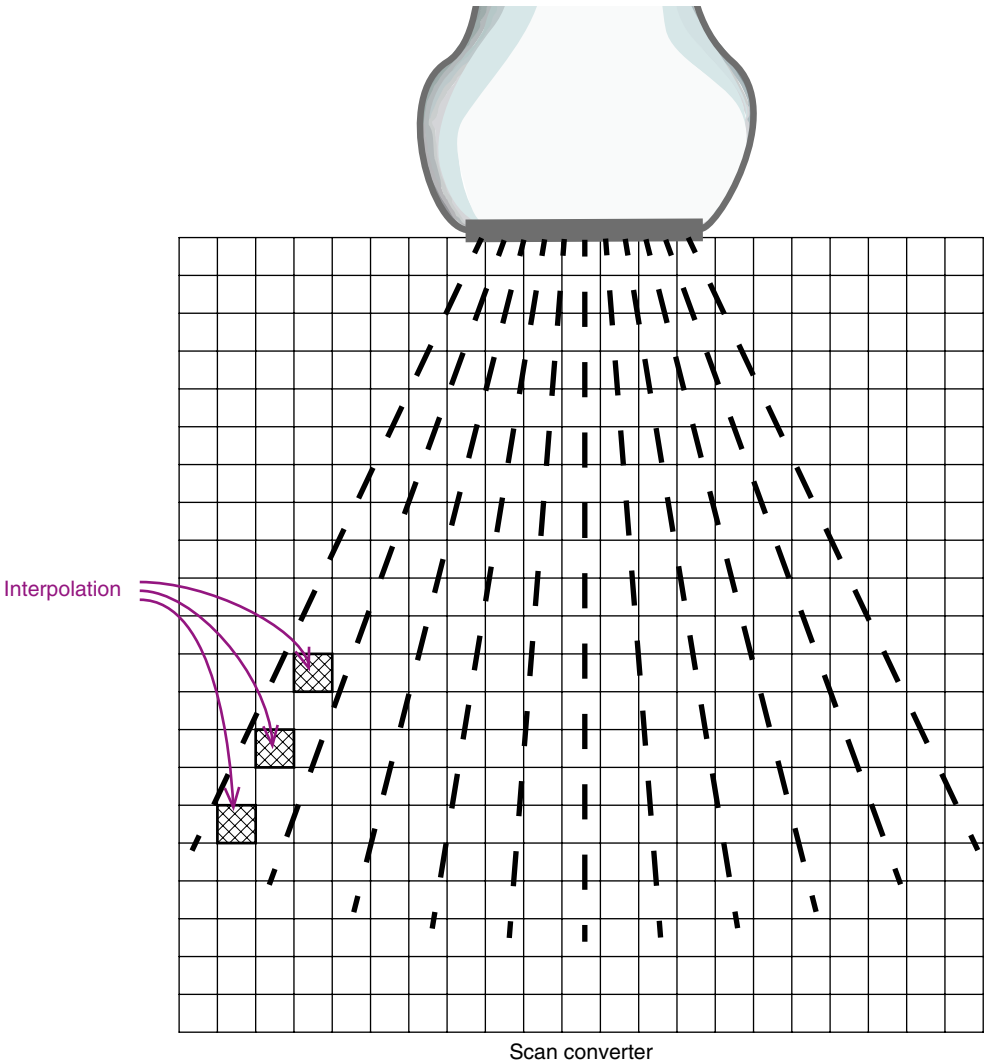

Fig. 1.20 Scan converter. The scan lines are converted from polar to Cartesian coordinates, and the information placed in a scan converter matrix, and used to construct a two dimensional image that can be visualized on a computer monitor. A common setup is a 525×525 pixel matrix, with each pixel having 8 bits of storage allowing 256 levels of gray scale. However, other matrix sizes and bits/pixels are possible. Interpolation is performed for those pixels in which no scan line information is available

obtained from: (a) angle of the scan line in relation to a reference axis, which is parallel to the surface of the array elements; (b) distance from the scan line to the reflector, as calculated from Eq. 1.6 above. These two coordinates are then converted into Cartesian *x* and *y* coordinates, which can then be placed into a large rectangular matrix suitable for pixel mapping on a 2D computer display. What becomes apparent during this conversion process is that, when the scan lines are superimposed upon the matrix, adjacent scan lines will not sample all of the pixels in the matrix. To fill in these areas, a process of *interpolation* is performed in which an averaged signal from nearby pixels is used to fill in the value of the blank (unsampled) pixel (Fig. 1.20).

In the scan converter, image data can be held in memory and continuously updated with new echo data. At the same time, information is continuously read out to a video buffer to provide real-time visualization of the scanned images on a video monitor. Most echocardiography systems now use a large digital computer monitor, generally one based upon liquid crystal display (LCD) technology. Various postprocessing techniques can also be performed on the digital image data stored in the computer memory; these techniques include contrast and edge enhancement, as well as smoothing and B-mode color. For echocardiography, image acquisition, updating, and display must occur in a rapid fashion to portray real-time cardiac motion. Almost all ultrasound systems also have a freeze option that stops image acquisition (still frame) and allows visualization of a single image (for measurements or text labeling), and also a review of short cine loops. This feature is very useful for echocardiography, because it provides the ability to slow down and review rapidly moving images associated with cardiac motion. It also facilitates visualization of the acquired data relative to the phases of the cardiac cycle as displayed by concurrent electrocardiographic monitoring.

Instead of sweeping a B-mode scan line in an arc to obtain a 2D image, a simpler (and less processor-intensive) method can be used to display the B-mode data. If the scan line remains fixed, and instead a continuous recording of the line is made over time, then an *M-mode* tracing is obtained—the M stands for motion (Fig. 1.21). This type of display was the principal form of echocardiography used in the 1970s and early 1980s. Because only one scan line is involved, a high PRF can be used and therefore this mode has excellent temporal resolution. Frame rates of 1,000–2,000 lines/second are possible, significantly increased compared to standard frame rates of 30–120 frames/second for 2D imaging. Axial resolution is also excellent, making M-mode ideal for linear and time measurements. For example, M-mode measurements are very useful for assessment of left ventricular dimensions and function, such as calculation of left ventricular end diastolic dimension and shortening fraction. Since there are published normal ranges and values for M-mode measurements, these measurements serve as an important method of distinguishing normal vs. abnormal cardiac size and function (discussed in Chap. 5). However, M-mode does not provide a real-time 2D display of cardiac anatomy, making interpretation more difficult, and limiting its effectiveness with CHD. Thus M-mode imaging has largely been supplanted by 2D and 3D echocardiography. While still available on modern echocardiography machines, it generally comprises a very small fraction of a total examination.

Image Resolution

Resolution is a term commonly used to describe the quality of an ultrasonic image. With ultrasonic imaging, and specifically with echocardiography, there are three major types of resolution: spatial, contrast, and temporal. These will be discussed below.

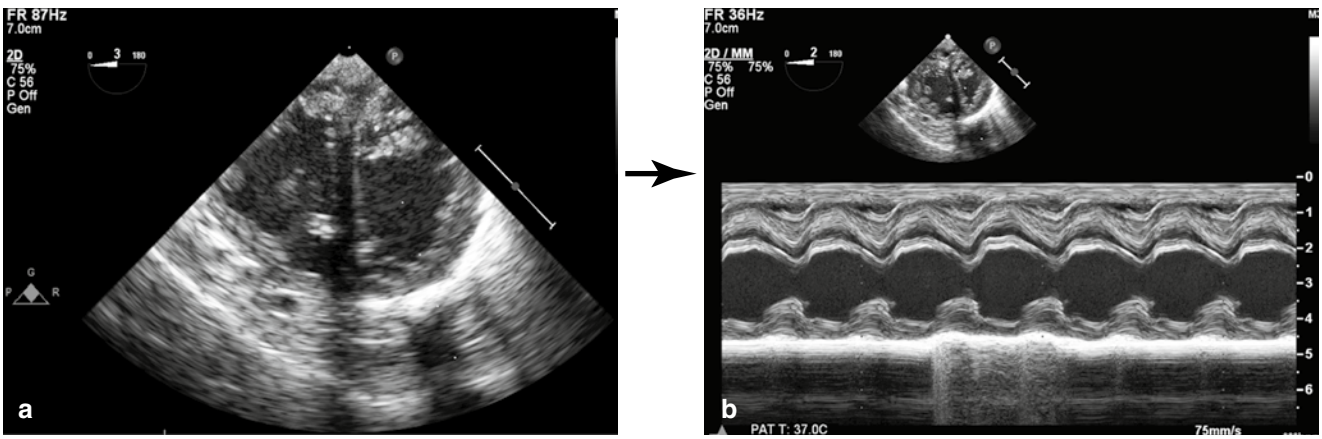

Fig. 1.21 Generation of an M-mode image. In this instance, the two-dimensional image (**a**) is used to guide the placement of the scan line (*dotted line*) for M-mode assessment (**b**). Real-time information is then obtained along the single scan line, plotted as time vs. depth from the transducer. M-mode imaging is characterized by excellent axial and temporal resolution

Spatial Resolution

Spatial resolution refers to the ability to discriminate objects in space, and applies specifically to 2D imaging. It is defined as the ability to distinguish two discrete objects located in close proximity to each other—in other words, the ability to resolve them as separate as opposed to overlapping structures. There are three types of spatial resolution: axial, lateral and elevational, representing the x, y, and z planes of a 2D ultrasonic/echocardiographic image (Fig. 1.22). Axial and lateral resolutions affect the two planes readily seen on a 2D image; elevational resolution refers to the "hidden" plane perpendicular to the other two planes, and not as apparent on 2D imaging. Factors affecting the resolution in each plane are discussed below.

Axial Resolution

Axial resolution describes the ability to discriminate two objects located along the axis of the sound beam (i.e. the scan line). It is determined principally by the transmitted ultrasonic pulse duration. The pulse duration is itself determined by two major factors: the number of cycles in the pulse, and the wave period (which is the inverse of frequency). In order to distinguish two separate objects along the axis of the sound beam, it is necessary that there be a short pulse duration (Fig. 1.10)—specifically, the time gap between the arrival of two pulses from two separate reflectors should be greater than the length (duration) of each pulse. Otherwise, there will be overlap of the two pulses and the two reflectors will not be resolved (Fig. 1.23). To improve axial resolution, the pulse duration should be decreased. This can be achieved by two methods. One is to use a higher frequency transducer, which decreases wavelength and wave period. The other is to improve damping of the "ringing" of the transducer so that each pulse will have fewer cycles. Broad bandwidth, high frequency transducers will provide the best axial resolution

The typical axial resolution for most modern ultrasound systems is between 0.3 and 2.0 mm; a rule of thumb is that the axial resolution of a system is 1.5 times the wavelength of the system. Therefore for a 7.5 MHz transducer, axial resolution is 0.3 mm [14]. In general, axial resolution tends to be the best of all the three dimensions. It is fairly constant with depth, though signal attenuation plays a role with the higher frequency transducers.

Lateral Resolution

Lateral resolution refers to the ability to distinguish two closely spaced reflectors positioned perpendicular to the axis of the ultrasound scan line. This is determined by two factors. The first is *beam width*: if the width of the beam is less than the distance between the two reflectors, then they can be resolved. Otherwise, if the beam is too wide, the images merge together and the two reflectors cannot be resolved (Fig. 1.24). Beam width changes with distance from the transducer; optimal beam width occurs within the near field (Fresnel) zone, prior to beam divergence. A long near field is therefore preferable for ultrasonography and echocardiography, and as noted previously in Eq. 1.4, the depth of the Fresnel zone is equal to $d^2/4\lambda$. Two important observations can be gleaned from this equation. First, lateral resolution can be improved by using a larger transducer aperture (diameter), which extends the depth of focus and lengthens the near field. Second, using a higher transmitted frequency will also extend the length of the near field, thereby improving lateral resolution further along the scan line (Fig. 1.25). However this latter point must be balanced by the greater attenuation of higher frequency sound waves, which can limit the depth of penetration. Focusing a beam (mechanically or electronically) will also enhance lateral

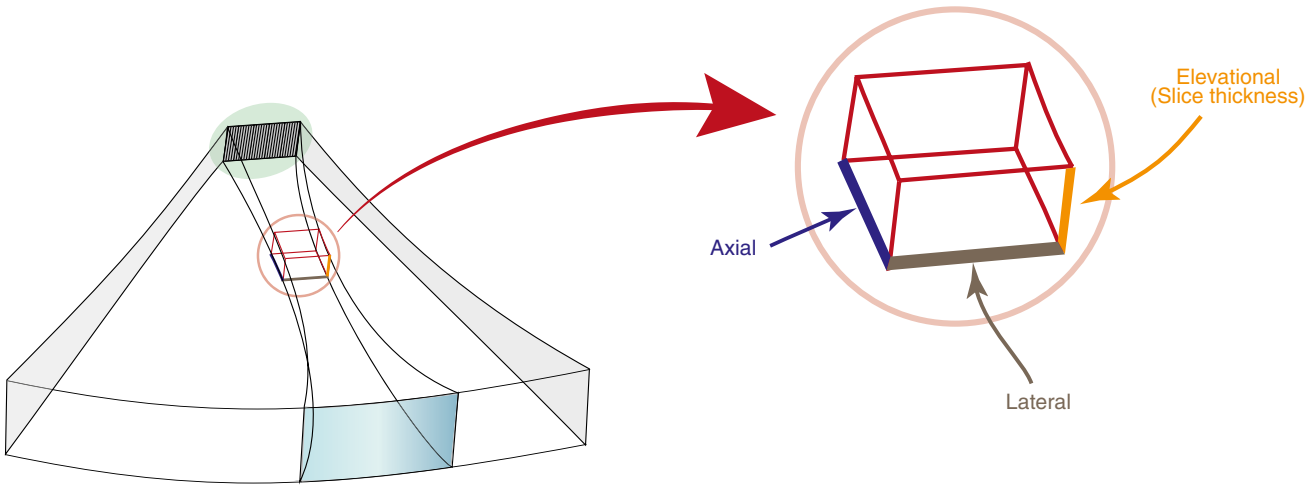

Fig. 1.22 The three spatial resolution planes: axial, lateral, and elevational (slice thickness)

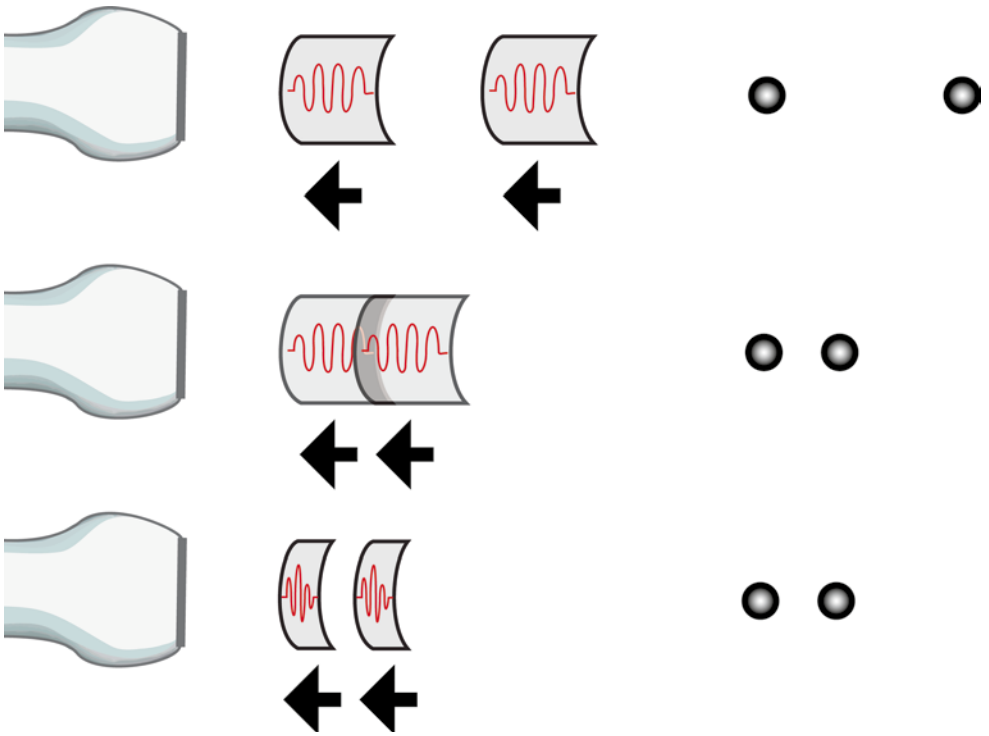

Fig. 1.23 Axial resolution. This diagram illustrates the effect of pulse duration on axial resolution. Each panel shows two pulses from two separate reflectors. In the *top panel*, the pulse duration is longer (which can be due to lower frequency, more cycles/pulse, or both). However because the two reflectors are spaced further apart, the longer pulses are still able to distinguish them as separate objects. In the *middle panel*, the reflectors are closely spaced and the long pulses are no longer able to distinguish the objects as separate; the two pulses overlap and appear to be one on the monitor. In the *bottom panel*, the two reflectors are still closely spaced (as in the *middle panel*) but pulse duration has been shortened by the use of a higher frequency and/or decreased number of cycles/pulse. The shorter pulse duration enables the two objects to be shown as separate objects on the screen, hence axial resolution has been enhanced

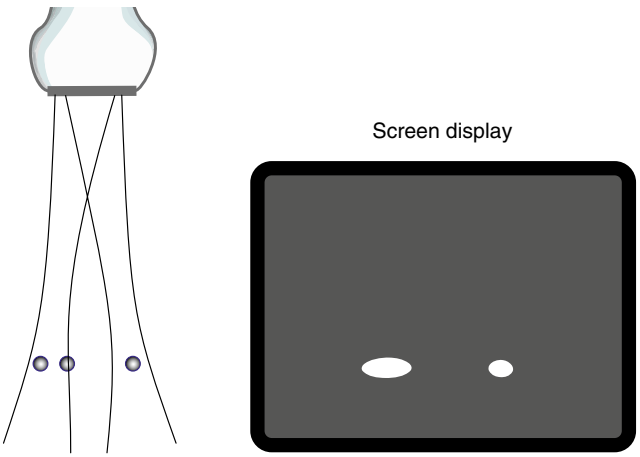

Fig. 1.24 Lateral resolution. This diagram illustrates the effect of beam width on lateral resolution. Two reflectors can be distinguished separately when the beam width is less than the lateral distance between two reflectors. When the beam is wider than this distance, the two objects cannot be resolved as separate reflectors

resolution by narrowing the beam width; the best resolution occurs within the focal zone, where the beam is narrowest (Fig. 1.14). With phased array transducers, dynamic adjusting of the focal zone to the desired depth can be performed to optimize the lateral resolution for that level.

The other important factor affecting lateral resolution is especially pertinent to echocardiography. This involves *line spacing or line density*. As will be discussed in the section on temporal resolution, the frame rates for real-time 2D imaging depend upon the depth of scanning as well as the number of scan lines per imaging sector. To improve frame rates, the number of scan lines can be reduced, with the result being less scanning time required per sector, but increased spacing between scan lines. This can reduce lateral resolution because even with a narrow beam width, if the line spacing is greater than the distance between two closely spaced objects, the objects still might be not be resolved as separate reflectors.

Typically, at a depth of 10 cm, a beam width of approximately 2 mm is achieved (obviously this will be affected by signal frequency and transducer size). Thus lateral resolution tends to be less than axial resolution, and unlike axial resolution, it exhibits depth-dependence. Nonetheless lateral resolution is a major factor determining the quality of ultrasound images. For this reason, modern

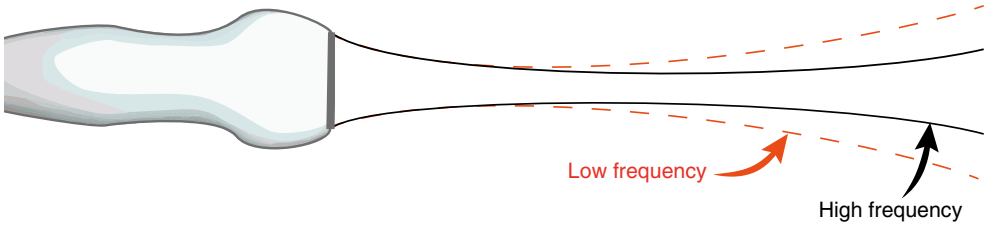

Fig. 1.25 Effect of frequency on near field length and beam width. In this diagram both beams have been focused. However even with a focused beam, using a higher frequency transducer lengthens the focal zone and near field, and there is less divergence in the far field

echocardiography manufacturers attempt to enhanced lateral resolution by utilizing combinations of time-delayed firing and changing beam aperture—available with phased array technology—to optimize focusing at different depths (also known as multiple focal zones). This effectively lengthens the focal zone. However as noted above, it requires multiple pulse sequences, which can reduce temporal resolution.

Elevational Resolution

Contrary to appearances, a 2D tomographic image is not flat. It is in fact a slice, and this slice has a thickness aspect, which is known as the elevational plane with an axis perpendicular to the imaging plane (Fig. 1.22). Similar to lateral resolution, slice thickness depends upon beam size—that is, the size of the beam in the elevational plane. However unlike lateral resolution, in most standard 2D transducers there is no electronic focusing available in this plane; a fixed focal length acoustic lens generally determines beam width in this dimension. Slice thickness is minimal closest to the focal zone, and widens beyond that point. As with lateral resolution, a higher frequency transducer improves the elevational resolution by lengthening the near field. Slice thickness is also determined by the width of the beam in the elevational plane.

What is the importance of elevational resolution? While the elevational plane is not displayed in a conventional 2D image, objects that exist within the slice can overlap with the 2D image being displayed, potentially causing slice thickness artifacts.

Of the three types of resolution, the elevational resolution is usually the worst. In most phased array transducers, elevational slice thickness ranges between 3 mm (near the focal zone) and 10 mm as the beam diverges [15]. While little information is available regarding elevational resolution in TEE transducers, slice thickness artifacts are likely to be minimized due to a several factors: (a) higher frequencies of the transducer; (b) some focusing from the transducer's acoustic lens; (c) reduced transducer depth, usually about 5–10 cm in the vast majority of patients for most TEE views except for the deep transgastric views.

Optimizing Spatial Resolution

From the above discussion it becomes apparent that *the best spatial resolution occurs in the near field and focal zone of the transducer*. Beyond this area, lateral and elevational resolution decrease as the beam diverges. Use of higher frequency transducers improves axial resolution and lengthens the near field, thereby improving lateral and elevational resolution. Focusing of the beam further decreases beam width at the focal zone, thereby improving lateral and elevational resolution. However focusing can increased beam divergence, and lateral/elevational resolution are reduced in the far field. While axial resolution does not change with depth, with greater depths there is reduced penetration of higher frequency ultrasound, thus lower frequencies must sometimes be used for imaging of more distant structures, leading to reduced resolution.

Therefore for echocardiographic 2D imaging, as a rule it is desirable to position the transducer as close as possible to the object of interest, and to use the highest frequency transducer possible. Fortunately these conditions can be achieved with most TEE imaging, as the close proximity between esophagus and heart (from most TEE windows) enables the optimization of all three types of spatial resolution.

Contrast Resolution

Contrast resolution refers to the ability to differentiate between body tissues that have slightly different properties, and therefore different acoustic impedances, using different shades of gray on the display. There are two components to contrast resolution. The first is the intrinsic contrast, and how this is encoded in the stored pixel values in the image memory. Intrinsic contrast depends upon the different tissue interfaces/acoustic impedances, as well as acquisition parameters (beam width, pulse shape) and processing (compression, edge enhancement). It also depends in part on how gray scale is encoded in the process of analog to digital conversion of the amplified voltage signal: the larger the number of bits per pixel, the larger the number of gray scale shades available. Extrinsic contrast translates these pixel values into brightness levels on the monitor, and is dependent upon operator-adjustable contrast and brightness controls. During this process, the *compression* can be adjusted by the operator

to vary the dynamic range of the signal amplitude. Increasing the dynamic range increases the range of gray scale and decreases contrast; decreasing the dynamic range does the opposite. It should be noted that improving the contrast often improves the ability to distinguish structures, thereby enhancing spatial resolution.

Temporal Resolution

Temporal resolution refers to the ability to visualize smooth real-time motion, and is related to image refresh speed, also known as frame rate. Frame rate is dictated by four factors: the speed of sound, sampling depth, the number of separate transducer beam lines used to form an image, and the number of focal zones. The equation relating these variables is given as follows:

$$F = \frac{c}{2DNn} \tag{1.7}$$

F = frame rate
c = speed of sound
D = sampling depth
N = number of sampling lines per frame
n = number of focal zones used to produce one image

Pulse repetition period and PRF play an integral role here. As noted previously, a small time period is required for a pulse to be transmitted and for collection of all echoes emerging from that scan line. The round-trip time per scan line in soft tissue (pulse repetition period) is 13 μs/cm of depth. Therefore for an image sector 10 cm deep (from the transducer), the pulse repetition period per scan line is 130 μs. If the image sector is composed of 100 scan lines, the time for one image equals 13 ms, thus the maximum frame rate is approximately 77 frames/s. This is with a single focal zone; if multiple transmit focal zones are used (advantageous for improving lateral resolution), then frame rate decreases because multiple pulse sequences must be generated per scan line. *What becomes apparent is that frame rate is principally affected by sampling depth and number of scan* (*beam*) *lines*. Deeper scanning depths as well as wider imaging sectors (requiring more scan lines) will appreciably lower frame rates. To improve frame rates, a smaller depth should be used. The number of scan lines can be decreased in one of two ways: (a) decreasing the number of scan lines while maintaining the same size imaging sector (however this increases lateral line spacing, thereby reducing lateral resolution); (b) narrowing the imaging sector while maintaining the same line spacing (which maintains lateral resolution but decreases the field of view) (Fig. 1.26). Of course, any combination of these maneuvers can further improve temporal resolution. In addition, newer technologies are now being employed including parallel processing, which allows more scan lines to be acquired at one time, thereby reducing the total time require to acquire the image.

In the realm of diagnostic medical ultrasound, temporal resolution considerations are especially applicable for echocardiography because of one simple fact: the heart is in constant motion. For visualizing a rapidly moving structure such as the heart, the image must be refreshed a minimum number of times per second to produce the appearance of smooth, real-time cardiac motion; otherwise a "strobe" effect is created and motion no longer appears smooth and can be difficult to interpret. The minimum frame rates needed to present smooth real-time motion will vary depending upon heart rate—the faster the heart rate, the greater the necessary frame rate. While no published standard exists, for visualizing cardiac motion it is generally desirable to have a frame rate that allows for at least 10 samplings (frames) per cardiac cycle; 20–30 frames/cycle will usually provide good temporal resolution. Conversely, when the rate decreases to less than five frames/cardiac cycle, cardiac motion ceases to be smooth and important information can be lost because of the inadequate sampling rate. Thus for a heart rate of 100/min, a frame rate of 50 frames/s will yield 30 frames/cardiac cycle, thereby providing acceptable temporal resolution. However a frame rate of 10 frames/s yields only 6 frames/cardiac cycle, which is barely adequate for most cardiac imaging. In such instances the operator should attempt to boost frame rates by using the maneuvers outlined above. Obviously one should strive for the highest frame rates possible, which will permit more detailed analysis of cardiac motion and function; this is especially pertinent given the higher heart rates found in young children. Very high frame rates are also desirable for precise evaluation of myocardial mechanics using methods such as tissue Doppler evaluation and strain/strain rate imaging.

Fortunately, with TEE the close proximity of the transducer to the heart means that smaller distances are needed to visualize the cardiac structures. Hence excellent temporal resolution is generally possible, even while at the same time being able to use higher ultrasound frequencies to optimize axial and lateral resolutions.

Tissue Harmonic Imaging

Tissue harmonic imaging is a technique used to enhance 2D imaging, particularly in patients with poor echocardiographic windows. It is based upon the detection of *harmonic frequencies* generated by beam propagation through tissue. It relies upon the fact that a relatively high-pressure amplitude sound wave changes shape during propagation, a phenomenon known as nonlinear wave propagation. The sinusoidal shape becomes distorted, and this change in shape corresponds to a change in frequency components of the sound wave—harmonic frequencies are generated from the original sound wave. These intensify with distance from the transducer as the waveform becomes more distorted. The harmonic components occur as multiples of the fundamental frequency: if the fundamental frequency is 2.5 MHz, the second harmonic is 5.0 MHz, the third

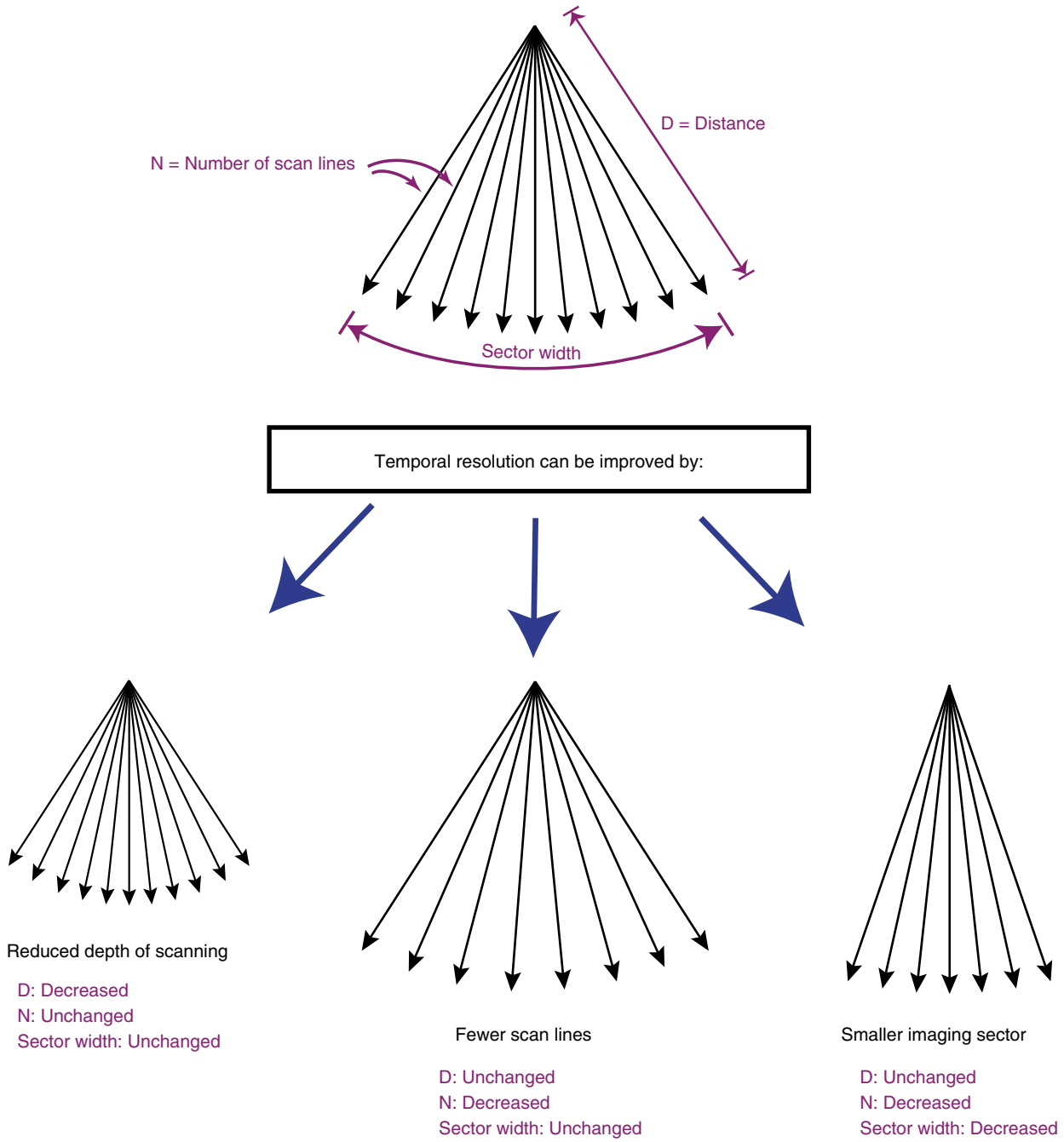

Fig. 1.26 Enhancement of temporal resolution. Temporal resolution is dependent upon sector depth and number of beam lines. It can be improved by several methods, including: (**a**) reducing sector depth (*leftward panel*); (**b**) reducing the number of scan lines without changing sector width, effectively reducing line density (*middle panel*); (**c**) narrowing the sector width, which also has the effect of decreasing the number of scan lines while maintain line density (*rightward panel*). Any combination of these maneuvers can be performed to enhance temporal resolution further

harmonic 7.5 MHz, etc. However the third and higher harmonics have weak amplitudes and therefore harmonic imaging is confined principally to the second harmonic frequency.

Tissue harmonic imaging relies upon the detection of this second harmonic frequency. The ultrasound machine can be configured to isolate this component for image formation. The advantage of this type of imaging is that artifacts are reduced or eliminated because they arise from the fundamental frequency, which is suppressed with tissue harmonic imaging. Thus signal to noise ratio is increased, and contrast resolution and border delineation are enhanced. Moreover the width of the main beam is effectively narrower than the main beam at the fundamental frequency, thus lateral resolution can be

enhanced. The drawbacks of harmonic imaging depend upon the methods used for second harmonic isolation. One method, known as harmonic band filtering, utilizes longer spatial pulse length to narrow transmission bandwidth and enhance separation of fundamental and harmonic frequencies. However, the longer spatial pulse length can lead to poorer axial resolution. The other method, known as pulse phase inversion, utilizes a two-pulse sequence in which the second pulse is shifted 180° in phase. With standard sinusoidal waveforms, summation of these two returning pulses would cancel each other out. However with nonlinear propagation, the returning harmonic components that are generated are not identical in amplitude, thus summation of the returning signals will isolate the harmonic frequency that has been produced. Broadband transmitted pulses with short spatial pulse length can be used, so this method preserves axial resolution; however, using the multiple pulse technique can reduce temporal resolution and produce motion artifacts [16].

Harmonic imaging has found great utility in transthoracic echocardiographic imaging of adult patients with poor windows, and occasionally it proves beneficial in selected pediatric patients because of its improvements in contrast resolution. It has less applicability with TEE because of the close proximity and generally excellent imaging afforded by the proximity of the esophagus to the heart [17].

Doppler Echocardiography

In addition to providing information about anatomy and function, ultrasound can also furnish important information about motion and velocity. This is particularly relevant in echocardiography, where knowledge of cardiac and blood flow velocities—made possible through the use of Doppler echocardiography—can be used to derive a wealth of noninvasive information on cardiac physiology. This section discusses the science of Doppler echocardiography.

The Doppler Principle

The Doppler effect was discovered and first described by the Austrian physicist Christian Doppler in 1842. While studying the light from the stars, he discovered that the colored appearance of moving stars was caused by their motion relative to the earth. The motion resulted in either a red or blue shift of the light's frequency, depending upon the direction of motion. Doppler mathematically described the shift that occurred, and also correctly surmised that the same type of perceived frequency shifts would occur for a stationary observer listening to sound waves produced from a moving source. The perceived frequency of sound would be higher (compared to the emitted frequency) for an approaching object, and lower for a retreating object (Fig. 1.27).

The Doppler principle can also be applied to ultrasonography, and specifically to echocardiography. The ultrasound transducer serves as the stationary observer, and emits a sound of known frequency toward a moving target. The signal reflected from the moving target will return with a different frequency (the Doppler shift), and this change in frequency is proportional to the velocity of the reflector. The velocity of the moving reflector can be calculated using the **Doppler equation**:

$$f_D = \frac{2 f_0 V \cos\theta}{c} \tag{1.8}$$

f_D = the Doppler frequency shift = $f_r - f_0$
f_0 = the transmitted frequency of sound
f_r = the received frequency of sound
V = reflector velocity
θ = the intercept angle between the ultrasound beam and the direction of blood flow
c = the velocity of sound

If this equation is rearranged to derive the reflector velocity from the frequency shift between transmitted and received ultrasonic signals, the following equation is obtained:

$$v = \frac{f_r - f_0}{\cos\theta} \times \frac{c}{2 f_0} \tag{1.9}$$

From these equations, three important points become apparent. First, the angle (θ) of the ultrasound beam relative to the direction of reflector motion (also known as the angle of insonation) is important—as θ becomes less parallel and changes from 0° to 90°, the Doppler frequency shift (f_d) is reduced by the factor cosine θ. When the direction of the beam is perpendicular to reflector motion, cosine 90° = 0 and no frequency shift is detected. Table 1.2 shows the reduction in calculated velocity (as compared to actual velocity) for a reflector moving at 1 m/s, as θ increases from 0° to 90°. Angles greater 30° result in significant decreases in calculated velocity. The message here is simple and straightforward: *when evaluating for a Doppler velocity, the angle of insonation must be as parallel as possible to the direction of motion.*

The second important point is that the Doppler frequency shift depends upon the frequency of the incident beam—for a given reflector velocity, the higher the incident frequency, the higher the Doppler shift. As will be seen, the incident frequency, and the magnitude of this frequency shift, are important in determining the limits of pulsed and color flow Doppler evaluation.

The third important point is that reflector direction of motion can be determined. As is evident from Fig. 1.27, the Doppler frequency shift incorporates directionality: approaching objects increase the returning frequency of the

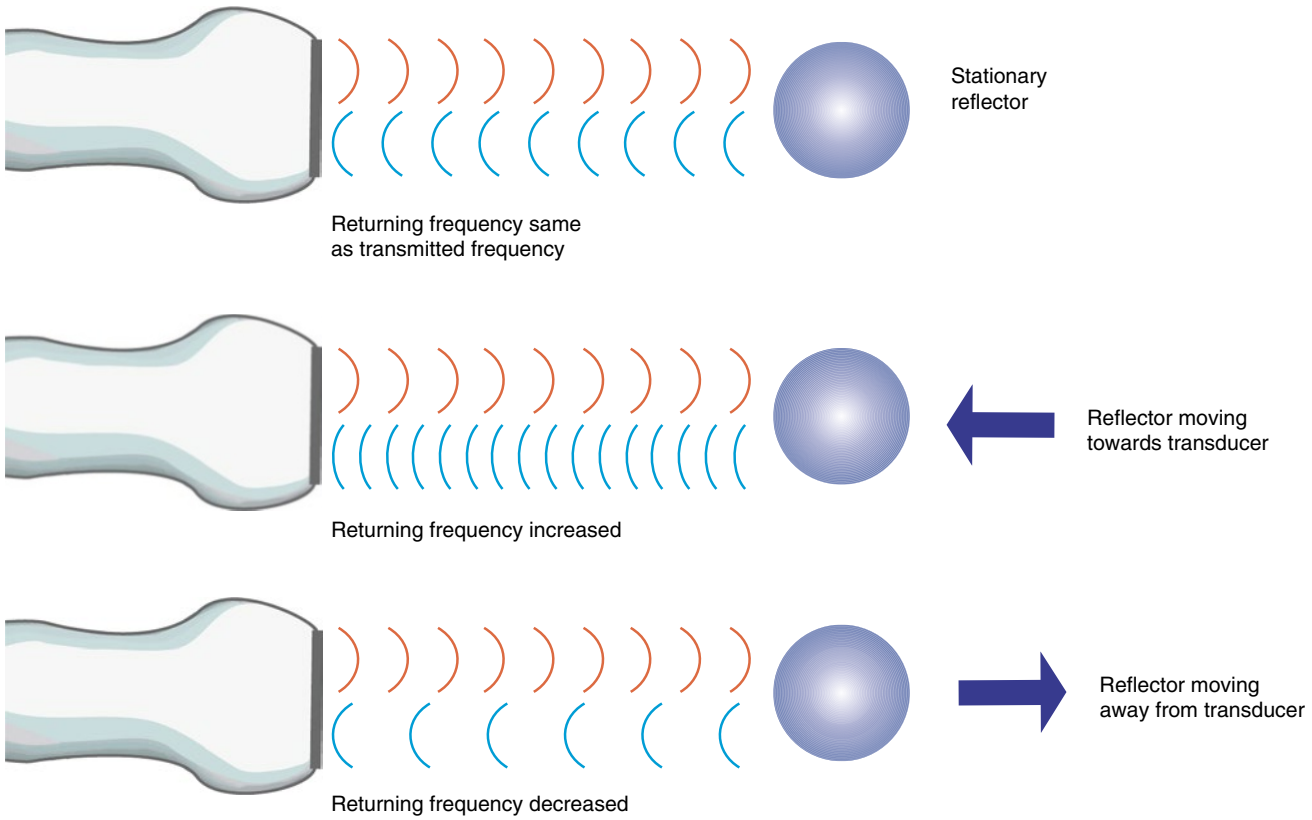

Fig. 1.27 The Doppler principle. When an ultrasound pulse of known frequency is transmitted, the returning pulse from a stationary reflector will have an identical frequency. However, the pulse returning from a reflector moving *towards* the transducer will have an *increased* frequency, and if the reflector is moving *away* from the transducer, the pulse will have a *decreased* frequency. The change between incident and reflected frequencies is known as the Doppler frequency shift, and from this shift, the reflector velocity can be calculated

Table 1.2 Doppler angle and velocities for a reflector velocity of 1 m/s, using a 5 MHz transducer

Doppler angle (degrees)	Doppler shift (kHz)	Actual velocity (cm/s)	Calculated velocity (cm/s)
0	6,494	100	100
30	5,624	100	87
45	4,592	100	71
60	3,248	100	50
75	1,681	100	26
90	0	100	0

signal, and retreating objects decrease the frequency. While the process in which the echocardiography machine determines reflector direction is not as straightforward as might appear from Eq. 1.9, the fact remains that reflector direction of motion is another important piece of information that can be extracted from the returning echo signal.

Doppler echocardiography plays a major role in the noninvasive hemodynamic evaluation of the cardiovascular system, primarily for the assessment of blood flow in the arterial and venous systems. Because red blood cells (Rayleigh scatterers) reflect ultrasound, blood flow evaluation by Doppler can readily be performed, and from this a great amount of hemodynamic information can be derived. In addition, myocardial motion can also be assessed by Doppler, yielding important information about myocardial systolic and diastolic function and mechanics.

There are several methods in which Doppler information can be displayed by echocardiography: spectral, color flow Doppler, and audible Doppler. These will be presented below.

Spectral Doppler

In the example given above, a single velocity was used to characterize a moving object. However it is a simplistic notion to view flow in the human blood vessel as a constant river or stream of one single velocity; in fact, quite the opposite is true. In the human body, blood flow in the heart, arteries and veins is not steady, and exhibits considerable variation during the cardiac cycle, especially given the pulsatile nature of cardiac output. Blood flow also varies with external factors such as inspiration/expiration. Moreover, even in the normal flow through a vessel, at any one point there is a distribution of velocities, with a much higher velocity in the

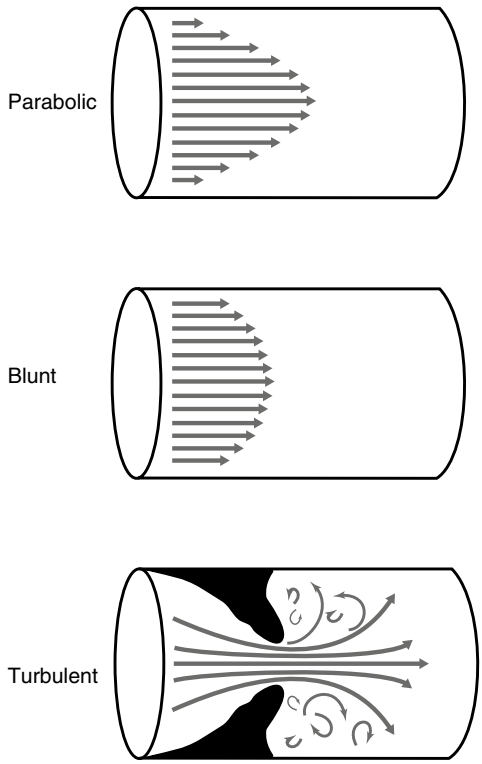

Fig. 1.28 Laminar vs. turbulent flow in a blood vessel. In normal vessels, the blood cells move fastest along the central axis of the vessel, and the velocity decreases virtually to zero next to the vessel wall. While blood flow direction is still orderly and well-organized, there is a parabolic appearance to the flow in the vessel (*top panel*). In larger vessels, this flow takes on a more blunt profile, with less variation in velocities in the center of the vessel (*middle panel*). When turbulence occurs, such as when blood passes through an area of obstruction, a disordered and chaotic flow pattern is produced (*lower panel*)

center of the vessel compared to flow near the periphery (adjacent to the vessel wall). This is known as *laminar* flow, and is due to the friction between layers, resulting in the lowest velocities along the wall, and the highest velocities centrally. Thus the velocity profile assumes a rounded or parabolic configuration, as noted in Fig. 1.28. A laminar flow pattern is characterized by a smooth, organized and orderly appearance. With higher blood flow velocities, such as those encountered with vessel or valve stenosis, there is a loss of orderliness in blood flow. This is known as *turbulence*. The blood flow pattern presents a chaotic picture, with flow orientation in a number of different directions, and considerable dispersion in detectable blood flow velocities (Fig. 1.28).

Whether laminar or turbulent, the returning Doppler signal from blood is seen as a complex wave representing a combination of frequency shifts produced by different velocities. Doppler **spectral analysis** is the process whereby this complex signal is broken down into simpler frequency components for analysis. In echocardiography, the process most commonly used is known as *Fourier analysis*, and the device used to perform the analysis is called a fast Fourier transform analyzer. A spectral analyzer then records the relative amount of signal for several discrete frequency "bins". This analysis allows the amount of Doppler signal present at different frequencies to be displayed as a function of time. When evaluating blood flow, the low velocity signals originating from myocardial motion are filtered. At any given time point, the distribution of velocities is shown on the y axis; for each velocity, pixel brightness corresponds to the quantity of red blood cells with that velocity. By obtaining successive signals, a continuous spectral display of velocity vs. time is obtained. In essence, a visual display is created showing the breakdown of velocities (frequencies) plotted as a function of time (Fig. 1.29). By convention, flow direction is depicted as above the baseline when flow is toward the transducer, and below the baseline when flow is away from the transducer (Fig. 1.30). When there is a narrow range of velocities present, such as that seen with smooth laminar flow, the spectral envelope displays a small band along the top edge of the spectral envelope corresponding to the range of velocities. The brightness of the pixels of a given velocity in the display corresponds to the number and frequency of reflectors with that velocity. A darker spectral "window" is seen underneath this band because no other velocities are present. With a wider range of velocities sampled, such as turbulent blood flow or with continuous wave Doppler, the spectral window becomes "filled in". This is also known as spectral broadening (Fig. 1.31).

Spectral Doppler evaluation represents the fundamental basis for quantitative noninvasive hemodynamic assessment. From the spectral curves, a number of important parameters can be used for analysis including peak velocity, mean velocity as calculated using the time-velocity integral (represented by the area under the curve for a single cardiac cycle), and acceleration. Applications for these will be discussed in subsequent portions of this chapter, and also in other chapters of this textbook.

There are two principal methods of spectral Doppler analysis: *continuous wave* and *pulsed wave* Doppler. These two methods will be discussed below. What will become apparent is that these two methods are complementary—each has its own strengths and weaknesses, but the strengths of one complement the weaknesses of the other, and ideally the two should be used together for a full Doppler evaluation.

For transthoracic, fetal, and transesophageal echocardiography, modern phased array transducers have the capability of performing B-mode imaging and spectral Doppler evaluation (such systems are sometimes called "duplex scanners"). These transducers can rapidly alternate between imaging and spectral Doppler evaluation. The transducer "time-shares" between both, displaying the spectral Doppler tracing while at the same time periodically updating the 2D image to verify location of the Doppler cursor. Broadband phased array transducers can also be optimized for both

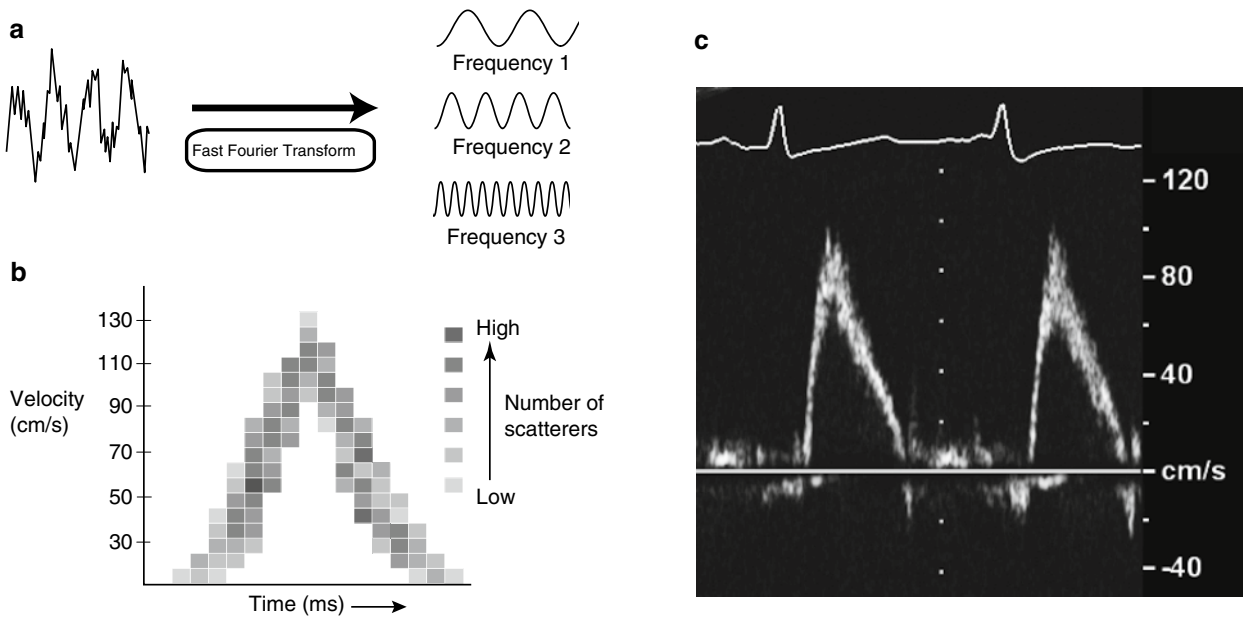

Fig. 1.29 Spectral Doppler display. The returning Doppler velocity profile is complex, and contains a range of different Doppler frequencies that can be analyzed into simpler frequency components by the use of a fast Fourier transform (FFT) analyzer (**a**). A spectral analyzer then produces a record showing the relative amount of signal within each of several discrete bins corresponding to the relative amount of each signal. The Doppler spectral display (**b**) provides a readout of velocity vs. time, with the pixel brightness reflecting the relative amount of scatterers with that velocity at that point in time. In this way, a spectral Doppler tracing is obtained (**c**)

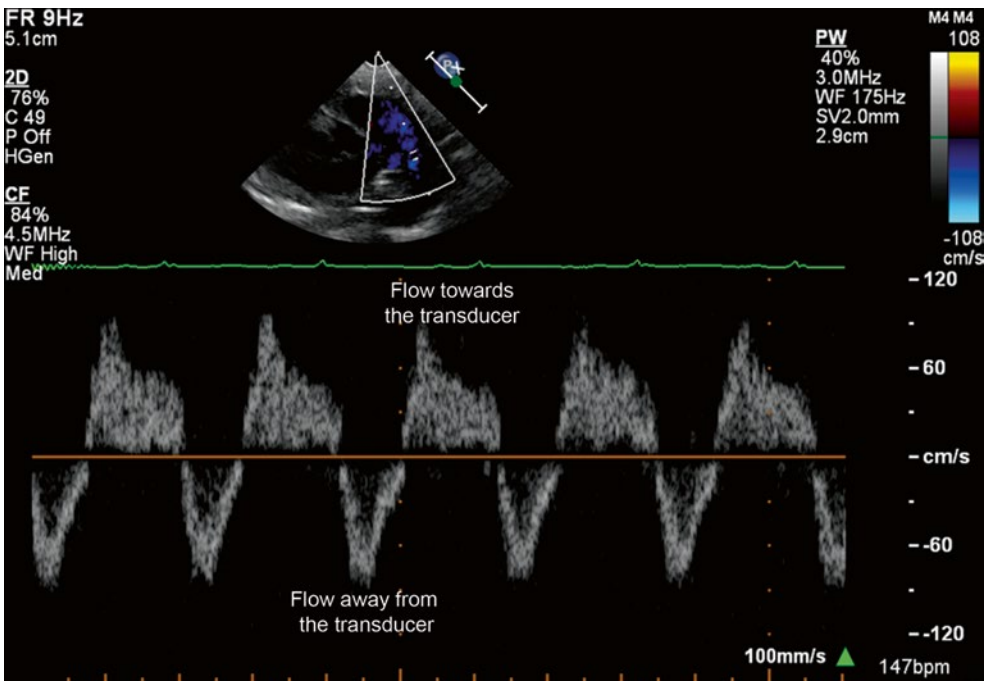

Fig. 1.30 Spectral Doppler from a transthoracic echocardiogram displaying flow directionality in this patient with to and fro flow across a patent ductus arteriosus. Flow below the baseline represents flow away from the transducer; flow above the baseline represents flow towards the transducer

modes—they can operate at lower frequencies in Doppler mode to optimize detectability of velocities at increased depths, and high frequency in imaging mode to optimize spatial resolution. In addition, these highly sophisticated transducers also have the capability of performing M-mode imaging, tissue Doppler imaging, and (in some instances) more advanced technologies such as 3D and strain imaging/speckle tracking.

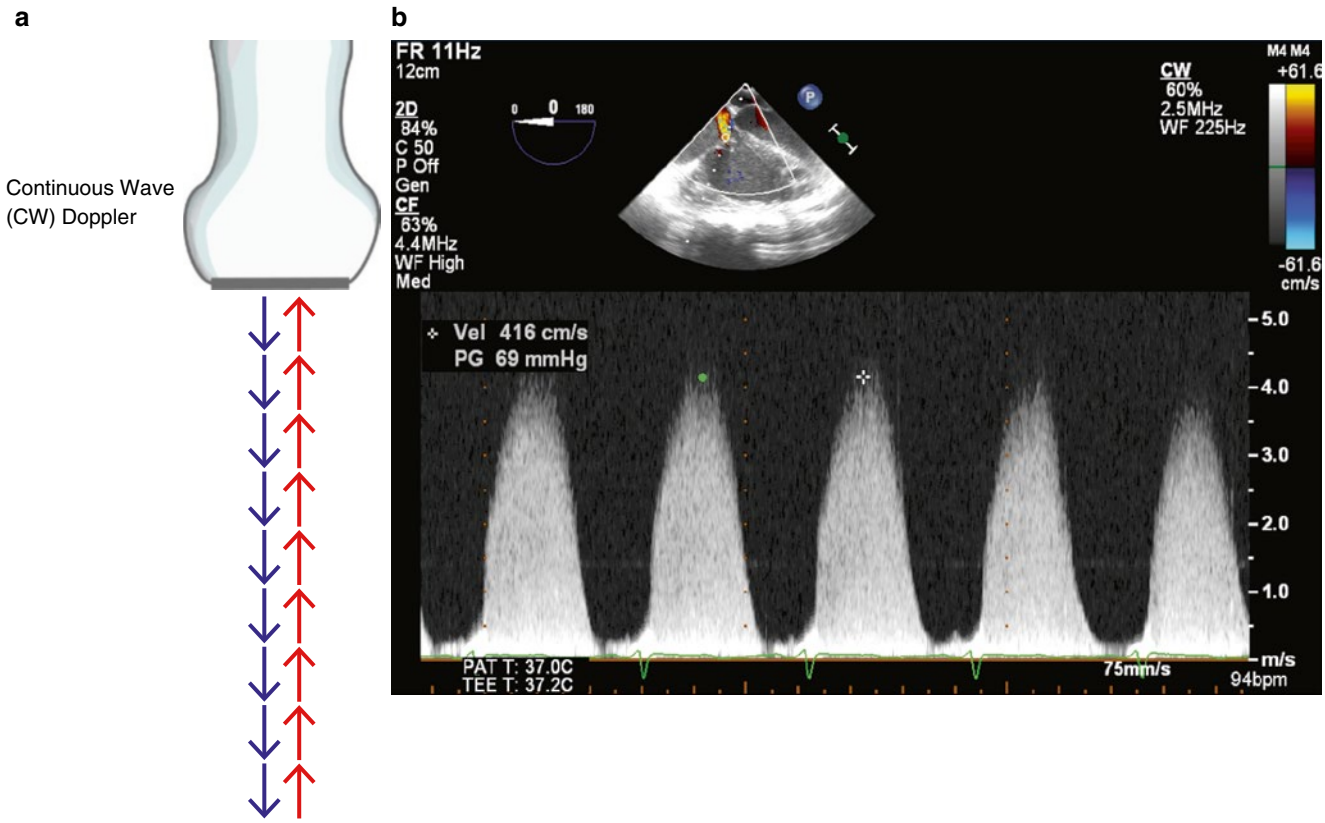

Fig. 1.31 Continuous wave Doppler. There are two basic components: a transmitter that continuously sends sound waves of known frequency, and a separate receiver that continuously receives all returning signals (**a**). The "difference frequency" is plotted as a function of time, yielding a spectral display with a wide dispersion of frequencies and significant spectral broadening (**b**). In this example, a high velocity tricuspid regurgitation signal of approximately 4.2 m/s is obtained. This study was performed with a transesophageal echocardiographic probe with broadband capabilities: B-mode imaging was performed at a frequency of 7 MHz; color flow Doppler at 4.4 MHz, and a frequency of 2.5 MHz was used for the continuous wave Doppler evaluation

Continuous Wave Doppler

Continuous wave (CW) Doppler is the simpler of the two spectral Doppler methods. The transducer is essentially divided into two separate elements: a transmitter and receiver. Two elements are needed because both operate continuously: the transmitter continuously excites the transducer to produce a reference signal of known frequency f_0 (Fig. 1.31a) The signals returning from reflection and scattering are amplified and combined with the reference (transmitted) signal to create a complex Doppler signal which is then demodulated to obtain the "difference" or "beat" frequency, which is equal to the Doppler frequency shift corresponding to the velocities of the reflectors. The beat signal is amplified, low pass filters remove high frequency signals, and high pass filters remove low frequency (wall) signals. This demodulation yields the Doppler shift, but gives no information regarding directionality. To obtain information about flow direction, a commonly used signal processing technique known as *quadrature detection* is used. This method sends the echo signal to two demodulators, and the phase relationship of the two resultant signals can be used to determine whether the Doppler shift is positive or negative. A spectral tracing of velocities vs. time is then created in the manner described above. In practice, many moving interfaces reflect signals to the receiver, thus many beat frequencies are produced. Because of this wide mixture of velocities being sampled, there is significant spectral broadening of the CW Doppler signal (Fig. 1.31b).

The advantage of CW Doppler is its ability to measure very high blood flow velocities, in excess of 6–7 m/s (or higher). Because the signal is continuously emitted and sampled, the spectral tracing will not be subject to aliasing (discussed below). This gives it great utility when evaluating areas of stenosis. However the disadvantage of this technique is a complete lack of depth specificity, also known as *range ambiguity*. A high velocity might be detected, but based upon the CW tracing alone, it is impossible to determine at what depth this velocity is located. Along the CW beam line, *all* velocities will be sampled and displayed in one spectral tracing. Therefore if there are several levels of obstruction, for example if high velocities are present along the line from two (or more) separate locations, it might be very difficult to separate the different velocities.

Pulsed Wave Doppler

Pulsed wave (PW) Doppler is used for the evaluation of Doppler signals at a specific range or depth. Using the

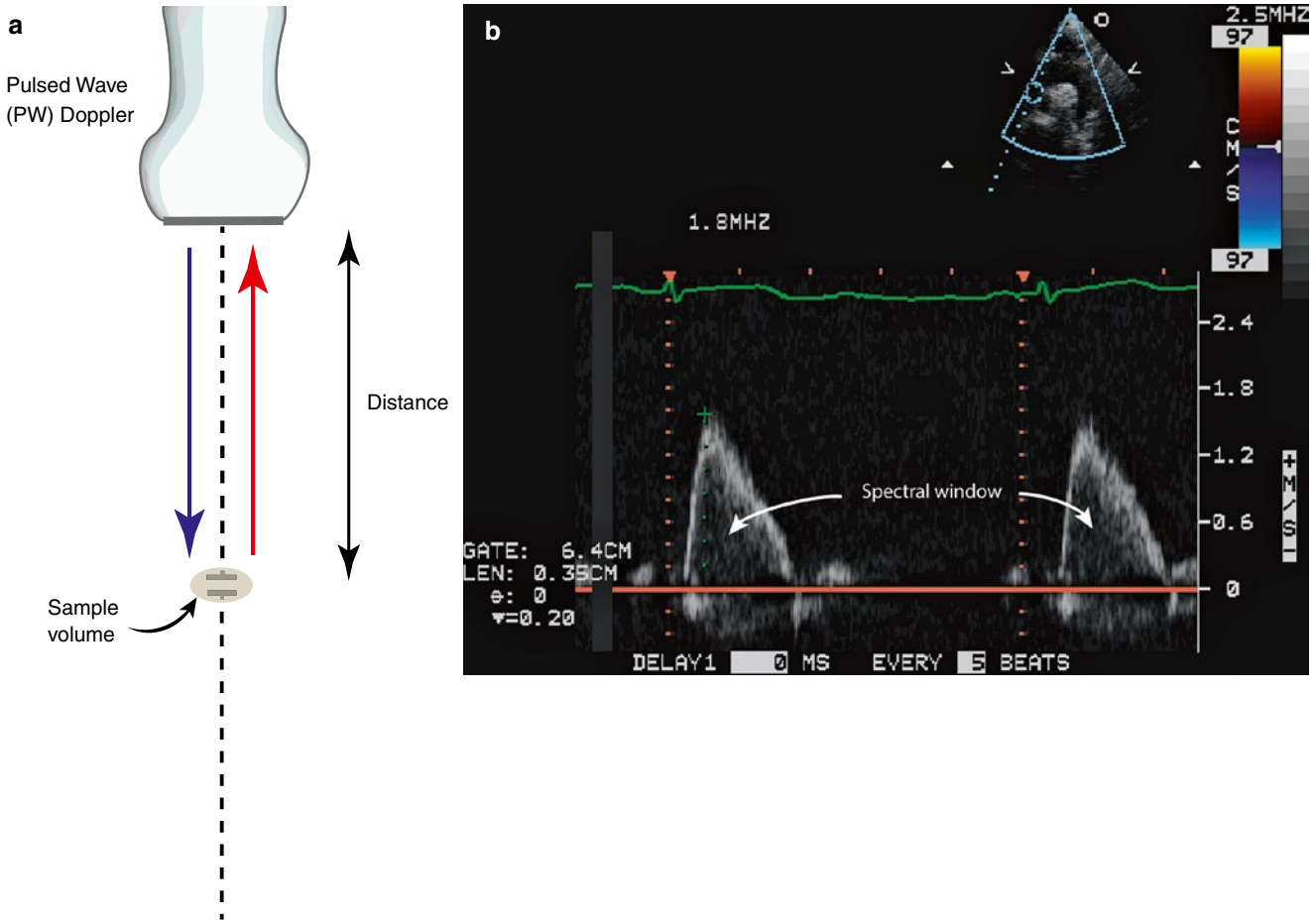

Fig. 1.32 Pulsed wave Doppler. This is used to evaluate Doppler signals at a specific range or depth, and relies upon the pulse-echo principle to determine which signals to sample. A sample volume is placed in the area where Doppler evaluation is desired (**a**). Pulses are transmitted over a beam line along which the sample volume is located; however only echoes returning in a time window equivalent to sample volume depth (depth ∝ (round-trip echo time/2)) are collected. The resultant signals are processed and a spectral display generated (**b**), in this example a spectral Doppler recording has been obtained by transthoracic echocardiography from the ascending aorta. Note that normal blood flow has a narrow range of blood flow velocities displayed as a band of *gray scale brightness*. This creates an open area underneath known as a "spectral window"

principle of pulse-echo 2D imaging, PW Doppler involves emitting a signal of known frequency, and by selecting transmission/reception time in conjunction with the speed of sound in soft tissue, returning signals originating from a specific depth can be isolated and evaluated. However unlike 2D imaging, the important information evaluated by PW Doppler is not signal amplitude, but rather the *Doppler frequency shift* of the returning signal, which can then be used to calculate reflector velocity and direction.

To perform PW Doppler evaluation, it is necessary to have updated 2D image information so that the desired region of interrogation can be selected; this region is designated on the image by the use of a *sample volume*, which is usually a pair of small parallel lines orthogonal to a visible scan line on the display. This sample volume can be adjusted for depth and position anywhere within the image (Fig. 1.32a). The sample volume or gate size can also be adjusted for size; increasing the gate size accepts Doppler signals from a longer axial region. Like pulse-echo imaging, the same PZE element serves as both transmitter and received of ultrasound pulses. These pulses tend to be longer in duration (spatial pulse length 5–25 cycles) to produce a narrow frequency bandwidth pulse and improved sensitivity, though this comes at the expense of poorer axial resolution and greater acoustic exposure. As previously noted, only the echoes returning during a specified time window (corresponding to the desired depth, as given in Eqs. 1.5 and 1.6) are selected for analysis. These echoes undergo the same processes of amplification, demodulation and filtering that are utilized with CW Doppler, yielding a velocity and directionality of the moving reflector. The signals are stored in a sample and hold unit, and held there awaiting the results of another transmit pulse. Subsequent ultrasound pulses are transmitted as soon as the previous pulses are received; the maximum frequency of transmission is the maximum PRF, which, as discussed earlier, is completely dependent upon the depth of the sample volume. In general, a PRF of 4,000–12,000 Hz is utilized with PW Doppler [1]. With each pulse

transmission-reception, the incoming signals are processed, resulting in the construction of the Doppler signal. The spectral tracing displays the range of velocities over time, with pixel brightness corresponding to the number of reflectors with a specific velocity. With laminar flow, there is a much narrower range of velocities displayed as a small band along the edge of the spectral envelope, and a spectral "window" underneath (Fig. 1.32b). This band broadens slightly with peak flow rates as a more parabolic shape of velocities occurs. As noted previously, turbulence results in a wider range of velocities and "fill-in" of the spectral window, also known as spectral broadening.

With current phased array transducer technology, 2D imaging and Doppler capabilities are all present on one transducer. For PW Doppler, the 2D image information is utilized for precise placement of the sample volume in the desired location. During the periods when the transducer is "listening" for the returning Doppler information, image pulses can be sent. Therefore an intermittent image update can occur even during the PW spectral Doppler display.

The advantage of PW Doppler is that, unlike CW Doppler, the sample volume can be precisely located anywhere within the field of view, enabling collection of velocity information from a specific location. However, this comes with a tradeoff—for PW Doppler there is an upper limit to the maximum velocity that can be measured unambiguously, and this limit varies with depth. This is discussed in the section below.

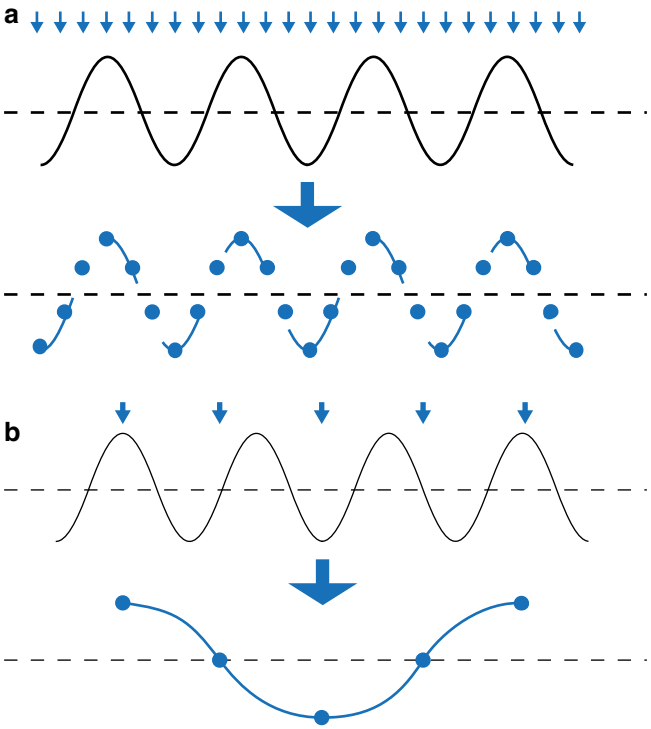

Fig. 1.33 Examples of adequate and inadequate signal sampling. To describe a wave accurately, there must be adequate sampling of the signal. The greater the sampling frequency, the better the signal is rendered. At the very minimum, sampling needs to occur at twice the frequency of the wave being sampled. Otherwise, *aliasing* will occur. (**a**) A sine wave is sampled frequently (*arrows*), allowing for an accurate rendering of the signal. (**b**) The sampling frequency of the same wave is inadequate, leading to aliasing and the erroneous rendition of a lower frequency wave

Aliasing and the Nyquist Limit

Unlike CW Doppler, sampling with PW Doppler cannot be performed continuously. The echo pulse transmit/reflect time must be used to determine sample volume distance, which means that one complete pulse must be sent and received before the next is sent. Therefore a Doppler signal must be sampled at discrete intervals. The greater the sampling frequency, the better the construction of the signal (Fig. 1.33a). For PW Doppler, the sampling frequency is equal to the pulse repetition frequency (PRF). The upper limit of the sampling frequency is given by the maximum PRF, which in turn is dictated by the distance from the transducer: the farther the distance between sample volume and transducer, the less the maximum PRF.

To provide an accurate measurement of a reflector's velocity by PW Doppler, at minimum the PRF needs to be high enough to sample the Doppler frequency shift unambiguously at least *twice* per wave cycle. If not, a phenomenon known as **aliasing** occurs in which the reported frequency shift will appear to be erroneously low (Fig. 1.33b) [18]. This is akin to the well-known example in movies of a rapidly spinning wheel—if the movie frame rate is not twice the frequency of the spinning wheel, aliasing occurs in which the wheel appears to be spinning slowly in the other direction. For PW Doppler, the minimum PRF needed to avoid aliasing is twice the Doppler shift frequency (f_d), as given by the equation: Minimum PRF = $2f_d$. When viewed in another manner, the maximum frequency shift (f_d)—which equates to the maximum nonaliased velocity measurable by a PW Doppler—is equal to PRF/2. This is known as the **Nyquist limit**. Doppler frequency shifts below the Nyquist limit can be determined accurately; those above the Nyquist limit result in aliasing and the erroneously production of a waveform of lower frequency. Aliasing of PW Doppler is manifest as a "wrapping around" of the signal from the top to the bottom on the spectral display (Fig. 1.34).

As an example, consider blood coming directly toward the transducer at 1 m/s. Using PW Doppler with a 5 MHz transmission frequency will result in a Doppler frequency shift of 6,490 Hz for the returning signal. If the sample volume is located 5 cm from the transducer, the maximum PRF at that point is 77,000 ÷ 5 or 15,400 Hz. This is more than twice the Doppler frequency shift of 6,490 Hz, hence at this distance the velocity can be determined accurately, without aliasing. However if the sample volume were located at 10 cm, the maximum PRF of 7,700 Hz (77,000 ÷ 10) is less than twice the Doppler frequency shift, and aliasing would occur at this level.

The Nyquist limit will vary both with sample volume depth as well as the frequency of the signal. The equation for calculation of maximum reflector velocity without aliasing is given as follows:

$$V_{\max} = \frac{c^2}{8 f_0 D \cos\theta} \tag{1.10}$$

V_{max} = the maximum measurable velocity of blood
c = the velocity of sound in tissue
f_0 = the transmitted frequency of sound
D = depth of interest
θ = the intercept angle between the ultrasound beam and the direction of blood flow

As previously mentioned, greater depth reduces PRF, thereby reducing the Nyquist limit for a given transducer. However, from Eq. 1.10 it is evident that, in addition to distance, there is an inverse relationship between transmitted ultrasound frequency and maximum detectable velocity using PW Doppler. Lower ultrasound frequencies enable detection of higher velocities than do higher frequencies, because the Doppler shifts are lower for the same reflector

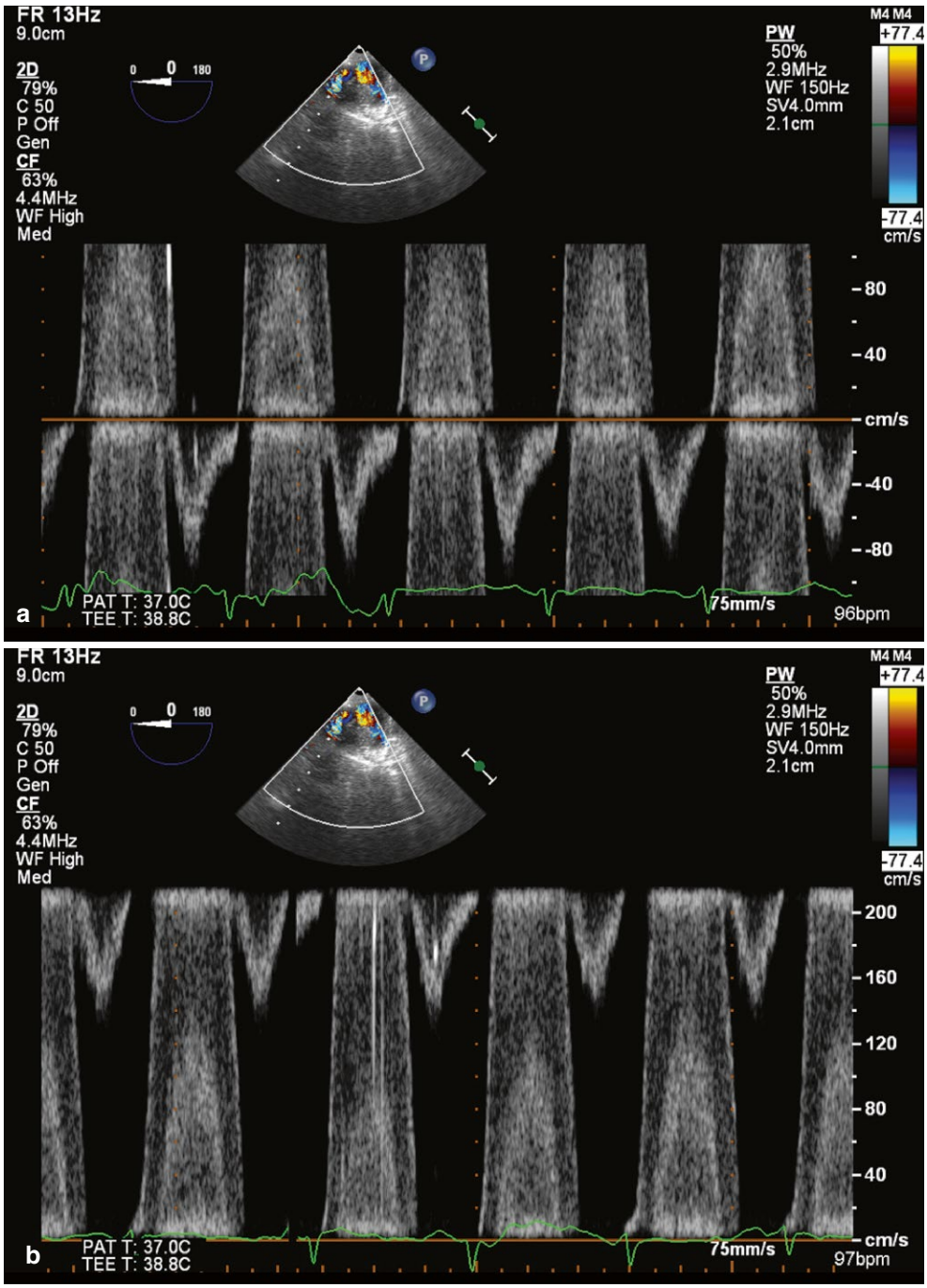

Fig. 1.34 Spectral display of aliasing by pulsed wave Doppler echocardiography in a patient with pulmonary conduit stenosis. The display "wraps around" so that the Doppler tracing is cut off at the top and appears to arise from the bottom of the screen, protruding through the baseline and up into the same wave (**a**). Even moving the baseline down to allocate the entire frequency range to the signal still results in an aliased signal (**b**). This indicates that the Doppler frequency of the signal is higher than the Nyquist limit for this particular transducer (operating at 2.9 MHz). When continuous wave Doppler evaluation is performed, a high velocity of over 4 m/s is measured, adequately resolved by this modality (**c**)

Fig. 1.34 (continued)

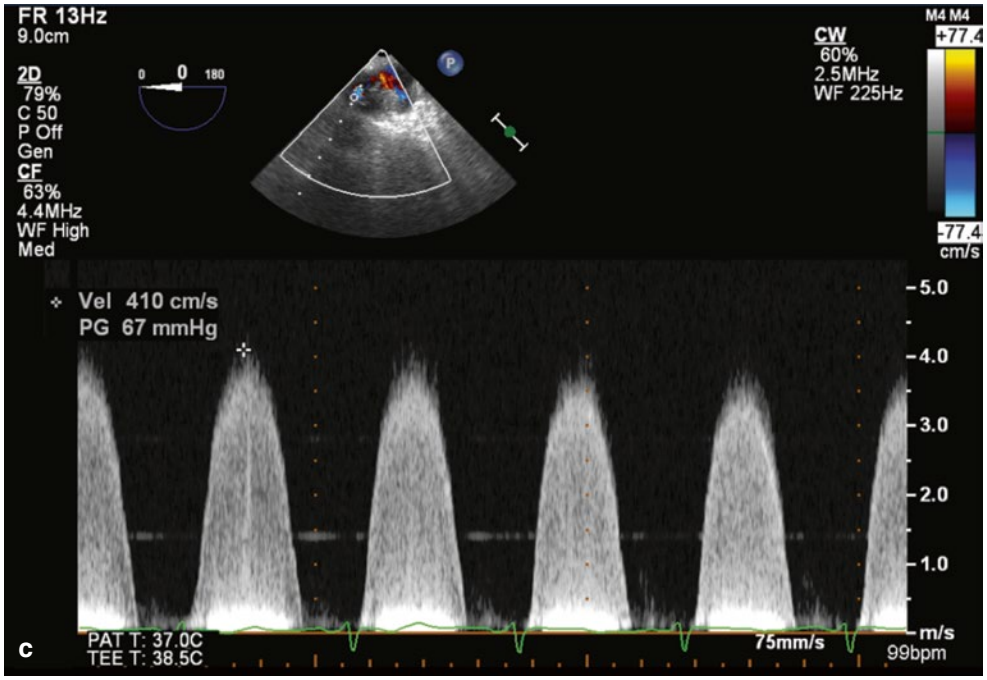

velocity. This is well shown on Fig. 1.35, which displays a graph of depth vs. calculated maximum detectable velocity for different transmitted ultrasound frequencies (assumed angle of insonation of 0°).

In summary, to maximize PW Doppler evaluation and minimize aliasing, several techniques can be performed:

- Increase the velocity scale, which increases PRF.
- Adjust the spectral baseline to the top or bottom. This allocates the entire frequency range to the maximum PRF available on the machine, though directional discrimination is lost.
- Use a lower frequency transducer.
- If possible, decrease the depth to the sample volume.

Some echocardiography machines provide a "high PRF" option for PW Doppler. This feature enables the use of a PRF higher than that allowed for the prescribed depth. This means that echoes are obtained from more than one sample volume, which in turn can lead to range ambiguity. Obviously if range ambiguity is not a concern, then CW Doppler should be used for the most accurate quantification of high velocities.

Combining the Spectral Doppler Modalities

With PW Doppler, precise depth information is available for localization, but there is a limit to the maximum measurable velocity due to the possibility of aliasing, particularly with deeper sample volumes. Conversely, CW Doppler has no such velocity limit but it can become difficult to determine the precise location of a high velocity signal. In practice, the two should be used in combination: PW Doppler for localization and quantification of blood flow through most structures, CW Doppler for quantification of high velocity jets such as stenotic valves and tricuspid regurgitant jets (as demonstrated in Fig. 1.34).

Avoidance of Artifacts with Spectral Doppler

Proper technique is important when performing spectral Doppler evaluation. As noted previously, the angle of insonation should be as parallel as possible to the direction of blood flow. With TEE, this can become even more challenging because of the confinement of the probe to the esophagus. In such cases, the different TEE positions and views (discussed in Chap. 4, as well as multiple chapters in this textbook) should be explored to determine an optimal Doppler angle of insonation—for example, the transgastric and deep transgastric views for evaluation of the left ventricular outflow tract. Visual assessment by color flow Doppler can be very useful to optimize this evaluation. Also, it is important to obtain a high quality Doppler signal with a well-demarcated, bright, and easily visualized spectral envelope. In some instances the signal is incomplete or weak, and increasing the gain settings results in significant artifact. "Feathering" (artifactual echo signals beyond the main spectral envelope) can also result in overestimation of the velocities [19]. During evaluation of flow across atrioventricular valves, some short, prominent valve closure signals can be mistaken for valvar regurgitation, resulting in erroneous estimation of regurgitant velocities. The operator should be well aware of all of these potential pitfalls.

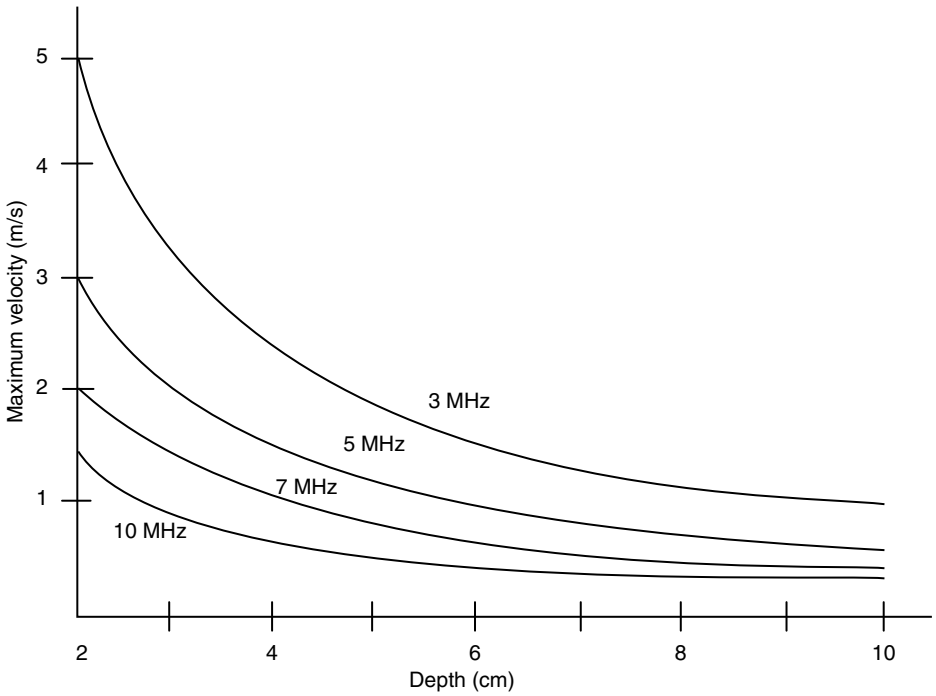

Fig. 1.35 Maximum detectable velocity without aliasing using pulsed wave Doppler, as plotted against depth of the sample volume. Four different transducer frequencies are plotted using the Nyquist equation (Equation 1.10) and assuming a 0° angle of insonation. Note that, for any given depth, lower transducer frequencies yield higher maximum detectable velocities

Spectral Doppler for Hemodynamic and Myocardial Assessment

Spectral Doppler serves as the basis for quantitative assessment of hemodynamics by echocardiography, and it is also useful for the evaluation of myocardial function. Using real-time spectral Doppler tracings that display velocity over time, important physiologic data can be derived in regard to pressure, flow, and function. These are discussed below.

Pressure Gradients and Intracardiac Pressures

This represents one of the most common and important applications of spectral Doppler. The calculation of pressure gradients is based upon Newton's law of conservation of energy, which states that the total amount of energy within a system must remain constant. Thus as blood flows through a stenotic orifice, kinetic energy (proportional to square of velocity) increases while potential energy decreases, and past the area of stenosis, some potential energy "recovers" while kinetic energy decreases. Using blood velocity as obtained by spectral Doppler (either PW or CW Doppler), the pressure gradient can be derived by using the Bernoulli equation:

$$\Delta P = \frac{1}{2}\rho\left(V_2^2 - V_1^2\right) + \rho\int_1^2 \frac{DV}{DT}DS + R\left(V\right) \qquad (1.11)$$

Convective acceleration (Kinetic)	Flow acceleration (Inertial)	Viscous friction (Shear stress)

ΔP = pressure difference across an obstructive orifice (in mmHg)
V_1 = flow velocity proximal to the obstruction
V_2 = flow velocity distal to the obstruction
ρ = mass density of blood
DV = change in velocity over time (DT)
DS = distance over which change in pressure occurs
R = viscous resistance in blood vessel
V = velocity of blood flow

The first term corresponds to kinetic energy resulting from acceleration through the stenosis; the second term represents energy loss from blood flow acceleration/deceleration; the third term represents energy loss due to viscous friction. Obviously the complete Bernoulli equation is quite complicated and requires the input of a number of different variables. However in clinical practice, the Bernoulli equation can be simplified because generally the effects of flow acceleration and viscous friction can be ignored when evaluating flow across a discrete area of stenosis. The value of $\frac{1}{2}\rho$ in blood is 4, thus yielding the *modified* Bernoulli equation: $\Delta P = 4(V_2^2 - V_1^2)$. In most clinical situations, V_2 is much greater than V_1 and therefore V_1 can be discounted and V_2 used by itself, yielding a simpler version of the modified Bernoulli equation often called the *simplified* Bernoulli equation: $\mathbf{\Delta P = 4V^2}$ (V is equal to the measured spectral Doppler velocity). For example, when the maximal instantaneous velocity across a stenotic valve is 3.5 m/s, the calculated pressure gradient = $4 \times (3.5)^2$ or 49 mmHg. Either PW or CW Doppler can be used, though in many situations,

Table 1.3 Noninvasive hemodynamic assessment by spectral Doppler

Pressure	Equation	Useful TEE view(s) for velocity measurement
RV/PA systolic pressure	4 [**V(TR)**]2 + CVP/RAp	ME 4 Ch ME RV In-Out TG RV In
RV/PA systolic pressure (VSD and left to right shunt present)	Systolic BP – 4[**V(VSD)**]2	ME 4 Ch ME RV In-Out ME AV SAX ME LAX
PA systolic pressure (PDA and left to right shunt present)	Systolic BP – 4[**V(PDA)**]2	UE PA LAX UE Ao Arch SAX
PA mean pressure	4 [**V(early PR)**]2 + CVP/RAp	ME RV In-Out DTG Sagittal
PA diastolic pressure	4 [**V(late PR)**]2 + CVP/RAp	ME RV In-Out DTG Sagittal
LA pressure	Systolic BP – 4 [**V(MR)**]2	ME 4 Ch ME 2 Ch ME LAX
LA pressure (ASD and left to right shunt present)	CVP/RAp + **mean gradient across ASD**a	ME 4 Ch ME Bicaval DTG LAX DTG Sagittal
LV end diastolic pressure	Diastolic BP – 4 [**V(AR)**]2	ME AV LAX DTG LAX DTG Sagittal TG LAX

Note: For each derived pressure, the velocity measured by spectral Doppler in shown in **bold**. All estimated pressures in mm Hg

[a]Mean pressure gradient is the Bernoulli-derived pressure gradient averaged over a selected period of time (e.g. one cardiac cycle), obtained by tracing the spectral Doppler envelope

Abbreviations: Ao aortic, ASD atrial septal defect, AR aortic regurgitation jet, AV aortic valve, BP blood pressure, Ch chamber, CVP mean central venous pressure, DTG deep transgastric, In inflow, LA left atrium, LV left ventricle, LAX long axis, ME mid esophageal, MR mitral regurgitation jet, Out outflow, PA pulmonary artery, PDA patent ductus arteriosus, PR pulmonary regurgitation jet, RAp right atrial mean pressure, RV right ventricular, SAX short axis, TG transgastric, TR tricuspid regurgitation jet, UE upper esophageal, V velocity, VSD ventricular septal defect. See Chap. 4 for a description of the individual transesophageal echocardiographic (TEE) views

particularly with the evaluation of stenosis, CW Doppler is needed due to the high velocities that cause aliasing with PW Doppler.

A few caveats are important regarding the simplified Bernoulli equation. First, as with all Doppler evaluation, the angle of insonation should be as parallel as possible in order to obtain an accurate Doppler gradient. Second, the simplified equation becomes less accurate when there is a long, tubular stenosis (such as a Blalock-Taussig shunt). In such cases, the effect of viscous friction becomes significant, and the simplified Bernoulli equation can underestimate the pressure gradient. Third, by changing the mass density (ρ) of blood, anemia and polycythemia can have an effect upon the gradient. Finally, in some clinical situations such as hypoplastic aortic arch/coarctation of the aorta, V_1 could become significant and therefore should be accounted for, i.e. the modified Bernoulli equation should be used.

The modified/simplified Bernoulli equations have many uses: evaluation of pressure gradients across stenotic valves or outflow tracts, derivation of ventricular chamber pressures using the velocity across ventricular septal defects, calculation of gradients in the great arteries (e.g. coarctation, ductus arteriosus), etc. In the absence of pulmonary outflow or pulmonary artery obstruction, a tricuspid regurgitant velocity can be used to calculate systolic pulmonary artery pressure using the simplified Bernoulli equation. Other chamber and blood vessel pressures can be also be derived noninvasively, sometimes with the use of additional information such as arterial blood pressure or central venous pressure. Some of these hemodynamic calculations are listed in Table 1.3. Most, if not all, of these measurements can be obtained from TEE. The modified and simplified Bernoulli equations have a wide variety of applications in CHD evaluation, and their various applications will be discussed in multiple sections of this book.

Cardiac Flow

Stroke volume and cardiac output can be calculated using spectral Doppler. Stroke volume is calculated from echocardiography by the equation:

$$Q = TVI \times CSA \tag{1.12}$$

Q = volumetric flow (stroke volume)
TVI = time velocity integral
CSA = cross sectional area of the area that velocity is measured

Assuming a circular cross sectional area, the cardiac stroke volume can then be calculated from the diameter measured at the selected area. For left sided cardiac output, the left ventricular outflow tract diameter, represented by aortic valve annulus diameter, can be best obtained from the mid esophageal aortic valve long axis view. Cross sectional area (in cm^2) is then calculated by the formula $\pi \times (\text{diameter}/2)^2$. The time velocity integral (in cm) is calculated by manual tracing of the spectral Doppler tracing, which for the aortic valve is best obtained from a deep transgastric long axis or sagittal view, or a transgastric long axis view (see Chap. 4 for description of individual views). Once the stroke volume is obtained, cardiac output (C.O.) can be calculated as follows:

$$C.O. = HR \times Q \tag{1.13}$$

HR = heart rate (beats/min)
Q = stroke volume (from Equation 1.12)

Cardiac index (C.I.), in l/min/m^2, is calculated as follows:

$$C.I. = C.O./BSA\ (m^2) \tag{1.14}$$

It should be noted that this calculation should be performed when there is laminar, not turbulent, blood flow across the area in question. Also, the aortic valve is best used for this measurement because of its circular cross section, which does not vary significantly throughout the cardiac cycle.

A similar principle of volume assessment can be applied to the calculation in the calculation of aortic valve area (in the case of aortic valve stenosis), using the *continuity equation*. This equation is based upon the principle of conservation of mass, which stipulates that volumetric flow remains equal as it passes from one site through another. Hence the continuity equation is given as follows:

$$CSA_1 \times TVI_1 = CSA_2 \times TVI_2 \tag{1.15}$$

In this case, the CSA_1 and TVI_1 are obtained from the left ventricular outflow tract below the aortic valve, using the method noted above. The spectral velocity tracing across the outflow tract is obtained by PW Doppler. The TVI_2 can then be calculated from the CW Doppler spectral tracing, and from these variables, the equation can be solved for CSA_2, which is the aortic valve area. It should be noted that this equation is predicated upon the assumption of a circular cross-sectional area of the left ventricular outflow tract. However recent 3D literature has suggested that the cross-sectional geometry of the outflow tract is more likely elliptical than circular [20, 21].

The continuity equation serves as the basis for the calculation of valve regurgitant orifice area as measured by the proximal isovelocity surface area (PISA) method. PISA is not widely used with congenital valve disease; it is utilized to a greater extent in adult cardiology, particularly with mitral valve disease [22, 23]. The continuity equation is also discussed in several other sections in this book, for example its use in adults with prosthetic heart valves for the calculation of valve effective orifice area (discussed in further detail in Chap. 16).

Myocardial Function

Doppler echocardiography plays an integral role in the assessment of myocardial mechanics, particularly as regards diastolic function. Spectral Doppler assessment of ventricular filling, as well as pulmonary and systemic venous Doppler waveforms, are methods used to evaluate left ventricular and left atrial diastolic properties. In addition, newer methods such as tissue Doppler imaging (also known as Doppler tissue imaging) utilize direct spectral Doppler evaluation of myocardial motion for assessment of ventricular diastolic function. This modality evaluates the low velocity, high amplitude signals of the myocardium that are filtered out by conventional spectral and color flow Doppler evaluation of blood flow (Fig. 1.36). A discussion of these methods is provided in Chap. 5.

Tissue Doppler imaging can also be used for strain analysis, one of the newer methods of myocardial functional assessment. Strain measures the extent of myocardial deformation, and strain rate measures the rate of change of this deformation. Tissue Doppler imaging was the initial technique used to evaluate these parameters—strain rate was derived from the gradient of the velocity over a sampling distance, and strain obtained as the integral of this. However the major limitation is that, like all Doppler techniques, strain could only be evaluated in one dimension—the direction along the scan line (i.e. longitudinal strain). Since myocardial strain occurs in several other directions (radial and circumferential), an alternative methodology of strain analysis has emerged to evaluate these other types of strain—that of speckle tracking. This is a 2D method that tracks a matrix of myocardial speckles corresponding to minute tissue structures. Using speckle tracking, strain can be tracked in any direction. While this method currently appears to be the preferred method of strain evaluation, tissue Doppler is still utilized. The discussion of strain evaluation is beyond the scope of this chapter; the reader is referred to Chap. 5 and other sources that provide more in-depth discussion of deformation analysis [24–26].

Color Flow Doppler

Color flow Doppler is one of the most important echocardiographic tools available, particularly for the assessment of CHD. This modality provides a visual depiction of Doppler

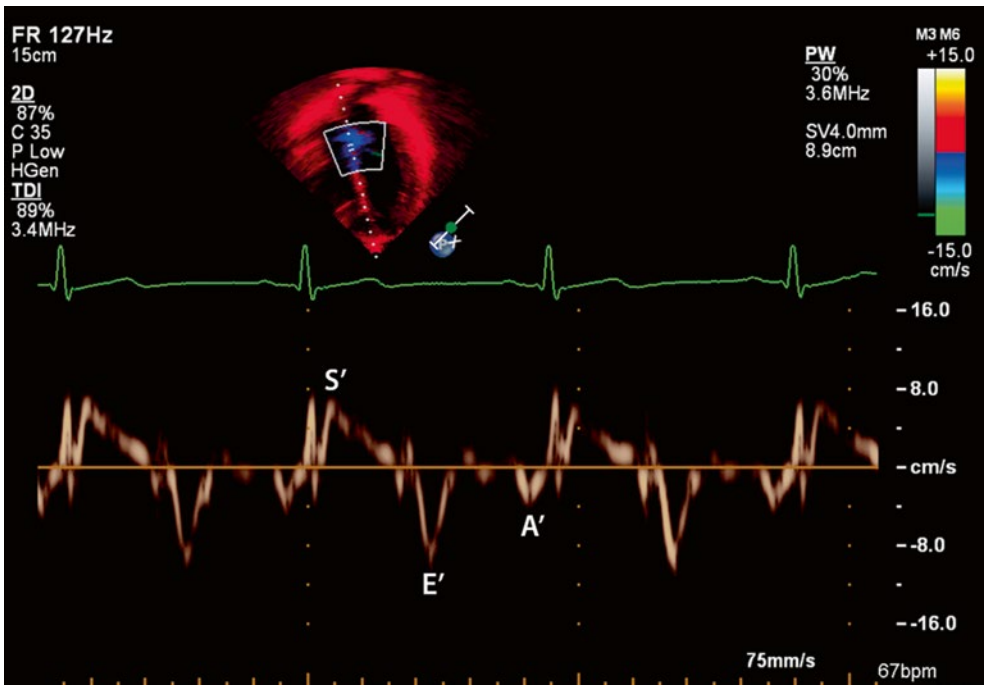

Fig. 1.36 Tissue Doppler imaging. This tracing is taken from a transthoracic echocardiogram apical four chamber view. The sample volume is placed at the level of the medial mitral valve annulus, and a pulsed wave spectral Doppler tracing is recorded. The E′ and A′ waves correspond to early and late diastolic filling (the E and A waves of mitral valve inflow), and the S′ wave corresponds to ventricular systole. Note the low tissue velocities (less than 10 cm/s), much lower than those normally found in blood pool

information for multiple reflectors and scatterers in motion—in general, these represent blood flow within the heart and arteries/veins. Doppler information is encoded as a color map, and overlaid upon the corresponding B-mode images, whether 2D, 3D, or M-mode displays. Thus real-time blood flow visualization and flow characteristics can be seen with a wide range of different physiologic situations and conditions.

The acquisition of color flow data is an extension of pulse-echo gray scale imaging, but instead of echo amplitudes, reflector velocities are determined. For each image, multiple scan lines are utilized, and multiple receiver "gates" are present for each scan line (Fig. 1.37). Ultrasound pulses are transmitted along the scan lines; these pulses are slightly longer in length than standard B-mode imaging to improve Doppler processing. Image (B-mode) data are acquired as outlined previously for 2D imaging. However in contrast to B-mode imaging, in which only one pulse-echo sequence is necessary per scan line, multiple pulse-echo sequences (known as a *pulse packet*) are sent along each beam line. Often 8–10 pulses are sent in one packet. The first returning signals, both from moving and stationary reflectors, are stored in a Doppler processing unit, in a series of registers corresponding to depth. The second set of returning signals are compared to the first set. Stationary reflectors will have identical signals and are therefore eliminated from further processing using a "stationary echo canceler". Moving reflectors will have different signals, and the differences are used to determine reflector velocities and direction. Several techniques can be used to estimate reflector velocity, but the best known is a mathematical technique termed *phase shift autocorrelation*, in which the change in phase from one transmit pulse to the next is compared, and a velocity calculated. Over the course of multiple pulses, an average or *mean* velocity is calculated. This process is repeated for all the pulses in a packet. There is a tradeoff here: the more pulses

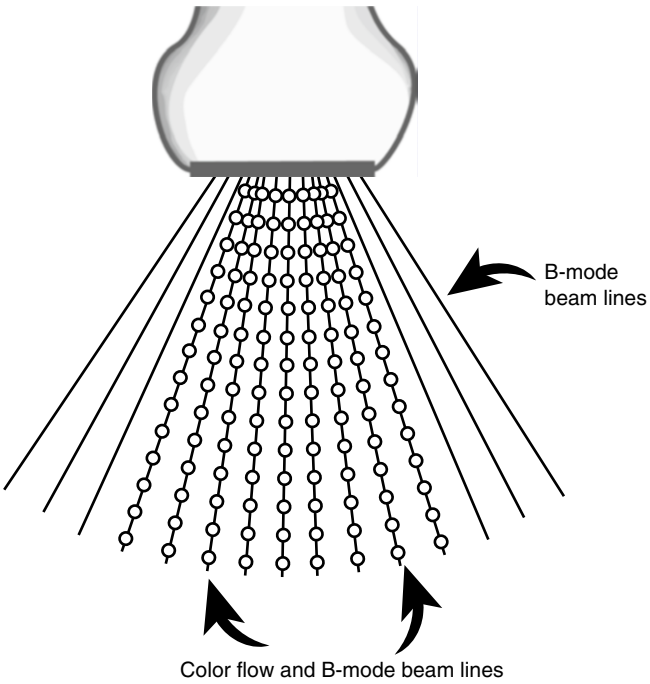

Fig. 1.37 Diagram of color flow Doppler. Both B-mode imaging and color flow Doppler are combined; the *scan lines* represent B-mode beam lines, and the *small circles* represent the multiple receiver "gates" located along the beam lines for color flow Doppler (these are combined color flow and B-mode beam lines). In general, only part of the imaging sector is used for color flow Doppler

in a packet, the better the estimates of reflector velocities but the longer the acquisition time, which slows frame rates.

Once the data from all pulse packets in one scan line have been obtained, the next scan line is evaluated. This process continues in sequence for each scan line, acquiring both color flow as well as B-mode image data, until the entire color Doppler sector has been acquired (a color flow sector tends to be smaller than the underlying B-mode imaging area). Like B-mode imaging, a sweep of the sector is continually repeated and rapidly processed to achieve real-time scan rates. Nonetheless, there are tradeoffs with color flow Doppler in both temporal and spatial resolution. Frame rates for color flow Doppler are inherently lower than B-mode imaging due to the multiple pulse sequences per packet. Increased frame rates can be achieved by reducing color sector depth, and/or reducing the total number of scan lines by either narrowing the color sector or reducing scan line density. This is analogous to the options available to improve B-mode temporal resolution, as discussed previously. Spatial resolution of color flow Doppler is also less than B-mode imaging. Because of the longer spatial pulse lengths used for Doppler evaluation, axial resolution is reduced. Also, a reduced number of scan lines (to improve temporal resolution) will reduce lateral resolution.

There are several ways in which information is displayed visually by color flow Doppler. Direction of flow is indicated by hue: by convention, red typically indicates flow *towards* the transducer, blue indicates flow *away* from the transducer (also known as "BART"—blue away, red towards). The brightness or saturation of the color can be used to indicate flow velocity, with brighter or whiter color indicating higher flow rates (Fig. 1.38). Some color flow mapping schemes include a *variance* mode in which wider variability among velocities in a single packet is indicated by a green or yellow color (Fig. 1.39a). Being a form of pulse-echo, color flow Doppler is subject to aliasing, which is displayed as color reversal or as a mosaic of multiple colors such as yellow, orange, green, etc. (Fig. 1.39a, b). With color flow Doppler, the velocity scale shown is for mean velocities; nonetheless the Nyquist limit is lower and aliasing will occur at lower velocities than PW Doppler due to the significant computational demands associated with color flow processing.

It should be noted that the method of signal processing used by color flow Doppler is fundamentally different from that used for CW and PW Doppler. This is because the fast Fourier transform methods utilized for spectral evaluation are more time-consuming and, if performed for multiple scan lines and reflectors in a designated sector, the rapid processing needed for display of real-time images could not be achieved.

Importance of Color Flow Doppler

Color Doppler echocardiography plays a vital role in the noninvasive evaluation of cardiac disease. No other imaging modality provides, in real-time, the rich variety of physiologic and functional information offered by this technique. This is particularly true with CHD, in which color flow Doppler interrogation has become indispensable for echocardiographic evaluation. Its importance cannot be overstated; in a number of instances color flow information is equally as important, if not more so, than standard 2D imaging. This is due to its exquisite sensitivity for abnormal flow velocities in

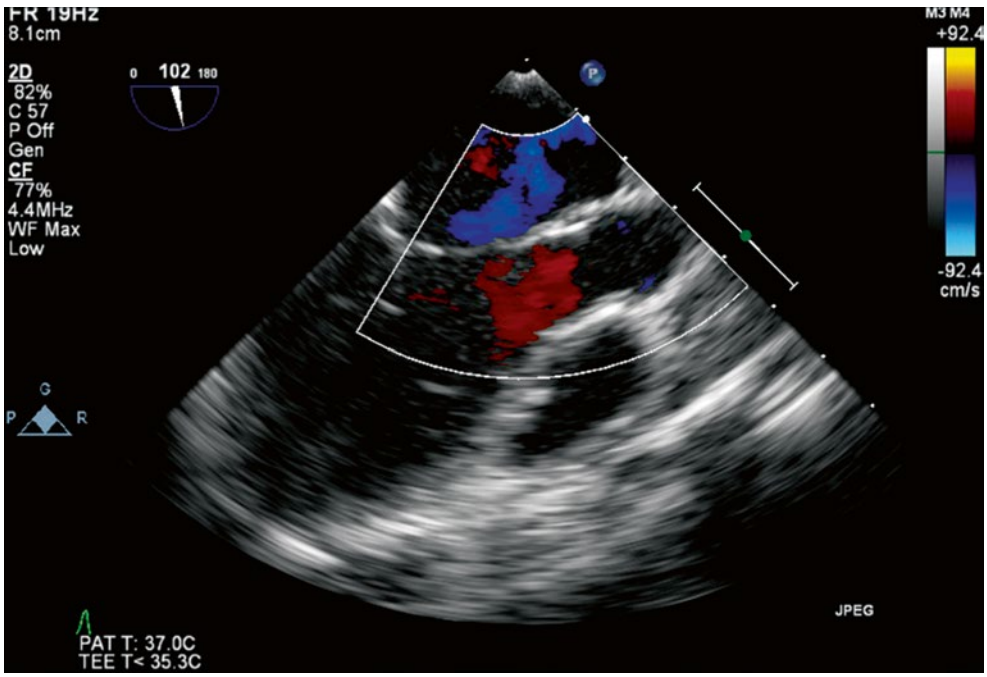

Fig. 1.38 Transesophageal echocardiogram, mid esophageal long axis view during systole showing color flow Doppler. The red flow represents normal flow velocity in the left ventricular outflow tract, the blue flow represents pulmonary venous blood returning to the left atrium

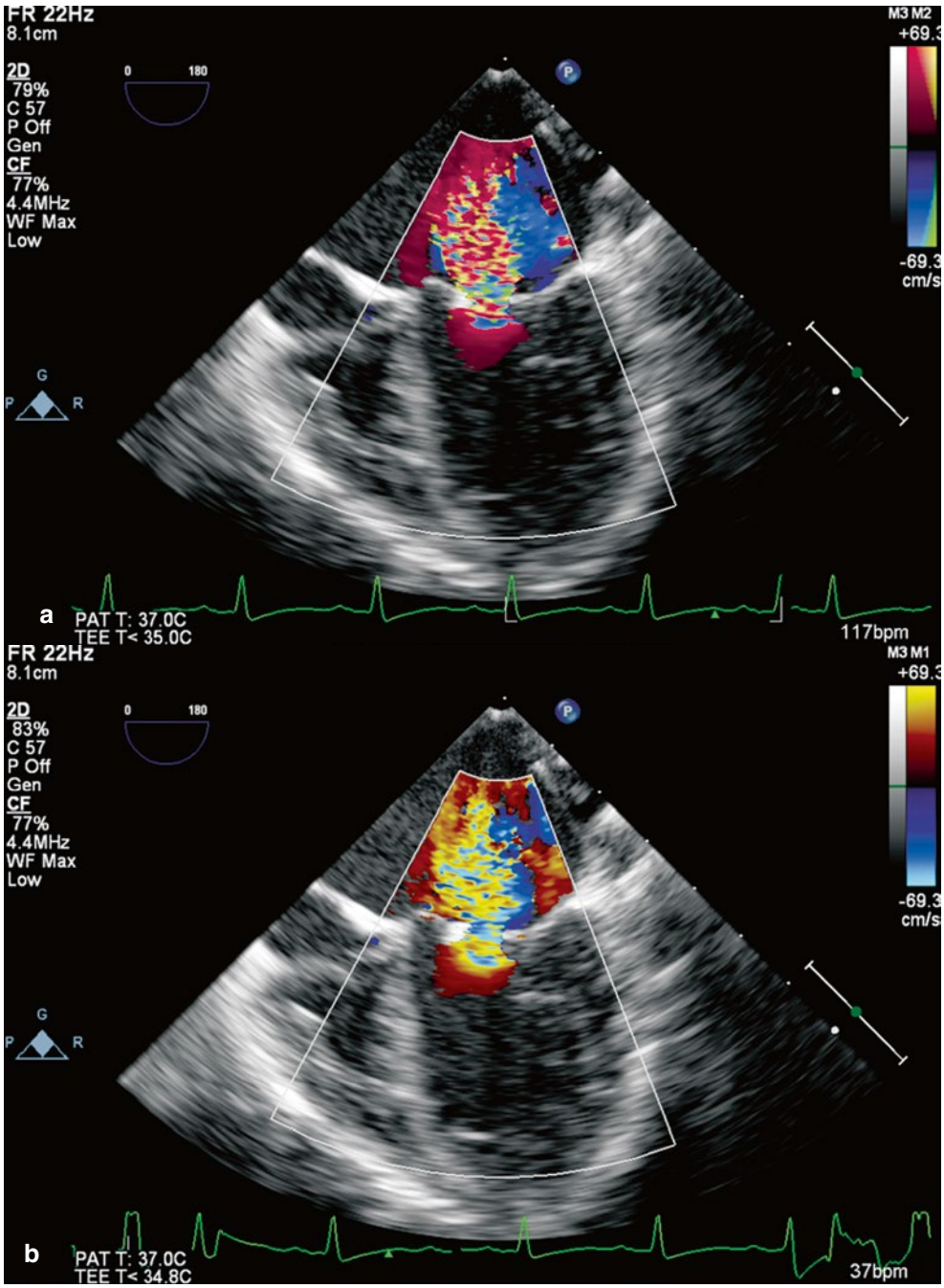

Fig. 1.39 Transesophageal echocardiogram, mid esophageal four chamber view in a patient with significant mitral insufficiency, obtained during systole, showing different color flow Doppler maps. (**a**) Shows the regurgitant jet using variance mode, (**b**) Shows the same jet using brightness mode

many different forms of congenital cardiac pathology. There are a number of congenital cardiac defects that cannot be fully assessed until color flow Doppler evaluation is performed—in some cases the pathology is incompletely seen or not even visible by 2D imaging alone (despite the superior spatial resolution of 2D imaging). Color Doppler is an essential part of the evaluation of shunts, vascular anomalies, and any pathology involving the atrioventricular and/or semilunar valves. It provides an important visual assessment of the location(s), extent, and severity of valvular stenosis or regurgitation and is very useful in directing the spectral Doppler evaluation of a stenotic/regurgitant jet by providing the optimal location and angle for spectral Doppler interrogation.

Color flow Doppler also has utility for a number of congenital heart defects typified by low velocity blood flow states. Examples of this include evaluation of Glenn and Fontan evaluation, and anomalous systemic and pulmonary venous pathways/connections. In these instances, the PRF is reduced (and wall filter settings can also be reduced) to decrease the velocity scale and improve color flow brightness/detectability for lower velocity reflectors. However the lower PRF results in a decreased frame rate.

In fact, color flow Doppler has become such an integral part of the echocardiographic examination that sometimes its potential shortcomings and limitations are not fully considered. As a form of Doppler evaluation, color flow Doppler is subject to the same limitations as PW Doppler. Like PW Doppler, aliasing will occur when the Nyquist limit is exceeded by the Doppler frequency shift of moving reflectors, and this will be reflected in the color flow reversal or mosaic patterns described above. Lower frequency transducers enable higher PRFs and Nyquist limits. Furthermore, the color (Doppler) signals will vary depending the angle of insonation; the more perpendicular the angle, the lower the Nyquist limit. As with any Doppler modality, whenever feasible, one should strive to utilize a color Doppler angle of interrogation as parallel to the intended flow as possible.

Another important reminder: it is easy to perform and record too much color flow Doppler. Because the color map is superimposed upon the real-time image, the examiner can also see the underlying anatomy while the color flow is being displayed. What can result is a study dominated by color flow Doppler evaluation and color flow Doppler recorded clips. However for a number of reasons, it is important to ensure that adequate B-mode imaging is performed. With color flow Doppler, the spatial and temporal resolution of the underlying B-mode images will be inferior to that of imaging alone; at times the disparity is striking, particularly the reduction in temporal resolution when color flow Doppler is activated. Also, the overlying color flow Doppler map has the potential to obscure important anatomic details, especially smaller structures. For this reason, the observer must be conscious of the need to strike a balance between adequate 2D imaging and judicious and proper use of color flow evaluation.

The other important fact to remember about color flow Doppler is that it is a map of mean velocities, and thus it is representative of blood in motion. It is not a map of blood or blood volume itself. This consideration applies particularly to valvular regurgitation, in which the color flow Doppler depiction of a regurgitant jet is often used as a visual estimate of the actual volume of the jet. However it is important to note that this jet can be made to appear larger or smaller due to a number of factors. Instrument settings can change the appearance of the jet size: the jet size can appear larger when the color gain setting is increased, and also when the PRF is decreased (i.e. the Nyquist limit is lowered). If the pressure in the receiving chamber is high (e.g. the left atrium with mitral regurgitation), the pressure gradient decreases more rapidly. This can lead to lower jet velocities and a smaller color flow jet area. Furthermore the extent and geometry of the regurgitant jet will vary depending upon whether it is central or adjacent to a cardiac boundary or wall (a "wall-hugging" jet). Even with the same regurgitant orifice, a jet next to a wall cannot entrain adjacent fluid, and therefore will appear smaller than the same jet seen in the center of the valve. Finally, color flow jets do not have the same degree of spatial resolution as the B-mode image, and often color flow jet or shunt margins are imprecise and tend to "bleed" over the 2D boundaries, thus the measurement of color flow jet diameter across, for example, a ventricular septal defect can overestimate the true defect diameter.

Audible Doppler

While ultrasound frequencies are measured in millions of Hz (or MHz), the Doppler shift produced by moving structures in the body generally falls within audible frequency range. For example, if a 5 MHz signal is sent towards a reflector moving straight towards the transducer at 1.0 m/s (a typical velocity for normal blood flowing through the great arteries), the Doppler shift would be 6,490 Hz (6.49 kHz), well within the human audible range of 20–20,000 Hz. Most echocardiography machines provide a sound system that can amplify and play these signals as audio. Using this signal is a useful method to guide spectral Doppler assessment—by listening for the pitch (frequency) and loudness of the signal, one can determine the optimal position for spectral Doppler evaluation, and also detect areas of turbulence/stenosis. Prior to the widespread availability of color flow Doppler, listening to the audio component served as an important part of Doppler evaluation. It was particularly helpful in screening for occult high velocity flow signals such as small ventricular septal defects that were not obvious by 2D imaging: the echocardiographer would pass a pulsed wave Doppler sample volume across the entire ventricular septum, listening for high frequency signals that might indicate a possible defect. This is a technique still used by some experienced echocardiographers. However, for many practitioners color flow Doppler has largely replaced audio because of its sensitivity and efficient evaluation of large volumes of real-time Doppler information.

Overview of the Echocardiography Machine

Competent performance of an echocardiogram requires an understanding and familiarity with all of the equipment. In the case of TEE, this includes not just the transducer and associated controls on the handle, but the cardiac ultrasound machine as well. Given the time constraints of many TEE studies, particularly those performed intraoperatively, it is essential that one proceed in a rapid and efficient manner. This requires the operator to have a thorough working knowledge of all aspects of the imaging system.

The layout of the echocardiography machine and its multiple controls/functions will vary with each manufacturer. Nonetheless, certain features are common to every

current system, and lend a certain degree of familiarity no matter what platform is used. All machines have a large high-resolution screen with which to view the live images. Most current machines now have "hard" keys assigned to certain unchanging functions and "soft" keys that can vary depending upon the mode of scanning performed (B-mode, color Doppler, etc.) (Fig. 1.40a). Most new machines incorporate these "soft" keys into touch screens with menus that will change and update depending upon the mode of scanning; each set of menus contains multiple options to optimize imaging and/or Doppler settings. There will also be a keyboard used for inputting of patient information as well as annotation/labeling in specific images; a trackball is also present and used for many functions including selection of specific images, movement of the cursor on the screen, etc. Other important features common to all echocardiography machines include a digital loop acquisition button, freeze frame/cine looping function that allows the user to scroll

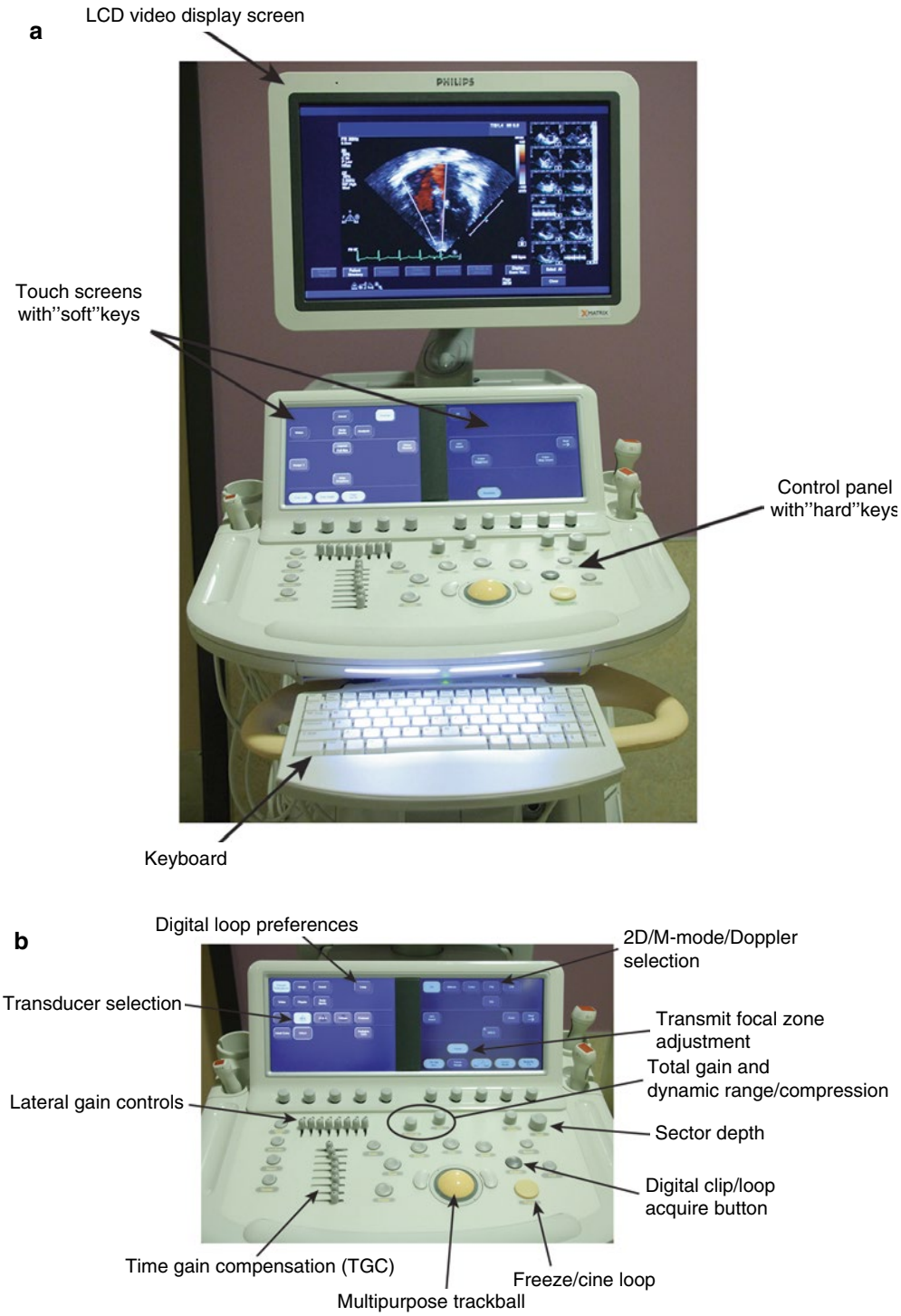

Fig. 1.40 Photograph of a standard echocardiography machine (Philips IE-33). The major components of an echocardiography machine are shown in (**a**). (**b**) The control panel and touch screen are shown in more detail, along with a number of important controls detailed in the text

through a loop frame by frame (very useful for fast heart rates), as well as calipers available for making measurements directly upon the screen (Fig. 1.40b). In addition, there are specific ultrasonic features common to all echocardiographic machines, some of which are listed below:

- **Transmit power**. Most machines allow the operator to adjust the output power, thereby providing higher intensity pulses with greater amplitude of the transmitted echo signals. This will improve visualization of the echo signal from weaker reflectors, but will also increase the exposure of the patient to greater acoustic energy (which can produce more heat). This control is variously labeled output, power, dB, or transmit. Thus during procedures that require continuous TEE monitoring (such as monitoring of cardiac function during surgery), it is advisable to decrease the output power to reduce the potential amount of heat generated. To help gauge the potential level of acoustic exposure, two standardized indices can be found on the display of the contemporary echocardiography machines from most manufacturers. It should be noted that these are calculated indices, based upon conservative assumptions, and represent "worse case" situations. The first, *Thermal Index* (*TI*), relates to the possibility of tissue heating due to absorption of ultrasound energy, and represents the ratio of acoustic power produced by the transducer to the power required to raise the temperature of tissue by 1 °C. There are several calculations used, depending upon whether bone is encountered along the ultrasound path; the measurement is called TIS when only soft tissue is encountered, TIB if bone is at or near the focal zone of the transducer (e.g. fetal scans), and TIC if bone is close to the transducer. The other index, known as *Mechanical Index* (*MI*), is related to the likelihood of cavitation produced by acoustic energy. As transmit power output increases, both the TI and MI will be noted to increase. These indices have been established to help guide echocardiographers in minimizing acoustic exposure, and standardization allows them to be used and compared across a number of different echocardiography platforms, regardless of manufacturer.
- **Temperature sensor**. Many TEE transducers have a built-in temperature sensor to monitor the patient temperature, and automatic shutoff if the temperature exceeds a predefined threshold. Nonetheless, if the probe temperature and/or local patient temperature (adjacent to the probe) is noted to increase significantly, transmit power should be reduced to decrease acoustic energy output.
- **Transmit frequency adjustment**. As has been previously noted, broadband frequency transducers (which include TEE transducers) provide the ability for the operator to alter transmit frequency to accommodate the particular clinical imaging needs. The transducer's default frequency is generally its center frequency, but the frequency can be increased for greater resolution (less penetration), or decreased for improved penetration (with less resolution). For TEE, given the generally excellent imaging afforded by most TEE views and windows, it is rare that significant frequency adjustment is necessary. The exception might be the deep transgastric views (see Chap. 4), in which the great distance from the transducer to certain cardiac structures could necessitate the use lower frequencies, particularly in larger patients.
- **Gain control**. This adjusts the amplification of the received signal in order to increase or increase the sensitivity of the instrument. It should be noted that this control, unlike transmit power, does not increase the acoustic exposure to the patient. It only increases the amplification of the received signal. There are several types of gain control. The first control is the *Overall Gain Control* and increases amplification at all depths. The second is are the TGCs, or *Time Gain Compensation* controls. These are the individual slider bars that provide adjustment of receiver gain at specific depth ranges. They are used to compensate for the attenuation of signals that occur at greater depths—in other words, a "slope" of TGCs occurs, with progression from less to more gain as the depth increases. Presently, most machines now provide an internal TGC feature that automatically corrects for depth, obviating the need for some manual adjustment of TGCs. Also, because a brief pulse of ultrasound contains a range of frequencies, manufacturers now provide a *dynamic frequency tracking* feature in which the transducer responds most effectively to higher frequencies arising from shallower depths, and to lower frequencies for greater depths. This feature capitalizes on the greater penetration of lower frequency signals, and the better resolution (but lesser penetration) of the higher frequency signals. Finally, some machines also offer lateral gain control settings as well. These adjust amplification along individual beam lines (laterally), but do not adjust for depth.
- **Dynamic range and compression**. Most machines have a control that varies the range of gray scale that can be displayed. In essence, it affects the contrast and contrast resolution on the monitor—low dynamic range produces higher contrast, and vice-versa. On some scanners, reducing dynamic range also eliminates low-level echo signals, thereby producing the effect of reducing overall gain. This control is also called compression, log compression, or dynamic range.
- **Transmit focus** (**focal zone**). This is a feature of phased array systems, and enables operator adjustment of the focal zone to various depths, based upon the timing of pulses from the individual elements. This feature helps to optimize lateral resolution.
- **Image invert**. Images can be presented with the apex of the sector at the top (the default setting for most systems) or inverted "up-down" so that the image is rotated 180° along its horizontal axis, and the apex of the sector is

located at the bottom of the screen. As will be discussed in Chap. 4, almost all TEE views in this book are presented with the apex of the sector at the top of the screen, with the exception of the deep transgastric views, which are inverted to display structures in their anatomic relationship. Of note, images can also be inverted "left-right" 180° along their vertical axis, though this is rarely (if ever) necessary, and can be very confusing.

- **Doppler invert**. Both color flow and spectral Doppler scales can be inverted so that the direction of flow can be reversed 180°. For color flow Doppler, this means that blue is flow towards the transducer, and red away from the transducer. For spectral Doppler, this means flow above the line is away from the transducer, and below the line is flow towards the transducer. It is rarely necessary to perform Doppler invert, and in fact it can be potentially confusing. Image and Doppler invert are performed independent of each other.
- **Image freeze/cine loop**. The image freeze/cine loop allows the user to "freeze" a short cine loop, which can then be scrolled backwards and forwards, frame by frame, enabling acquisition and storage of selected single images. Cine loop also enables measurements to be performed on appropriate images (these can also be stored). It should be noted that, while in freeze, the TEE transducer does not emit any ultrasound, therefore this mode should be selected when it is desirable to avoid heating adjacent tissues (for example, if the TEE probe is kept in a patient's esophagus between pre and postoperative studies).
- **Digital loop preferences**. Preferences for digital loop acquisition are generally available as a secondary menu, sometimes selected with one of the soft keys. Clip duration can be selected as a prescribed number of beats (if an ECG is present), or alternatively as a defined time period (number of seconds). In addition, some systems provide the choice of capturing clips prospectively or retrospectively.
- **Sector depth**. The depth of scanning can be reduced, which has the effect of improving frame rates, and also increasing the size of the structures visualized.
- **Sector size and line density**. These are controls available for imaging and color flow Doppler. Decreasing sector size, depth and line density can increase frame rates. However decreased sector size will reduce the field of view; decreased line density will reduce lateral resolution.
- **Zoom**. This is a function that allows a selected area of imaging sector to be magnified and expanded. There are two types of zoom: read and write. Read zoom takes the image data already existing in the scan converter and magnifies the existing pixels so that the selected zoom area fills the whole screen. This can be done on a frozen image. However, the existing data can appear coarse and pixelated. In contrast write zoom allows the operator to select the zoom area first, then transducer rescans only that area and writes only the data from the zoom area to the scan converter. Theoretically, this method can result in better image detail than the read zoom function because all scan converter pixels are assigned to the zoom area. However in practice, imaging improvements will ultimately still be limited by beam width and spatial pulse length (i.e. lateral and axial resolution).
- **Sweep speed**. The speed of certain displays such as M-mode and spectral Doppler can be varied; the usual settings are between 25 and 100 mm/s. Slower speeds allow display of more information and variation of information over time (for example, to visualize Doppler velocity variation with respiration, or spectral Doppler signals during bradycardic heart rates). Faster speeds allow more precise quantitative measurements, such as measurement of a Doppler waveform TVI.
- **Reject**. This is a form of electronic noise reduction in which low-level echoes and "noise" are eliminated from the display. It applies both to image as well as Doppler displays.

There are of course many other controls available, some of which focus primarily upon one mode of imaging. Again, the soft keys seen will change depending upon mode selected, and there will be variation in both terminology and layout depending upon the manufacturer. It is important that the operator become very familiar with the operational aspects of whichever machine is being used.

Artifacts

The nature of ultrasonic imaging is such that artifacts will inevitably be encountered. Artifacts are structures and features on an image that are either spurious, or whose displayed position does not correspond to the actual position of the object being scanned [27]. Ultrasound artifacts are can be produced by the changes in sound wave direction that occur while traveling through the body (i.e. reflection, refraction) as well as the use of reflector transmit/receive time as the proxy for reflector distance. A number of different artifacts are possible, many more than can be discussed in this section. For a complete discussion the reader is referred to several references [1–3]. Nonetheless it is important for the echocardiographer to be aware of some of the more common artifacts that might be seen. A few will be discussed below.

Mirror Image Artifacts

Mirror image artifacts arise from regions where an object is located next to a very strong reflector such as diaphragm.

When a transmit pulse encounters the object, it is reflected back to the transducer, producing the first image. However some sound is transmitted through the object and then continues to the interface beyond the object. The sound that returns from that interface undergoes partial reflection at the object, and this secondary echo returns back to the interface, where it is reflected again, giving rise to a secondary object that appears to be beyond the interface and appears as a mirror image. This is shown in Fig. 1.41. Mirror image artifacts can also occur with color flow Doppler. One such example is with the descending aortic long axis view, in which a color flow signal can be seen posterior to the aorta.

Mirroring can also be seen with the Doppler spectral display. This is different from the mirror image artifacts described above. A complete mirroring of the spectral tracing is seen on the opposite side of the baseline. This can be produced by a 90° angle between Doppler beam and direction of blood flow, or sometimes with too high a Doppler gain setting (Fig. 1.42).

Reverberation Artifacts

Reverberation artifacts occur when there is a fairly large impedance mismatch between interfaces (soft tissue-gas, fat-muscle, etc.). If the interface is oriented perpendicular to the direction of propagation, the reflected sound creates a strong echo. Some of this reflected sound is received by the transducer (creating an initial image), but some is also reflected from the transducer face back toward the interface, which then reflects back toward the transducer. This process can continue several times—in essence, sound "bounces" between the two surfaces. Each time, some of the returning sound is received and registered at an increased depth due to the perceived additional transmit-receive time (Fig. 1.43). Reverberation signals can be detrimental in that they can partially obscure actual echo signals on the display, and also produce additional "acoustic noise".

Another type of reverberation artifact is when multiple internal reflections occur within a small but highly reflective object, often a metallic object such as a needle, clip, or staple. This creates a series of echoes "ringing" within the object; some of the sound returns to the transducer, resulting in a number of small bands, known as **comet tails**. These produce a distinctive image on the display. Comet tails can also be seen distal to a strong reflector (Fig. 1.41).

Side Lobes and Grating Lobes

There are two important artifacts associated with transducer beams. The first is *side lobe* artifacts, which are secondary low intensity projections of ultrasound energy adjacent to the mean beam. They result from radial vibrations of the PZE elements, as opposed to the longitudinal vibrations used to generate the main beam. Side lobes can create imaging artifacts and noise in the image that can degrade lateral resolution. These artifacts tend to be of low intensity, but if a side lobe encounters a highly reflective surface outside the main beam, the object will appear to be incorrectly positioned as an image along the path of the main beam (Fig. 1.44). These artifacts can be recognized by their

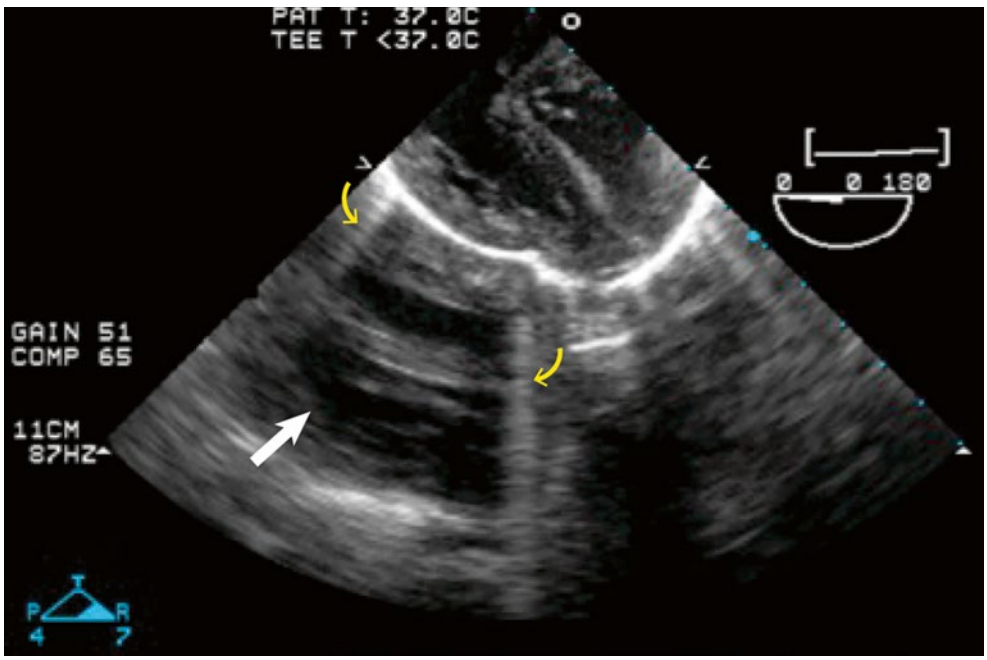

Fig. 1.41 Example of a mirror image artifact (*white arrow*) from a transesophageal echocardiogram in a mid esophageal four chamber view. The mirror image is seen on the opposite side of a large specular reflector, in this case, pericardium. Comet tail artifacts (*yellow arrows*) are also seen

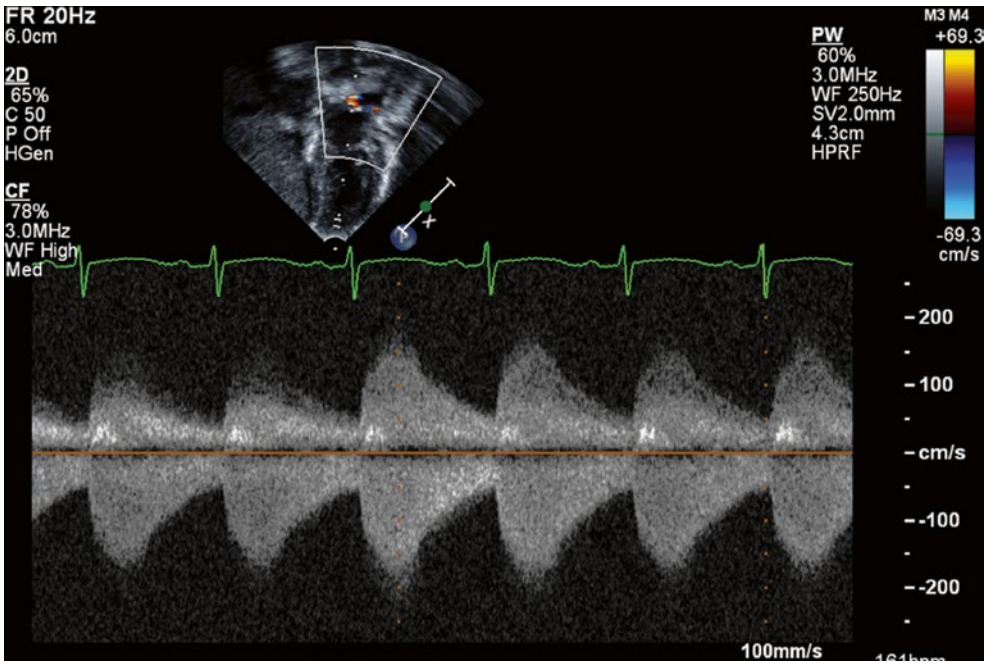

Fig. 1.42 Example of a spectral Doppler mirror image artifact in a patient with a patent ductus arteriosus. In this case the transducer was nearly perpendicular to the direction of blood flow, producing the artifact. Spectral broadening is also seen

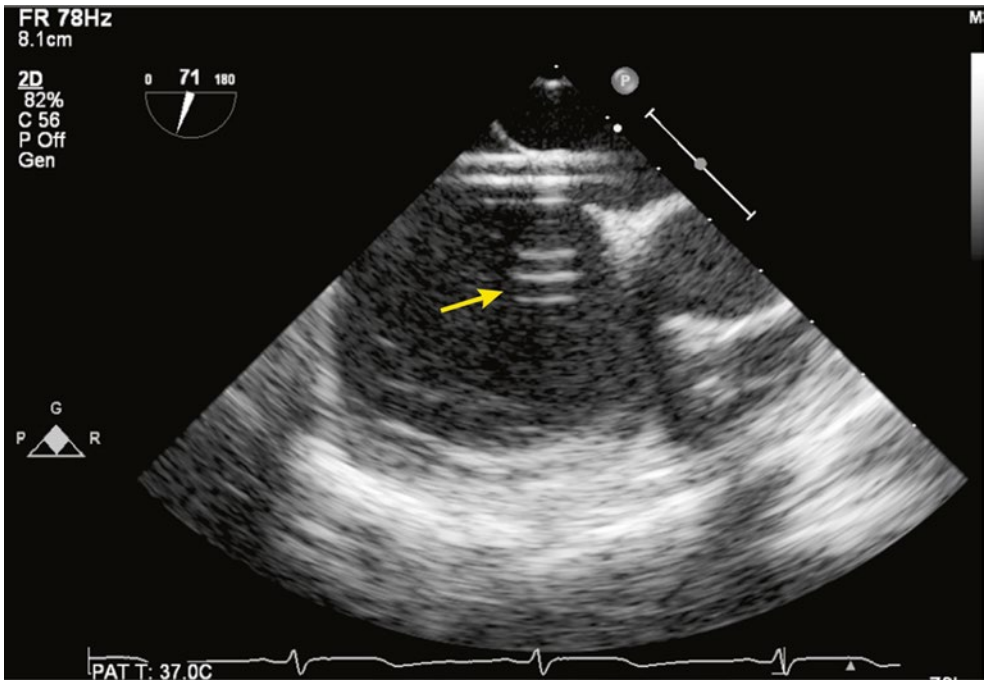

Fig. 1.43 Example of a reverberation artifact in a patient undergoing transcatheter closure of an atrial septal defect. The catheter sheath in the left atrium presents a large impedance mismatch; at the points perpendicular to the ultrasound path, reverberations are seen (*arrow*)

appearance of crossing anatomic borders such as cardiac walls (Fig. 1.45). They have an inconstant appearance; with adjustment of sector depth or transducer angle, they can disappear. The other type of artifact is *grating lobes*, which are a by-product of array transducers. These are multiple low intensity accessory beams that appear near the transducer face, but at large angles from the main beam. Ghost images can occur. These grating lobes can also degrade lateral resolution. Grating lobes can be eliminated by using very thin, closely spaced elements.

Acoustic Shadowing

When an interface is encountered with significant acoustic impedance mismatching, virtually all incident sound is reflected and none is transmitted. Thus, no imaging information is available past the interface. This leads to shadowing beyond the interface, characterized by a dark, anechoic area (Fig. 1.46). Acoustic shadowing is typically seen at the interface between blood/soft tissue and very dense objects such as metal or calcium; however it can also

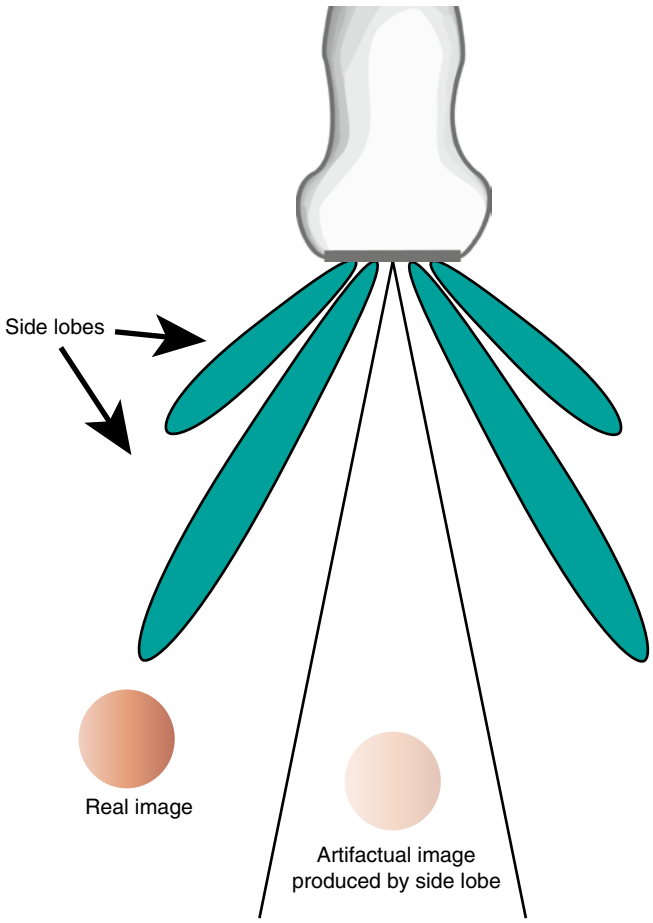

Fig. 1.44 Diagram of side lobes and the artifact that is can be produced. In this case an object encountered by one of the side lobes appears to be incorrectly positioned in the path of the main beam

be seen at soft tissue/lung interface. Whenever shadowing is encountered, other transducer positions should be attempted (if available) to circumvent the interface and visualize the area beyond it.

Digital Image Storage and DICOM

For a number of reasons, proper, secure recording and storage of echocardiographic information is imperative. First, all of the images, Doppler tracings, measurements and calculations obtained by echocardiography represent patient-related information, and need to be stored permanently as part of the medical record. Second, it is vital for the different medical/surgical subspecialists to have access to the actual echocardiographic images and data, not just the reports, when making decisions about medical/surgical therapy. Third, access to the actual data from past echocardiographic studies is useful in many ways: for comparing new information to older studies, for quality control, for research and education, and for medical-legal reasons.

Virtually all current echocardiographic machines and systems now store their information digitally in accordance with DICOM, the universal open standard created to ensure imaging intercompatibility among all medical imaging vendors and imaging modalities, including ultrasound, computerized tomography, magnetic resonance imaging, angiography, and radiography. It was expressly created to avoid proprietary, closed technology developed by different vendors. DICOM, which stands for **D**igital **I**maging and **CO**mmunications in **M**edicine, is not merely a file format, but rather an extensive

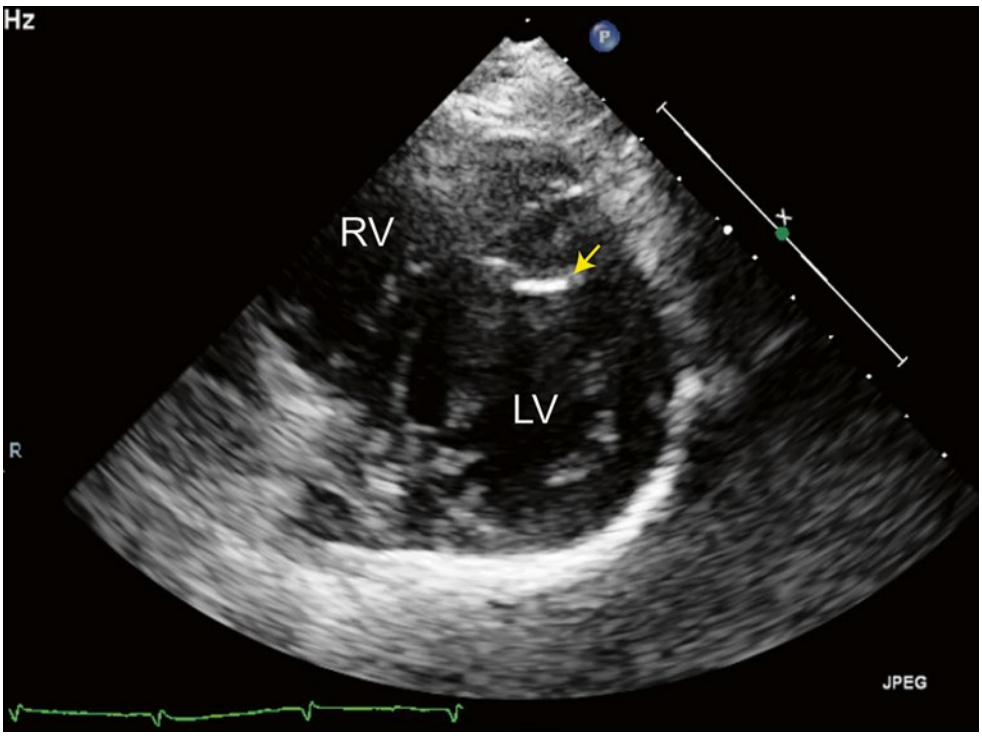

Fig. 1.45 Example of side lobe artifact, as shown with a transthoracic echocardiogram obtained from a standard parasternal short axis window, which was used to image the left ventricle (LV) and right ventricle (RV). The patient was known to have a central venous line in the right atrium. However on this image, the artifactual catheter tip (*arrow*) appeared to be located between ventricular septum and left ventricular cavity. This is due to side lobe energy giving the appearance of the catheter tip within the main beam

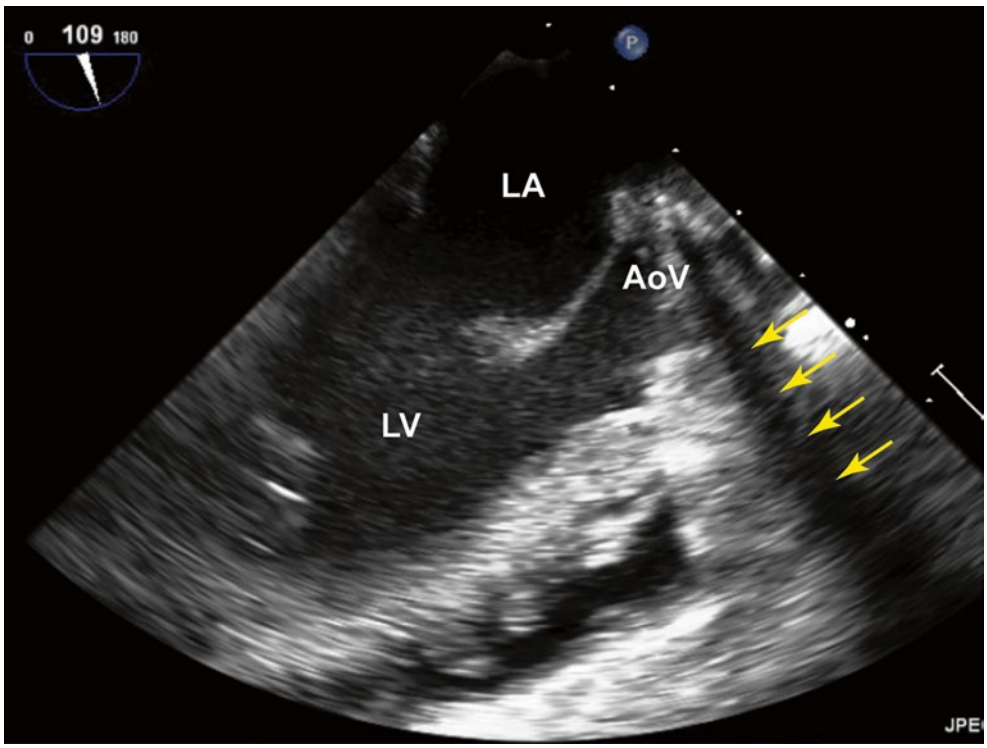

Fig. 1.46 Acoustic shadowing in a patient with a mechanical prosthetic aortic valve (AoV), as viewed from the transesophageal mid esophageal long axis view. The metal prosthetic ring causes significant acoustic impedance mismatching, such that no sound is transmitted beyond that point and a *dark*, anechoic wedge of shadowing is produced (*yellow arrows*). Reverberation is also present. *LA* left atrium, *LV* left ventricle

set of rules and protocols written in a number of separate sections, and crafted to specify the terminology, rules, equipment, file formats, image compression standards, hardware, and structured reporting that facilitate exchange of medical images [28–30]. The individual sections in the DICOM standard include networking standards based on Transmission Control Protocol/Internet Protocol (TCP/IP) to allow communication and transfer of information within an imaging network, also known as a PACS (**P**icture **A**rchiving and **C**ommunication **S**ystems) network. Other sections define a syntax and commands that can be used for the exchange of information. The use of these standards allows the integration of number of different devices (printers, scanners, workstations, servers, and storage devices) and imaging modalities on the same PACS network. Moreover, the stored images can be read on any computer or other device equipped with DICOM reading software. A DICOM file not only contains images, but a wealth of other information including patient information, study information, calibration information for the images (allowing offline measurements and adjustments to be made), etc. To assure intercompatibility, each vendor must publish a DICOM conformance statement. The DICOM standard is regularly reviewed and updated by the National Electrical Manufacturers Association (NEMA); new supplements and sections (parts) are routinely being added to keep the standard current with technology advances in the industry. As of this writing, the DICOM standard consists of 18 parts (Table 1.4), with more parts undoubtedly to follow in the future. Further information regarding DICOM can be obtained from the DICOM/NEMA website, http://medical.nema.org.

Table 1.4 DICOM standard (2011)

PS 3.1	Introduction and overview
PS 3.2	Conformance
PS 3.3	Information object definitions
PS 3.4	Service class specifications
PS 3.5	Data structures and encoding
PS 3.6	Data dictionary
PS 3.7	Message exchange
PS 3.8	Network communication support for message exchange
PS 3.10	Media storage and file format for data interchange
PS 3.11	Media storage application profiles
PS 3.12	Media formats and physical media for data interchange
PS 3.14	Grayscale standard display function
PS 3.15	Security profiles
PS 3.16	Content mapping resource
PS 3.17	Explanatory Information
PS 3.18	Web access to DICOM persistent objects (WADO)
PS 3.19	Application hosting
PS 3.20	Transformation of DICOM to and from HL7 standards

Source: DICOM/NEMA website—http://medical.nema.org

When recording an echocardiographic study, it is important for the operator to be aware of the need to record images carefully and adequately. In the videotape (analog) era, this was a simpler process—the recording could be started with the press of a button, and large portions of the study could be taped

continuously without heed to storage space requirements. The paradigm changed with digital recording. Digital studies are superior in so many ways—improved image quality, non-linear viewing capabilities, instantaneous accessibility from multiple networked sites, as well as the tremendous amount of additional information (aside from the images) contained in a recorded study. However the modern digital DICOM study is not recorded continuously with the simple press of a button, but rather as a series of individual clips/loops that can be as short as one beat in length. A typical transthoracic study for CHD can vary widely between 30 and 150 separate clips/loops, depending upon study complexity. It is an active process: the operator must regularly press the "capture" button (or its equivalent) in order to record a clip, and at times the clip length must be adjusted several times during a study. However recording must be performed assiduously, otherwise it is easy to produce a digital recording that contains only a small number of images and therefore an inadequate record of the entire study. This can be true especially with TEE, in which a rapid study is sometimes necessary due to the limited time available, particularly in the intraoperative setting. When ongoing monitoring is performed, the operator must be selective about the information acquired so as not to accumulate repetitive images. With CHD, sweeps are often necessary to develop a 3D appreciation of the anatomy, and a longer capture (3–5 s or more) might be necessary to record the desired information [29]. With modern echocardiography machines, the captured loop/sweep can be reviewed immediately to determine whether the information is adequate recorded, or whether more clips/loops are necessary. With TEE, it is even more important to record enough sweeps and clips, as there might not be another opportunity to repeat the study.

When a report is generated for the TEE study, it should be constructed with an eye toward readability and completeness. The report should provide an accurate, complete description and interpretation of the information contained within the images. Ideally, the report should contain essential elements including important patient demographic information, indications for the study, a description of study findings, any quantitative measurements, and a summary of pertinent positive and negative findings [31, 32].

Summary

This chapter provides a concise summary of the many important aspects regarding the science of ultrasound and echocardiography, as well as the use and control of the echocardiographic machine. Knowledge of the different technical aspects is important for all who perform echocardiography and TEE. By understanding the important concepts presented in this chapter, echocardiographers will have a solid foundation of knowledge, which will give them the necessary tools to optimize their echocardiographic imaging and Doppler evaluation of CHD. They will also have an appreciation of the many strengths, as well as the limitations and potential pitfalls, associated with echocardiography.

References

1. Zagzebski JA. Essentials of ultrasound physics. St. Louis: Mosby; 1996.
2. Hendee WR, Ritenour ER. Medical imaging physics. 4th ed. New York: Wiley; 2002.
3. Hedrick WR, Hykes DL, Starchman DE. Ultrasound physics and instrumentation. 4th ed. St. Louis: Mosby; 2004.
4. Gibbs V, Cole D, Sassano A. Ultrasound physics and technology: how, why and when. Edinburgh/New York: Churchill Livingstone/Elsevier; 2009.
5. Feigenbaum H. History of echocardiography. In: Feigenbaum's echocardiography. 7th ed. Philadelphia: Wolters Kluwer Health/Lippincott Williams & Wilkins; 2010. p. 1–8.
6. Denny MW. Air and water: the biology and physics of life's media. Princeton: Princeton University Press; 1993.
7. Hendee WR, Ritenour ER. Ultrasound waves. In: Medical imaging physics. 4th ed. New York: Wiley; 2002. p. 303–16.
8. Shankar H, Pagel PS. Potential adverse ultrasound-related biological effects: a critical review. Anesthesiology. 2011;115:1109–24.
9. Gauvin A, Cloutier G, Germain M. Principles of ultrasound. In: Denault AY, Couture P, Vegas A, Buithieu J, Tardif J-C, editors. Transesophageal echocardiography multimedia manual: a perioperative transdisciplinary approach. 2nd ed. New York/London: Informa Healthcare; 2011. p. 1–18.
10. Hendee WR, Ritenour ER. Ultrasound transducers. In: Medical imaging physics. 4th ed. New York: Wiley; 2002. p. 317–29.
11. Prager RW, Ijaz UZ, Gee AH, Treece GM, Wells PNT. Three-dimensional ultrasound imaging. Proc Inst Mech Eng H J Eng Med. 2010;224:193–223.
12. Rabben SI. Technical principles of transthoracic three-dinensional echocardiography. In: Badano LP, Lang RM, Zamorano JL, editors. Textbook of real-time three dimensional echocardiography. London: Springer; 2011. p. 9–24.
13. Salgo IS. 3D transesophageal echocardiographic technologies. In: Badano LP, Lang RM, Zamorano JL, editors. Textbook of real-time three dimensional echocardiography. London: Springer; 2011. p. 25–32.
14. Maslow A, Perrino AC. Principles and technology of two-dimensional echocardiography. In: Reeves ST, editor. A practical approach to transesophageal echocardiography. 2nd ed. Philadelphia/London: Lippincott Williams & Wilkins; 2008. p. 3–23.
15. Erb J. Basic principles of physics in echocardiographic imaging and Doppler techniques. In: Feneck RO, Kneeshaw J, Ranucci M, editors. Core topics in transesophageal echocardiography. Cambridge/New York: Cambridge University Press; 2010. p. 13–33.
16. Hedrick WR, Hykes DL, Starchman DE. Real-time ultrasound instrumentation. In: Ultrasound physics and instrumentation. 4th ed. Philadelphia: Elsevier Mosby; 2005. p. 129–54.
17. Bulwer BE, Shernan SK, Thomas JD. Physics of echocardiography. In: Savage RM, Aronson S, editors. Comprehensive textbook of perioperative transesophageal echocardiography. 2nd ed. Philadelphia: Lippincott Williams & Wilkins; 2010. p. 3–41.
18. Evans DH, McDicken WN. Doppler ultrasound: physics, instrumentation, and signal processing. 2nd ed. Chichester/New York: Wiley; 2000.
19. Lopez L, Colan SD, Frommelt PC, et al. Recommendations for quantification methods during the performance of a pediatric echocardiogram: a report from the Pediatric Measurements Writing

Group of the American Society of Echocardiography Pediatric and Congenital Heart Disease Council. J Am Soc Echocardiogr. 2010;23:465–95.
20. Gaspar T, Adawi S, Sachner R, et al. Three-dimensional imaging of the left ventricular outflow tract: impact on aortic valve area estimation by the continuity equation. J Am Soc Echocardiogr. 2012;25(7):749–57.
21. Saitoh T, Shiota M, Izumo M, et al. Comparison of left ventricular outflow geometry and aortic valve area in patients with aortic stenosis by 2-dimensional versus 3-dimensional echocardiography. Am J Cardiol. 2012;109:1626–31.
22. Otto CM, Bonow RO. Valvular heart disease: a companion to braunwald's heart disease. 3rd ed. Philadelphia: Saunders Elsevier; 2009.
23. Armstrong WF, Ryan T. Hemodynamics. In: Armstrong WF, Ryan T, Feigenbaum H, editors. Feigenbaum's Echocardiography. 7th ed. Philadelphia: Wolters Kluwer Health/Lippincott Williams & Wilkins; 2010. p. 217–40.
24. Armstrong WF, Ryan T. Evaluation of systolic function of the left ventricle. In: Armstrong WF, Ryan T, Feigenbaum H, editors. Feigenbaum's Echocardiography. 7th ed. Philadelphia: Wolters Kluwer Health/Lippincott Williams & Wilkins; 2010. p. 123–57.
25. Chassot P-G, Toussignant C. Basic principles of Doppler ultrasound. In: Denault AY, Couture P, Vegas A, Buithieu J, Tardif J-C, editors. Transesophageal echocardiography multimedia manual: a perioperative transdisciplinary approach. 2nd ed. New York/London: Informa Healthcare; 2011. p. 19–49.
26. Gorcsan J, Tanaka H. Echocardiographic assessment of myocardial strain. J Am Coll Cardiol. 2011;58:1401–13.
27. Zagzebski JA. Image characteristics and artifacts. In: Essentials of ultrasound physics. St. Louis: Mosby; 1996. p. 123–47.
28. Thomas JD. The DICOM image formatting standard: what it means for echocardiographers. J Am Soc Echocardiogr. 1995;8:319–27.
29. Thomas JD, Adams DB, Devries S, et al. Guidelines and recommendations for digital echocardiography. J Am Soc Echocardiogr. 2005;18:287–97.
30. Pianykh OS. Digital Imaging and Communications in Medicine (DICOM): a practical introduction and survival guide. Berlin: Springer; 2008.
31. Evangelista A, Flachskampf F, Lancellotti P, et al. European Association of Echocardiography recommendations for standardization of performance, digital storage and reporting of echocardiographic studies. Eur J Echocardiogr. 2008;9:438–48.
32. Picard MH, Adams D, Bierig SM, et al. American Society of Echocardiography recommendations for quality echocardiography laboratory operations. J Am Soc Echocardiogr. 2011;24:1–10.